Technische Universität München
TUM School of Natural Sciences

TUM

Zero-order drug delivery systems

Laura Tebcharani

Vollständiger Abdruck der von der TUM School of Natural Sciences der Technischen

Universität München zur Erlangung einer

Doktorin der Naturwissenschaften (Dr. rer. nat.)

genehmigten Dissertation.

Vorsitz: Priv.-Doz. Dr. Alexander Pöthig

Prüfer*innen der Dissertation:

1.   Prof. Dr. Job Boekhoven
2.   Prof. Dr. Angela Casini

Die Dissertation wurde am 16.08.2023 bei der Technischen Universität München eingereicht und durch die TUM School of Natural Sciences am 09.10.2023 angenommen.

I Abstract

Drug delivery technologies are a major part of the biopharmaceutical industry. Plenty of dosage forms exist that can release a range of drugs with different kinetics. However, up to now, formulations that release drugs with zero-order kinetics remain rare. Especially hydrophobic and oligonucleotide-based drugs are challenging to deliver linearly. Existing zero-order drug delivery platforms have high manufacturing costs and are usually complicated. The thesis will start with an introduction to different drug delivery systems and their release mechanism and kinetics. Moreover, I will discuss the state of the art, the advantages, and the limitations of these systems, which belong to the conventional, sustained, or zero-order release formulations, respectively. Furthermore, the importance of hydrogels, emulsions, and emulgels in drug delivery will be discussed. Hydrogels are widely used in biomedical applications as biocompatible systems, while emulsions are known for improving the delivery and bioavailability of hydrophobic drugs. Emulgels combine these desirable properties of hydrogels and emulsions and thus are ideal drug delivery platforms. A zero-order drug delivery system based on a chemical reaction network is also introduced in Chapter 1. Due to the phase separation of the activated precursor, a hydrophobic drug can be incorporated into the formed oil droplets. A unique self-protection mechanism of the activated precursor leads to the linear release of the drug molecules. Chapter 3 focuses on the optimization of this chemical reaction network-based system by simplifying the platform. The final formulation, a gellified emulsion, comprises hydrolyzable oil droplets of a hydrophobic anhydride embedded into a hydrogel. Hydrophobic drugs can be incorporated into the oil droplets and released linearly due to the zero-order hydrolysis of the droplets. The drug release rate and period can be easily adjusted by varying the initial oil and drug concentrations. Moreover, this chapter develops a tool based on partitioning the drug between the oil and the aqueous phase to predict compatible drugs. Furthermore, the formulation is biocompatible and can be stored at −20°C for several weeks. In Chapter 4, the compatible drugs are expanded to cholesterol-conjugated oligonucleotides, accumulating on the oil droplets' surface. The release follows a rapid burst with a through-the-initial oil concentration tunable onset. We combine this formulation into a dual-release platform that can release a hydrophobic drug with zero-order kinetics, followed by a rapid burst release of cholesterol-modified DNA. To show that the released cholesterol-conjugated DNA remains functional, we developed a method to delay the disassembly of gold nanoparticle aggregates. Here, the emulgel platform contains a cholesterol-tagged target DNA strand that can induce the disassembly of DNA-modified nanoparticles *via* toehold-mediated strand displacement. In Chapter 5, I examined how the drug delivery formulation performs under close to physiological conditions and discussed its limitations which lay in the reactivity

of the hydrolyzable oil with amine moieties present in a biological medium. Finally, I suggest boronic esters and orthoesters as alternative hydrolyzable oils to overcome the limitations of the anhydride-based formulation. Both compounds are potential drug delivery platforms but need further studies to achieve optimal drug release. With its simplicity and versatility, our system is a promising platform for the zero-order release of the drug.

II Zusammenfassung

Technologien für die Arzneimittelverabreichung stellen einen großen Teil der pharmazeutischen Industrie dar. Es existiert eine Vielzahl an unterschiedlichen Dosierungstechnologien die ein Spektrum an Wirkstoffen mit verschiedener Kinetik freisetzen können. Formulierungen die Wirkstoffe linear abgeben können sind jedoch selten. Existierende Systeme haben meist hohe Produktionskosten und sind kompliziert in der Anwendung. Vor allem die Verabreichung von hydrophoben und Oligonukleotid-basierte Medikamenten mit zero-order Kinetik ist eine Herausforderung. Diese Doktorarbeit beginnt mit einer Einführung in verschiedene Arzneimittelverabreichungstechnologien und ihre Freisetzungsmechanismen und -kinetik. Des Weiteren werde ich den heutigen Stand der konventionellen, der verzögerten und der linearen Arzneimittelverabreichungstechnologien, sowie ihre Vor- und Nachteile diskutieren. Außerdem wird die Bedeutung von Hydrogelen, Emulsionen und Emulgelen im Bereich der Wirkstoffabgabe herausgearbeitet. Aufgrund ihrer Biokompatibilität finden Hydrogele schon eine breite Anwendung im Bereich der biomedizinischen Anwendungen, während Emulsionen die Bioverfügbarkeit von hydrophoben Arzneistoffen verbessern kann. Emulgele vereinen diese erwünschten Eigenschaften von Hydrogelen und Emulsionen und sind deshalb ideale Plattformen zur Medikamentenverabreichung. Zusätzlich wird in Kapitel 1 eine Plattform zur linearen Wirkstoffabgabe vorgestellt, welche auf einem chemischen Reaktionszyklus basiert. Durch die Phasenseparierung eines aktivierten Produkts entstehen Öltröpfchen die einen hydrophoben Wirkstoff einschließen können. Der Selbstschutzmechanismus des aktivierten Produkts führt zu einer linearen Abnahme des Tröpfchen Volumens und dadurch zur linearen Freisetzung des Arzneistoffes. In Kapitel 3 fokussiere ich mich auf die Verbesserung und Vereinfachung dieser Reaktionszyklus-basierten Plattform. Die finale Formulierung, eine gelierte Emulsion, setzt sich aus hydrolysierbaren Öltröpfchen eines hydrophoben Anhydrides zusammen, welche in einem Hydrogel immobilisiert sind. Hydrophobe Wirkstoffe die in die Öltröpfchen eingeschlossen werden können, werden aufgrund der linearen Tröpfchen-Hydrolyse linear freigesetzt. Durch die Wahl der Anfangskonzentration von Öl und Wirkstoff kann die Einstellung von Freisetzungsrate und -periode festgelegt werden. Zudem wird in diesem Kapitel ein Werkzeug basierend auf Verteilung des Arzneistoffs zwischen Öl- und Wasserphase eingeführt um kompatible Wirkstoffe vorherzusagen. Außerdem kann die biokompatible Formulierung bei – 20°C mehrere Wochen gelagert werden. In Kapitel 4 wird die Palette an kompatiblen Wirkstoffen um Cholesterol-konjugierte Oligonukleotide erweitert. Diese lagern sich an der Oberfläche der Öltröpfchen an und werden schlagartig freigesetzt. Dabei kann der Beginn der rapiden Freisetzung über die Anfangskonzentration des Öls

eingestellt werden. Daraus haben wir eine duale Freisetzungsplattform entwickelt, die zuerst einen hydrophoben Arzneistoff linear abgibt und von einer schlagartigen Freisetzung Cholesterol-modifizierter DNA gefolgt wird. Um die Funktionalität der abgegebenen DNA zu zeigen, nutzen wir diese Plattform um Disassemblierung von Goldnanopartikel-Aggregaten zeitlich zu verzögern. In Kapitel 5 untersuche ich wie unsere Arzneimittelverabreichungsplattform unter physiologischen Verhältnissen abschneidet und diskutiere die Limitationen dieses Systems. Diese liegen in der Reaktivität des hydrolysierbaren Öls mit Amin-Gruppen, welche in biologischen Medien vorhanden sind. Schließlich führe ich in Kapitel 6 Orthoester und Borsäureester als hydrolysierbare Öle ein, um die Limitationen der Anhydrid-basierten Formulierung zu überwinden. Beide Verbindungen zeigen Potential als Wirkstoffabgabeplattform, erfordern jedoch weitere Studien um eine ideale Wirkstofffreisetzung zu gewährleisten. Durch die Einfachheit und Vielseitigkeit ist unser System eine vielversprechende Plattform für lineare Wirkstoffabgabe.

III Abbreviations

DMEM	Dulbecco's Modified Eagle Medium
EDC	1-ethyl-3-(3-dimethylaminopropyl)carbodiimide hydrochloride
e.g.	*exempli gratia*, for example
et al.	*et alii,* and others
FBS	Fetal Bovine Serum
i.e.	*id est*, that is to say
LB	Lysogeny Broth
PBS	Phosphate-Buffered Saline
PEG	Polyethylene glycol
PLGA	Poly(lactic-co-glycolic acid)
TBO	Tributyl orthoformate
TPO	Tripropyl orthoformate

IV Table of contents

1 Introduction

Abstract

Despite great progress in the field of drug delivery, there are still challenges that need to be overcome to improve the quality, efficiency, and safety of therapies. This chapter will overview conventional, sustained, and zero-order drug delivery systems. Here, I will discuss these drug delivery platforms' release mechanism, applications, advantages, and disadvantages. A common approach to overcoming the limitations of conventional and sustained delivery systems is the application of zero-order release platforms. However, these platforms come with their drawbacks that have not been solved yet. Furthermore, I will show that emulsions are important vesicles to increase the bioavailability of hydrophobic drugs. Combined with highly biocompatible hydrogels, emulgels that possess the desirable properties of hydrogels and emulsions can be formed. As a consequence, such emulgels are ideal drug delivery platforms. Finally, in this chapter, I will introduce a by paper Wanzke *et al.* developed drug delivery platform that is based on a chemical reaction cycle and can deliver hydrophobic drugs with zero-order kinetics. However, due to the low biocompatibility and complicated and impractical formulation of this emulgel-based platform, further optimization is needed.

1.1 Conventional drug delivery systems

Drug delivery technologies became a major part of the biopharmaceutical industry, especially due to economic factors. For example, developing a new pharmaceutic agent is more time-consuming and expensive than developing a new drug delivery vehicle. Moreover, new drug delivery platforms can increase the market value and competitiveness, and extend the patent life of existing drugs. On average, 6 years can be saved by developing a new delivery system (3-4 years) instead of a novel active agent (10-12 years). Furthermore, developing a new drug delivery platform cost only $20-50 million compared to over $500 million for the discovery of a new pharmaceutic compound. Thus, a lot of focus is put on the research and improvement of drug delivery platforms to achieve optimal efficiency and safety of new and existing drugs.[1-6]

Drug delivery describes administering a pharmaceutical compound to achieve a therapeutic effect. Usually, this is achieved by a drug delivery system, which consists of the active agent and additives that induce shape and structure to the formulation. After administration, these formulations transport the active agent into the body to the desired target site where it is released. Furthermore, they increase the drug release's stability, efficiency, and safety by controlling variables like the release rate or period. Since the drug delivery system is the interface between the drug and the patient, allowing accurate dosage and safe handling are essential properties of these formulations.[1, 3, 7-10]

An ideal drug delivery system has several important characteristics. Most importantly, the active agent needs to be transported to the site of action, so that the drug can achieve its therapeutic effect. However, a drug delivery platform should be safe and reliable and allow easy administration for optimal patient compliance. This means that the active agent should be released within the therapeutic window, which is the drug concentration range that provides a therapeutic effect without causing negative side effects.[1, 11, 12] Furthermore, the drug delivery system should be biocompatible and increase the bioavailability of the pharmaceutical compound, especially for hydrophobic drugs and drugs with a short circulatory half-life.[2, 13, 14] Ideally, the platform gives control over the drug release rate and period to get a maximum therapeutic effect.[15, 16] Finally, economic factors need to be considered. For example, the production of the formulation should be cost-effective and reproducible manufacturing with a defined quality must be ensured.[1, 9, 14, 17, 18]

Moreover, to achieve the most efficient therapeutic effect, the selection of the administration route is crucial. The selection of this delivery route depends on the properties of the active compound and if a targeted or systemic therapeutic effect is desired.[1, 12, 19] Oral, transdermal, transmucosal administration and parenteral delivery belong to the major route of drug

administration. Historically, oral administration *via* the gastrointestinal tract is the most important route due to its simplicity and widespread patient acceptance. Examples are solid dosage forms like pills, tablets, and capsules. However, the harsh conditions in the gastrointestinal tract can lead to the disintegration of the active compound, and low drug solubility can reduce bioavailability.[9, 18, 20-22] For transdermal and transmucosal administration, mostly semi-solid formulations such as gels, creams, and ointments, but also solid or liquid dosage forms like transdermal or transmucosal patches are used.[12, 18, 23] Parenteral administration, which describes the intravenous, intramuscular, and subcutaneous injection of a substance, is the most commonly used invasive delivery route. These injectable solutions, emulsions, or suspensions are especially used in emergencies when a rapid onset of the drug action and a high degree of flexibility in dosage adjustment is necessary.[9, 18, 24] In addition, the intrinsic chemical and physical drug properties, such as solubility, partition coefficient, pH value, and stability, must be considered when developing a formulation.[18]

Another important factor in developing dosage forms is the kinetic release profile of the therapeutic compound. Most clinically applied drugs are administered as conventional immediate-release formulations. This includes dosage forms such as pills and capsules and injectable formulations for parenteral administration. These immediate-release formulations are characterized by a rapid release of the active agent and, thus a fast increase of the plasma drug concentration as well as the immediate onset of the pharmacodynamic effects (**Scheme 1**). During this period the concentration lies within the therapeutic window. However, this stage is followed by a rapid decrease until the plasma drug concentration eventually falls below the minimum effective concentration (MEC), the concentration that is needed to achieve a therapeutic effect. Consequently, repeated administration and high dosages are required to remain within the therapeutic window, which is crucial for optimal therapy. However, this can result in poor patient compliance and increases the probability of under- or overdosing, thus leading to therapeutic inefficiency or even failure.[11, 21, 25-29]
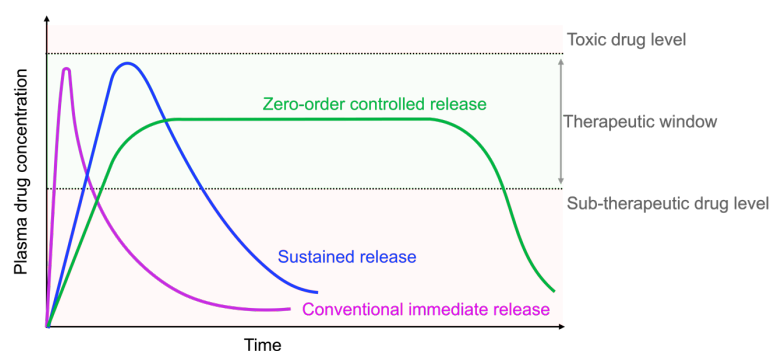
Scheme 1: Release profile of a conventional immediate (purple), sustained (blue), and zero-order controlled release platform (green).

1.2 Sustained drug release state of the art

To enhance the effectiveness of therapies, systems have been developed to sustain the release of the active agent in a predetermined manner. These sustained-release dosage formulations are characterized by releasing the therapeutic compound following first-order kinetics after an initial rapid burst release (**Scheme 1**). This means that the plasma drug concentration stays longer within the therapeutic window compared to immediate-release formulations, which translates into improved clinical efficiency of the drug. Furthermore, sustained-release formulations require less redosing, thus improving patient compliance.[16, 25, 30]

Three major mechanisms are utilized by sustained release platforms: dissolution-controlled, diffusion-controlled, and erosion-controlled release. When the formulation requires oral administration, the sustained release mechanism is often based on the dissolution of a drug-loaded matrix (monolithic system) or a coating that encapsulates the therapeutic compound (reservoir system, **Scheme 2**). Here the slow dissolution of the matrix or coating is the rate-determining step of the drug release, provided that the drug has a fast dissolution rate in an aqueous solution. Upon contact with the dissolution medium, *i.e.*, gastric or intestinal fluid, the matrix or coating will slowly dissolve, releasing the incorporated active agent. The Noyes and Whitney equation describes the dissolution rate. It depends on the drug concentration, solubility, and diffusion and on the matrix or coating's exposed surface area and thickness. This means that the dissolution rate and, thus, the drug release rate may change over time due to changes in the matrix or coating dimension during the release process. For monolithic systems, the active compound, such as theophylline monohydrate, is incorporated in a polymer matrix, *i.e.,* a combination of magnesium stearate, α-lactose monohydrate, and crystalline cellulose. Reservoir systems comprise single drug particles or granules, that are coated with polymers like cellulose, polyethylene glycol (PEG), or polymethacrylates and subsequently accumulated in a capsule or compressed into a pill. [10, 16, 30-32]

Monolithic system   Reservoir system

Soluble drug

Slowly dissolving matrix   Slowly dissolving coating
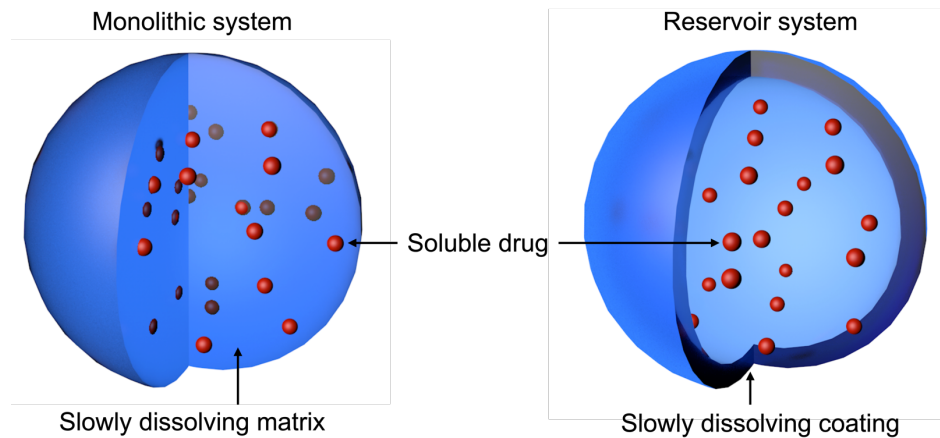
Scheme 2: Scheme of a monolithic release system with a soluble drug embedded in a slowly dissolving matrix and a reservoir system comprising soluble drug particles that are coated with a slowly dissolving polymer.

Another approach to sustaining drug release is the application of diffusion-controlled systems. Like dissolution-controlled platforms, diffusion-based drug delivery formulations come as monolithic systems, where the drug is embedded in a matrix or reservoir systems, where the drug is encapsulated into a thin membrane. But in contrast to the dissolution-controlled system, the matrix or the coating is inert, water-insoluble, and does not degrade or change during the release process. Consequently, the drug release is controlled by the diffusion of the drug out of the matrix or through the membrane into the surrounding medium. The diffusion of the drug is the rate-determining step, and the drug release can be described by the first and the second Fick's law (**Equation 1**).[10, 30, 32, 33]

$$F = -D\frac{\partial c}{\partial x} \quad \text{and} \quad \frac{\partial c}{\partial t} = D\frac{\partial^2 c}{\partial x^2}$$

Equation 1: Fick's first and second law where F is the flux, D is the diffusion coefficient, c is the concentration, x is the position and t is the time.[33]

The drug release from a diffusion-controlled formulation depends on the matrix or membrane properties, such as thickness and porosity, as well as on the physiochemical properties of the drugs, including molecular size and partition coefficient. In reservoir systems, porous, non-swellable membranes like ethyl cellulose can release drugs through micropores. Monolithic platforms can comprise hydrophilic, swellable polymer matrices such as alginates or hydroxypropyl methylcellulose that contain a homogeneously dispersed active agent.[10, 30, 32]

Hydrogels are a typical example of diffusion-based monolithic formulations. Here, the release profile of the drug can be influenced by the properties of the hydrogel network, *i.e.,* the mesh

size and the swelling ability, as well as by the drug properties like hydrophobicity and charge. Noteworthy, if the mesh size of the hydrogel is larger than the drug molecule ($r_{mesh}/r_{drug} > 1$), the drug molecules can move freely within the hydrogel network and are released rapidly following first-order kinetics. However, the diffusion process can be slowed down by decreasing the mesh size to be closer to the drug molecule size ($r_{mesh}/r_{drug} \sim 1$). As a consequence, the drug release can be decelerated and extended. Hennink *et al.* could show this by using a triblock copolymer (ABA) comprising a poly-(N-(2-hydroxypropyl) methacrylamide lactate) modified with methacrylate moieties (A) and poly(ethylene glycol) (B) (**Figure 1a**). Different degrees of crosslinking can be achieved by varying the polymer content (20% and 35% w/w). Gels with a high degree of crosslinking (35% w/w) showed an extended lysozyme release of 100 hours compared to the 50-hour release period from a less crosslinked polymer gel (20% w/w, **Figure 1b**).[2, 34, 35]
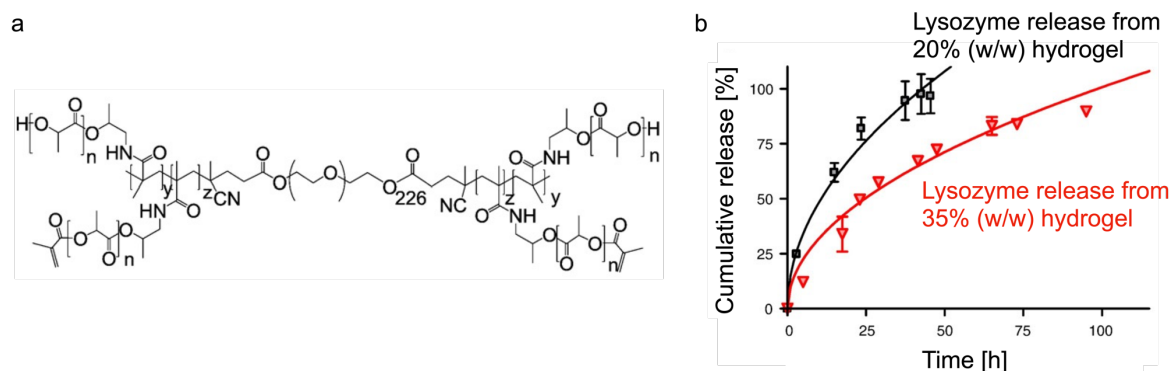
Figure 1: a) Chemical structure of the ABA triblock copolymer consisting of partly methacrylated poly(N-(2-hydroxypropyl)methacrylamide lactate) and PEG 10,000. **b)** Cumulative release of lysozyme from a 20% w/w and a 35% w/w hydrogel in PBS at 37°C. Reprinted from reference [33] by permission from Elsevier Ltd., Copyright © 2009.[35]

Finally, a sustained release formulation can be achieved through controlling the erosion of a matrix. Here the drug, which is dispersed in a polymer matrix, releases as the matrix is degraded by bulk or surface erosion. For example, a therapeutic compound can be dispersed in poly(lactic-co-glycolic acid) particles (PLGA particles), which have good biocompatibility and can be administered *via* injection. PLGA particles undergo bulk erosion since the water diffusion into the particle bulk is faster than the hydrolytic cleavage of this copolymer. As a result, the drug release follows first-order kinetics. However, by increasing the porosity of the PLGA particles, the release profile can be drawn to near zero-order kinetics. Siepmann *et al.* prepared lidocaine-loaded PLGA-microparticles with different porosities (**Figure 2a**). In non-porous microspheres, the release profile indeed showed first-order kinetics, no matter the particle size (**Figure 2b**). In contrast, the release of lidocaine follows near zero-order kinetics

when porous PLGA microparticles were used (**Figure 2c**). This can be explained by the reduced effect of the autocatalysis of PLGA through the increased porosity: if pores are present, the catalytic, acidic degradation products diffuse out of the particle bulk.[36, 37]
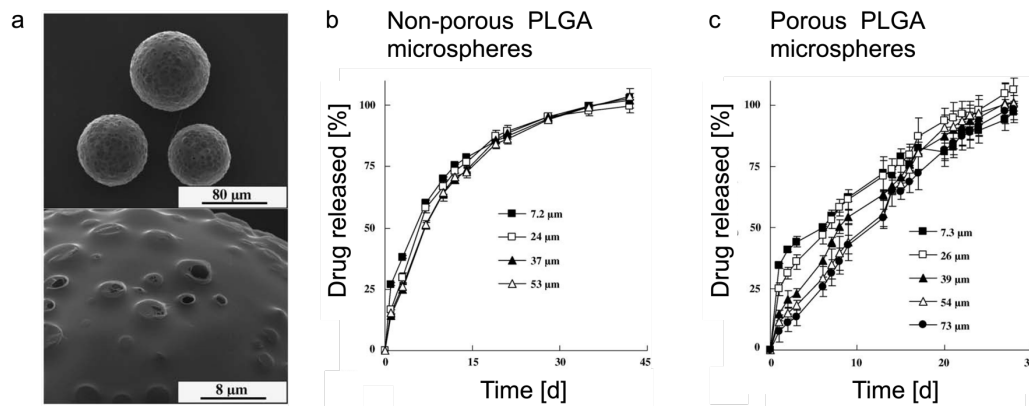
Figure 2: a) SEM image of the surface (lower and higher magnification) of lidocaine-loaded, PLGA microparticles before exposure to PBS. **b)** Cumulative release of lidocaine from non-porous PLGA microparticles and **c)** from porous PLGA-based microparticles with different radii in PBS over time. Reprinted from reference [34] by permission from Elsevier Ltd., Copyright © 2006.[36]

Further methods to achieve near zero-order release with PLGA copolymers is increasing the lactic compound, which leads to a more crystalline structure, adding surface-eroding compounds such as trimethylene carbonate, or choosing a rod-like structure. However, the physiochemical properties of the drugs have a huge influence on the release profile, thus, the system is limited by the selection of the drugs. Moreover, these rods can only be applied as implantable devices, which might decrease patient compliance.[38, 39]

Theoretically, polymer drug delivery systems that degrade *via* surface erosion mechanism should release their incorporated active agent at a rate proportional to the surface area. This could be achieved by choosing a polymer with a faster hydrolytic degradation rate than the bulk penetration by water, i.*e.,* polyanhydrides or polyesters. However, these polymer particles are typically spherical, resulting in a decrease in surface area over time. Consequentially, the release rate changes over time also decreases with time such that the release profile resembles the profile of a bulk erosion formulation.[40-42]

Even though the above-described systems can sustain the drug release, it is also a first-order process and the drug release rate. Thus, the plasma drug concentration are not constant. While such platforms can be successfully used to deliver drugs within a large therapeutic window, administering drugs with a narrow therapeutic window is difficult. To avoid frequent

redosing, these drugs require a release with a constant rate over the entire release period. This can only be achieved by zero-order drug delivery systems.[25]

1.3 State of the art, advantages and challenges of zero-order drug delivery systems

To overcome the limitations of conventional and sustained drug delivery systems, platforms that release their therapeutic compounds at a constant rate over an extended period have huge potential. These systems follow zero-order release kinetics, ensuring a constant plasma drug concentration during the entire release period (**Scheme 1**). As a consequence, the plasma drug concentration stays within the therapeutic window, thus decreasing adverse side effects. Usually, for these systems, less frequent administration is required, which improves patient compliance.[1, 11, 25, 43]

One example of zero-order drug delivery systems is osmotic pumps for oral use or as implantable devices. These systems rely on osmotic pressure, which is caused by the movement of solvent molecules across a semipermeable membrane. The membrane only allows the passage of the solvent molecules, usually water, that move from a region of low solute concentration to a region of high solute concentration. The osmotic pressure is proportional to the concentration and the temperature. Thus, a constant osmotic pressure can be achieved if the same solvent and solute are used on both sides of the membrane. This leads to a constant influx of solvent, which can be utilized for zero-order drug release. These platforms are independent of the pH, hydrodynamics of the dissolution medium, and other physiological parameters.[25, 44, 45] Osmotic pumps consist of a semipermeable membrane, *e.g.,* cellulose acetate, which encapsulates a drug and an osmotic agent. The osmotic agent can be an osmogenic salt like sodium chloride, fructose, citric acid, or the drug itself. The simplest form of an osmotic pump formulation is the elementary osmotic pump, a single-compartment system that releases the drug through a delivery orifice in the semipermeable membrane (**Figure 3a**). The influx of water, which is caused by the osmotic pressure, dissolves the encapsulated drug. Moreover, the water increases the volume and, thus, the hydrostatic pressure in the core leading to the effluxion of the dissolved drug through the delivery orifice. In general, the drug release rate from elementary osmotic pumps can be described by **Equation 2**.

$$\frac{dM}{dt} = \frac{dv}{dt}c$$

Equation 2: The drug release rate through the delivery orifice *dM/dt* is given by the flow into the tablet *dV/dt* and the concentration *c* of the drug in the dispensed solvent.[46, 47]

Optimization of the orifice size, the membrane properties, drug solubility, and the selection of the optimal osmogen and its concentration can achieve zero-order drug release. While generic elementary osmotic pumps can only release moderately soluble drugs, systems with a modified core can achieve zero-order release of drugs with low solubility.[10, 44, 46-50] One example is the successful zero-order release of nifedipine from a swellable elementary osmotic pump developed by Nokhodchi *et al.* (**Figure 3b**). The tablets comprise a cellulose acetate membrane with a delivery orifice diameter of 350 and 800 µm and a water-swellable polymer core (HPMC E50LV) containing potassium chloride as an osmotic agent. However, only a sufficient size of the delivery orifice, *i.e.,* 800 µm, achieves zero-order kinetics. If the orifice size is too small, *i.e.,* 350 µm, the hydrostatic pressure might not be fully relieved therefore leading to deformation of the tablet and thus unpredictable drug release.[49] In contrast, highly water-soluble drugs diffuse through the delivery orifice of the elementary osmotic pump resulting in first-order release kinetics.[50]
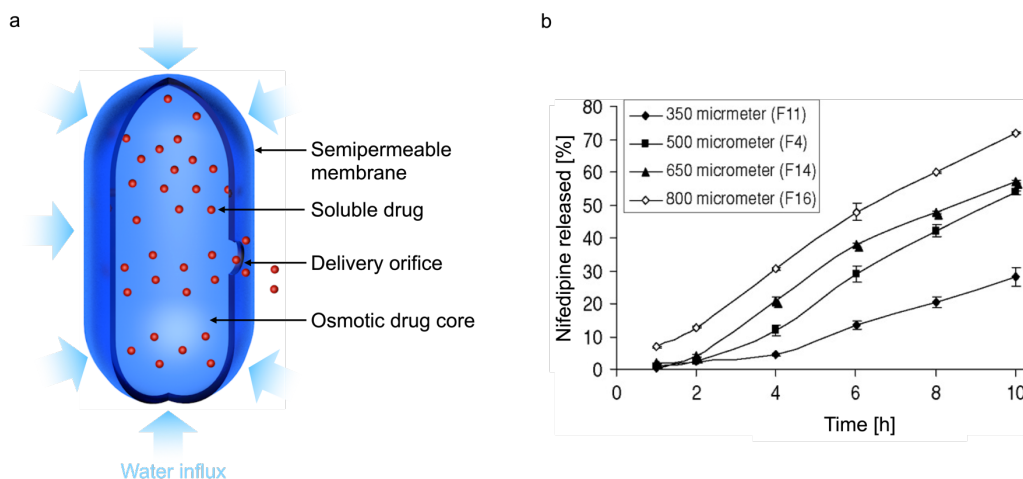
Figure 3: a) Scheme of an elementary osmotic pump with a semipermeable membrane, an osmotic drug core, and a delivery orifice. **b)** Cumulative release of Nifedipine from swellable elementary osmotic pumps with delivery orifices between 350 and 800 µm. Reprinted from reference [47] by permission from Informa UK Limited, trading as Taylor & Taylor & Francis Group, Copyright © 2008.[49]

Further variations of osmotic pump systems are controlled porosity osmotic pumps (**Scheme 3a**) and push-pull osmotic pumps (**Scheme 3b**), which overcome the limitations of elementary osmotic pumps and can release hydrophilic as well as hydrophobic drugs following zero-order kinetics. In contrast to elementary osmotic pumps, the semipermeable membrane of controlled porosity osmotic pumps contains water-soluble leachable compounds that induce pore formation upon contact with aqueous fluids. These pores function as delivery orifices. Here the drug release not only depends on the osmotic pressure, the drug solubility, and the membrane thickness but also on the pore formation. As a result, the release kinetics can be tuned by selecting the properties and amount of used porogens.[25, 45, 51-54] For example, the release of etodolac, an anti-inflammatory drug, follows zero-order kinetics if the cellulose acetate membrane contains only 5% polyethylene glycol (PEG 400) as a pore-forming agent. However, a higher concentration of pore-forming agent (10% and 20% PEG 400) creates a more porous membrane structure, and the drug release is diffusion controlled and follows first-order kinetics.[51] The same strategy was used to linearly release the analgesic drug tapentadol hydrochloride. Since this drug has a short half-life, linear release *via* controlled porosity osmotic pump tablets can reduce the frequent administration necessary when using immediate-release tablets.[54] Sucrose nano- or micro-suspensions as pore-forming agents can also achieve zero-order drug release, *e.g.,* diltiazem hydrochloride.[55, 56]

Push-pull osmotic pumps consist of a bilayer core: a drug layer containing the drug and a push layer containing an expanding hydrophilic polymer. Both layers contain an osmotic agent. A semipermeable membrane with a laser-drilled orifice at the drug layer surrounds this core. Constant swelling of the push layer leads to the zero-order release of the drug, which is either dissolved or readily with a suspension agent. Examples are the linear release of lithium carbonate to treat bipolar disorder or pramipexole to treat Parkinson's disease.[57-60] However, producing osmotic pump drug delivery systems is still costly, and special equipment for drilling the delivery orifice is needed.[25, 44, 45, 51]
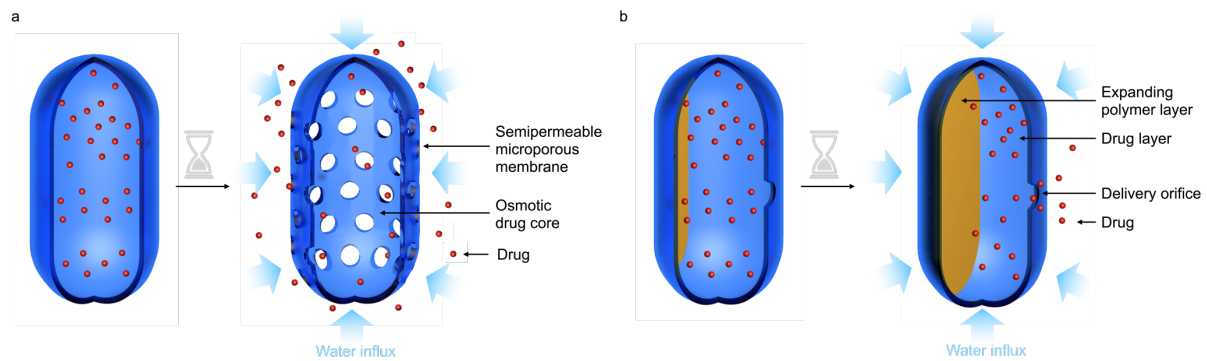
Scheme 3: a) Scheme of a controlled porosity osmotic pump before (left) and after (right) contact with an aqueous medium. **b)** Scheme of a push-pull osmotic pump before (left) and after (right) contact with an aqueous medium.

Another strategy to achieve zero-order drug release, especially for long-term drug delivery, is using actuated infusion pumps with a continuous flow. These pumps are implanted into the body, usually the abdomen. Such infusion pumps consist of a drug chamber, which can hold up to 50 mL of drug solution, and a propellant chamber, which contains a propellant like chlorofluorocarbon (**Figure 4a**). The transition from the liquid propellant to its gaseous state at body temperature leads to the compression of the drug reservoir. Consequently, the drug is pushed out of the reservoir and delivered to the target site *via* an implanted catheter. Due to the constant body temperature, the drug release is constant at a steady rate.[25, 61, 62] One example is the Codman® 3000 pump (Codman & Shurtleff, Inc., Raynham, MA, USA) which can be used to administer the anti-HIV drug darunavir to dogs at a constant rate over four weeks (**Figure 4b**).[63] Further applications of this pump are the intraspinal delivery of morphine and continuous administration of the skeletal muscle relaxant baclofen. Patient compliance can be improved drastically due to delivery periods of up to one month. In contrast, oral baclofen administration requires up to six doses daily.

Moreover, the delivery directly to the target site can reduce negative side effects.[62, 64-66] Although actuated infusion pumps are suitable for long-term zero-order drug release, especially for chronic diseases, several limitations exist. For example, the pumps require invasive surgical implantation posing a risk for the patient. Furthermore, changes in the body temperature can increase the vapor pressure of the propellant, which leads to an increase in the drug release rate. Overdosing can also be caused by pump malfunction or during the refill process and might be lethal due to the large drug reservoirs. Moreover, manufacturing actuated infusion pumps are expensive; up to date, only two systems are commercially available in Europe. At the same time, no pumps are available in the United States. For

example, the Codman® 3000 infusion pump was discontinued for economic and logistic reasons.[25, 61-63]
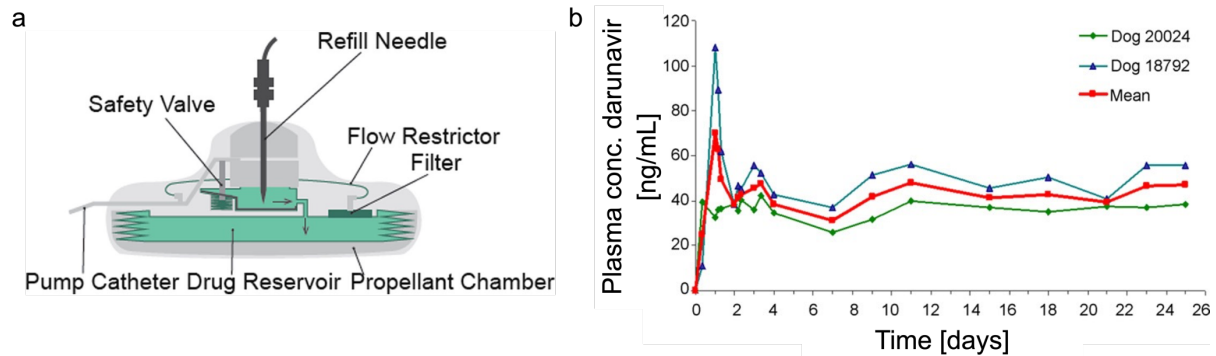
Figure 4: a) Scheme of an infusion pump with a collapsible drug reservoir and a propellant chamber. Reprinted from reference [59] by permission from Springer Nature Ltd., Copyright © 2019.[61] **b)** Plasma drug concentration profile of darunavir given as a continuous infusion to dogs at a constant rate (25 mg/dog/day) for 4 weeks with an adapted Codman® 3000 pump. Reprinted from reference [61] by permission from Elsevier Ltd., Copyright © 2008.[63]

As described in Chapter 1.2, diffusion-controlled drug release from a reservoir or matrix system results in first-order release kinetics, which can be sustained to prolong the drug release. However, microchip or capsule platforms containing a nanopore membrane with geometrically defined channels can achieve zero-order drug release. Here, the drug release is determined by physio-electrostatic confinement. These systems comprise a drug-containing reservoir sealed with a nanochannel membrane (**Figure 5a**). Through tailoring channel parameters such as height, the diffusion of molecules through the nanopore membrane can be physically and electrostatically constrained, thus leading to zero-order release kinetics. Furthermore, the dimensions and number of the nanochannels can be adjusted for individual therapeutic agents, making this system very versatile.[67-71] Based on the physiochemical properties of five different drugs, A. Grattoni, and co-workers selected different nano channel heights to achieve the zero-order release of each compound. The nanochannels lay between a silicon and silicon nitride layer and possess negative surface charges. The channel arrays are organized parallel to the membrane surface to which they are connected *via* inlet and outlet channels (**Figure 5b**). For small drug molecules like letrozole, a small channel height of 3.6 nm was used, while huge therapeutic molecules like interferon α-2b require a channel height of 22 nm to be released linearly (**Figure 5c-d**).[67] Similarly, capsules containing a silicone nanopore membrane linearly release fluorescein isothiocyanate (FITC)-labeled

bovine serum albumin over 60 days.[68] However, nanochannel microchips and capsules require surgical implantation, which means the risk of infection and complication might outweigh the benefits such as precise control over the release kinetics and protection of the drug in a sealed reservoir. Furthermore, high manufacturing costs and low drug-loading capacities may limit the clinical application of such devices.[25, 72, 73]
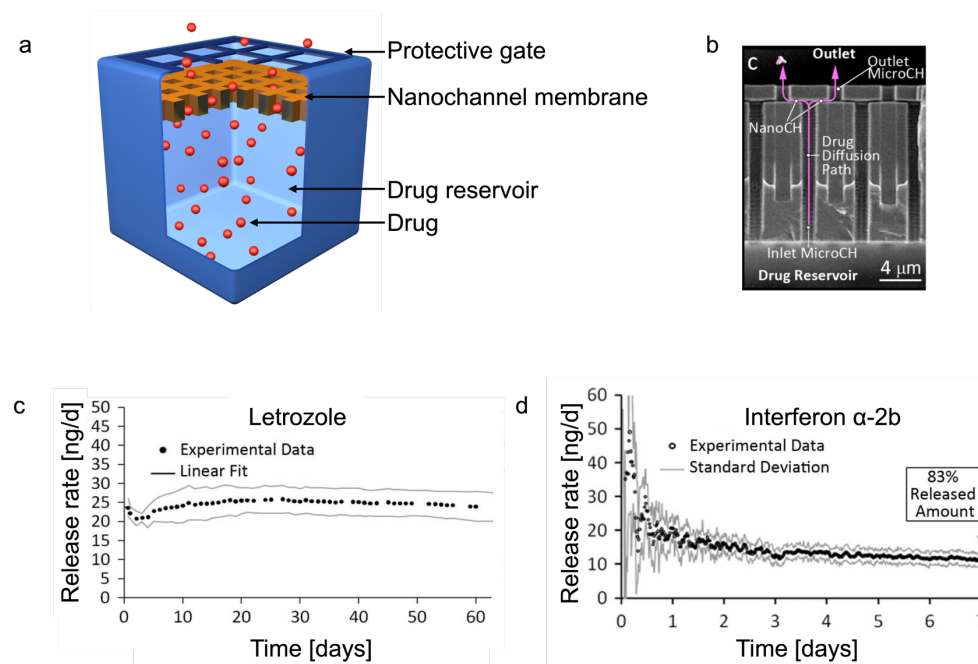
Figure 5: a) Scheme of a drug reservoir platform containing a nanopore membrane with geometrically defined channels. **b)** A cross-section of a membrane showing the vertically oriented inlet and outlet microchannels that are connected by the horizontally oriented nanochannels. The thinner layer on top of the nanochannels is deposited silicon nitride, while the thicker layer on the bottom is silicon. The pink arrows depict how diffusing drugs will travel across the membrane. **c)** *In vitro* release profile of letrozole (~24 µg/day). **d)** *In vitro* release profile of interferon α-2b (~15 µg/day). Reprinted from reference [65] by permission from Elsevier Ltd., Copyright © 2013.[67]

Finally, zero-order release kinetics can be achieved with electrospun nanofibers. These fibers consist of a polymer like cellulose acetate or poly-(DL-lactide-co-glycolide) (PLGA), which can be dissolved in a solvent. By applying high voltages, the electric force creates a charged thread of the polymer solution, forming a mesh of nanofibers. The active agent is dissolved in the polymer-solvent solution to produce the drug delivery system and directly spun into drug-containing nano-fibers.[74-79] For example, individually spun PLGA meshes promoted the zero-order release of the anti-inflammatory drug budesonide over 28 days while achieving a total cumulative release of 60%. S. Samavedi *et al.* suggested that the inherent solid-state drug

solubility in the PLGA polymer drives the linear release. By co-electrospinning PLGA with poly(caprolactone) (PCL) in different ratios, the drug release period can be tuned between 28 and 15 days. However, only pure PLGA nano-fibers achieved zero-order kinetics, while PLGA/PCL blends only achieved first-order release kinetics.[75]

This problem was not reported if core-shell nanofibers were used to release ferulic acid, a poorly soluble drug that would have a better bioavailability if released linearly. Yu and Liu *et al.* prepared such nanofibers by modified triaxial electrospinning. These fibers comprise a drug-loaded gliadin protein core and cellulose acetate shell (**Figure 6a-b**). They pointed out that only the core fluid containing gliadin and the drug is spinnable and supports the unspinnable middle cellulose acetate fluid and the outer solvent fluid. While the cellulose acetate forms the nanofiber shell, the outer solvent fluid's purpose is to stabilize the electrospinning process. By adjusting the flow rate of the cellulose acetate fluid, the final shell thickness of the fibers and, thus, the release rate and period of the drug can be tuned (**Figure 6c**). This means a thick cellulose acetate shell of 30.2 nm releases the ferulic acid over 40 hours, while a thinner shell of 5.2 nm releases the drug in 16 hours. Yu and Liu *et al.* suggested that the drug release is determined by its diffusion through the core matrix and the polymer shell. In contrast, when a monolithic nanofiber consisting just of the drug-loaded gliadin core is used, the release follows first-order kinetics. The researchers claim that the cellulose acetate shell can be replaced with other polymers and that this method can potentially release a range of drugs.[76]
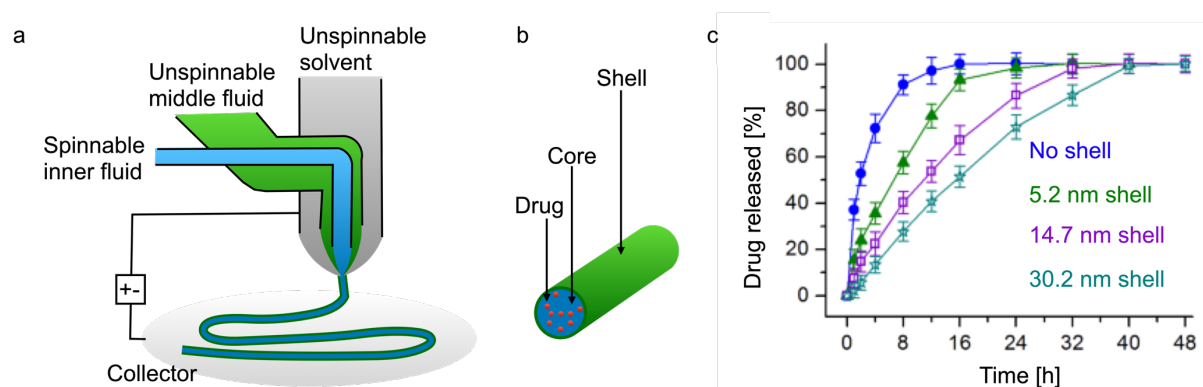
Figure 6: a) Scheme of a modified triaxial electrospinning setup that produces core-shell nanofibers. The drug is dissolved in the spinnable inner fluid. **b)** Scheme of an electrospun core-shell nanofiber that contains a therapeutic compound in the core. c) *In vitro* cumulative release profile of ferulic acid from nanofibers with different shell thicknesses. Reprinted from reference [74] by permission from Elsevier Ltd., Copyright © 2019.[76]

The paragraphs above show that nanofibers are versatile drug delivery systems, but there are still some drawbacks to these platforms. Especially the up-scaling of the production of core-shell nanofibers remains challenging and expensive. Furthermore, due to high solvent consumption up-scaling the manufacturing of nanofibers can result in environmental burden, safety concerns, and huge amounts of chemical waste. To date, no FDA-approved zero-order core-shell nanofibers for clinical applications are available.[79]

To summarize, researchers have shown that zero-order drug release can be achieved with osmotic pumps, actuated infusion pumps, passive microchips, and core-shell nanofibers. Furthermore, several systems are FDA-approved and are already used in clinical settings. These methods have many advantages compared to conventional and sustained release systems and have the potential to deliver hydrophobic, hydrophilic, and biomolecular active agents safely and efficiently while keeping a constant release rate. Thus, osmotic pumps, actuated infusion pumps, microchips, and nanofiber platforms can deliver drugs within narrow therapeutic windows and minimize adverse effects. Moreover, release periods between several hours up to 60 days, depending on which method is employed, can reduce the frequency of administration and improve patient compliance.

Despite the advantages, there are several drawbacks to each technique. While osmotic pumps are available as oral tablets and implantable devices, actuate infusion pumps and passive microchips require surgical implantation. Invasive surgical procedures always pose a risk for the patient and might prevent the patient from choosing such a therapy. Another common limitation that osmotic and infusion pumps, microchips, and core-shell nanofibers have is the high manufacturing cost and the need for special manufacturing equipment. This economic factor cannot be discarded because it can lead to the discontinuation of the product, *i.e.,* the Codman® 3000 infusion pump, regardless of the advantages over conventional systems.

1.4 The importance of emulsions to deliver hydrophobic drugs

To treat diseases and illnesses, therapeutic agents are the most important part as they are the compounds that actively treat the disease. To do so, therapeutic agents have internal characteristics such as functional moieties. However, this also has an influence on the rate and extent to which the body absorbs the active compound and becomes available at the target site. This relation is described by bioavailability, which is one of the most important parameters that need to be considered in drug development and delivery. Further influences on the bioavailability are the physiochemical drug properties like solubility, partition coefficient,

and dissolution rate, as well as physiological factors such as protein and tissue binding and site-specific absorption.[18, 80-82] Form these parameters, Amidon *et al.* developed a classification system, which became a powerful tool for improving the bioavailability of therapeutic agents. The biopharmaceutics classification system (BCS) categorizes active agents according to their solubility and permeability into four classes (**Scheme 4**). BCS class I drugs with high solubility and permeability, *i.e.,* paracetamol[83], can be easily administered *via* the oral route and thus have a high bioavailability. However, delivering especially poorly soluble drugs with a solubility below 100 µg/mL (BCS class II and IV) is challenging because only the solubilized drug at the target site is available for absorption. Currently, more than 40% of new therapeutic agents are hydrophobic and have low bioavailability. Examples of BCS class II drugs are nitrendipine, mebendazole, and ritonavir.[82, 84-87]
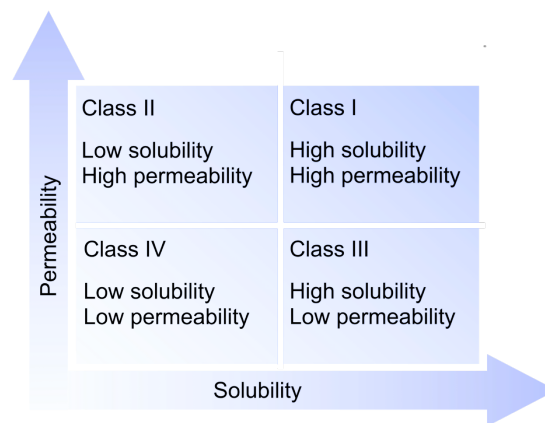
Scheme 4: Diagram of the biopharmaceutics classification system (BCS) with drug solubility and permeability as x- and y-axis, respectively, and BCS classes I to IV.

There are several approaches to increase the bioavailability of BCS class II drugs, including modifying physiochemical properties, such as the chemical structure, crystal modification, amorphization, or particle size reduction.[86] For example, the reduction of the particle size of Nitrendipine crystals from 36.6 µm to 200 nm resulted in a 5.1×10^4 higher dissolution rate. As a consequence, the bioavailability of Nitrendipine could be increased to 61%.[88] However, these methods are difficult to scale up.[86, 89]

In recent years, surfactants and other lipid-based formulations have become a common approach to improve the bioavailability of BSC class II drugs. Such formulations comprise an active compound that is incorporated into an inert delivery vehicle like oils, liposomes, emulsions, as well as self-emulsifying formulations.[86, 90-92] Emulsions like oil-in-water emulsions are widely known for improving the bioavailability of hydrophobic drugs by increasing their water solubility. Common emulsions for drug delivery applications comprise an oil- and a water phase, which is immiscible, a hydrophobic active agent that is dissolved or

dispersed in the oil phase, and a suitable emulsifying agent.[93, 94] For example, the intralipid system, which consists of a soybean oil emulsion that is stabilized with egg-lecithin, can be used to achieve a fiftyfold higher hexamethylmelamine drug concentration in mice compared to the administration in saline solution.[95] Furthermore, easy manufacturing and administration by all common routes, including oral, topical, parenteral, and aerosolization to the lung, make emulsions relevant drug delivery platforms. However, drawbacks are the sensitive and metastable properties of emulsions, which may hurt drug delivery. [90, 93, 96]

Besides conventional emulsion-based drug delivery systems, self-emulsifying drug delivery systems evolved as platforms to improve the bioavailability of hydrophobic drugs. Self-emulsifying drug delivery systems are isotropic mixtures of oils, surfactants, and co-solvents that emulsify to oil-in-water-emulsions upon dilution with an aqueous medium, *i.e.,* the gastrointestinal fluid. Depending on the size of the formed droplets, self-emulsifying systems with an average oil droplet size between 100 nm and 50 nm can be formed. Fatty acids and medium or long-chain hydrocarbons are most commonly used in the oil phase, *i.e.,* triglyceride oils or vegetable oils. To stabilize the emulsions, non-ionic surfactants with a high hydrophilic-lipophilic balance, such as ethoxylated polyglycolyzed glycerides or poly oxy-ethylene-20-oleate (Tween 80), are widely used. It is suggested that self-emulsification occurs when the entropy that favors dispersion is greater than the energy required to increase the surface area of the dispersion. The emulsifying agents, which form monolayers on the droplet surfaces, stabilize the emulsion and provide a barrier to prevent coalescence. Various self-emulsifying formulations exist, including capsules, pellets, powders, and liquids, allowing administration *via* oral, parenteral, or topical routes.[87, 90, 97-99] For example, the bioavailability of the poorly soluble Curcumin, which can act as an anti-inflammatory and antibacterial compound, can be improved with a self-emulsifying formulation (**Figure 7a**). If Curcumin is released from a self-emulsifying drug delivery pellet or liquid, which consists of Capyol 90 and Labrafac PG as oil phase and Labrasol as well as Cremophor EL as a surfactant, the bioavailability in rats is 16-fold higher compared to an unformulated suspension of Curcumin in water (**Figure 7b**).[100, 101]

Moreover, self-emulsifying formulations for several hydrophobic drugs are already commercially available. Novartis, for example, distributes Neoral, a self-emulsifying formulation containing the immunosuppressant cyclosporine A, the antiepileptic drug formulation Convulex is sold by Pharmacia and various HIV 1 antiviral drug formulations is available as soft gelatin self-emulsifying capsules from Roche, Boehringer Ingelheim, GlaxoSmithKline, and Abbott.[87] This shows that lipid-based drug delivery systems like self-emulsifying formulations are major platforms for administering hydrophobic drugs and achieving sufficient bioavailability.
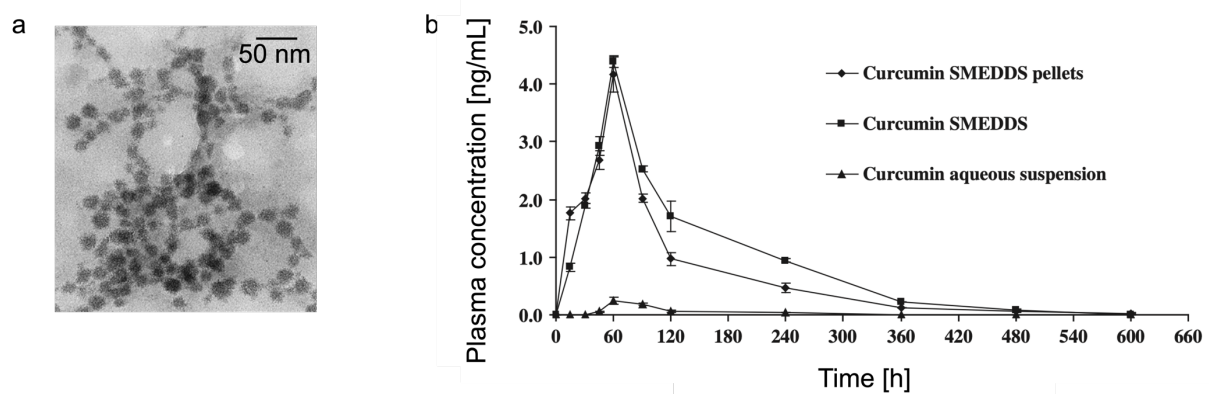
Figure 7: a) TEM image of a curcumin-self-emulsifying formulation. **b)** Plasma drug concentration profile of orally administered curcumin as a self-emulsifying liquid formulation, self-emulsifying pellets, and aqueous suspension (dose 50 mg/kg) to rats. Reprinted from reference [99] by permission from Elsevier Ltd., Copyright © 2010.[101]

1.5 Hydrogels and emulgels as drug delivery platform

Hydrogels have become a popular and important platform for drug delivery and are applied in various clinical settings such as oncology, wound healing, and pain management. Especially their biocompatibility due to the high water content and the physiochemical resemblance to biological tissue makes hydrogels a particularly appealing drug delivery system.[102, 103] Hydrogels are three-dimensional networks of water-soluble polymers, which can be of natural or synthetic origin. Examples of hydrophilic, natural polymers that form hydrogel matrices are agarose, collagen, and chitosan. Synthetic polymers commonly used in hydrogel synthesis are polyethylene glycol (PEG) and polylactide (PLA). The polymer chains are chemically or physically crosslinked to form a hydrogel *via* covalent bonds or hydrogen bonding, hydrophobic and ionic interactions. As a consequence, the hydrogel is resistant to disintegration during swelling in an aqueous environment. The equilibrium swelling level depends mainly on the density of the crosslinks, and the amount of water in the hydrogel determines the absorption, partitioning, and diffusion of solutes through the matrix. Due to the porous structure, drugs can be loaded into the hydrogel matrix and released. As described in Chapter 1.2, the drug release from simple hydrogel matrices is a diffusion-controlled process that follows first-order kinetics, which the cross-linking density can tune.[102-106]

However, modifications of the polymers can give the hydrogel more desirable properties like chemical, biochemical, or physical responsiveness to achieve a controlled drug release. For example, the drug release can be controlled by the swelling behavior of the hydrogel and induced by external stimuli such as temperature, pH, or sensitivity to glucose.[107-113] Hussain *et al.* reported that pH-controlled release of aceclofenac is possible with a stimuli-responsive AV-hydrogel derived from *Artemisia vulgaris* seeds. In an acidic environment (pH 1.2), the pH-responsive carbonyl moieties are not ionized, and thus the hydrogel shows minimal swelling. In contrast, higher pH (pH 7.4), leads to a high electrostatic repulsion of the polymer chains and, therefore, higher swelling due to the complete ionization of the carbonyl groups. As a consequence, the release of incorporated aceclofenac from the hydrogel matrix only reaches between 15.8 and 25.3% in simulated gastric fluid (pH 1.2)[114]. In comparison, between 88.2 and 98.2% could be released in simulated intestinal fluid (pH 6.8)[115] depending on the used formulation. Mimicry of the gastrointestinal tract conditions (pH and transit time) shows that drug release in the stomach could be prevented due to less swelling at low pH. In contrast, high pH in the intestinal tract enables drug release (**Figure 8a**).[116]
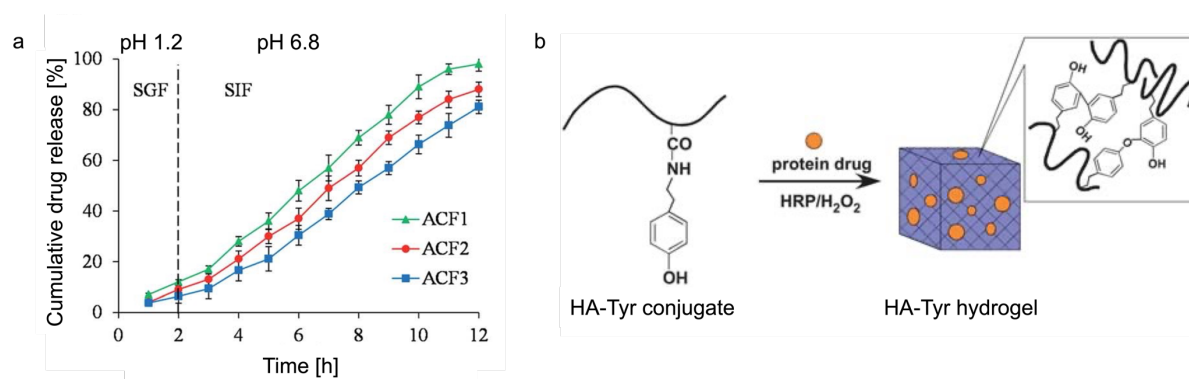
Figure 8: **a)** Cumulative drug release profile of aceclofenac from different AV-hydrogel (*Artemisia vulgaris*) formulations in simulated gastrointestinal fluid. The first 2 hours simulated gastric fluid (pH 1.2), and the remaining 10 hours simulated intestinal fluid (pH 6.8) was used to mimic the gastrointestinal tract. Reprinted from reference [114] by permission from the Royal Society of Chemistry, Copyright © 2020.[116] **b)** *In situ* forming of hyaluronic acid–tyramine hydrogel by enzyme-catalyzed oxidation, which can be used for protein delivery. Reprinted from reference [115] by permission from the Royal Society of Chemistry, Copyright © 2010.[117]

Moreover, biodegradability or dissolution of the hydrogel can be achieved by integrating moieties that are susceptible to enzymatic or hydrolytic cleavage. Additionally, high control over the cross-linking density and, thus the physical properties can result in injectable hydrogels.[118] For example, a hyaluronic acid–tyramine (HA–Tyr) hydrogel can be formed *in situ* by an enzyme-catalyzed oxidation reaction (**Figure 8b**). The liquid precursors can be

injected and form a hydrogel at the target location. The hydrogel network can incorporate and release protein drugs and even protect these proteins from degradation. Thus, hydrogels are efficient platforms to overcome the challenges of protein drug delivery, namely poor stability, short half-life, and rapid proteolysis.[117, 119-123] Furthermore, biodegradable, injectable hydrogels can significantly enhance patient compliance because surgical procedures are not necessary to administer or recover the formulation.[103, 118] Besides as a drug delivery system, hydrogels are also applied as wound dressings or in tissue engineering.[117, 124]

Another emerging drug delivery platform are emulgels, consisting of an oil-in-water or water-in-oil emulsion and a gelling agent. These formulations possess the advantages of emulsions and hydrogels, such as increasing the bioavailability of hydrophobic drugs, protecting protein drugs, and having high biocompatibility. Furthermore, physiochemical properties like the mechanical strength, porosity, and release profile of the emulgel can be controlled. Emulgels are already widely applied, especially as topical drug delivery systems to treat skin diseases or to relieve muscle pain. A commercially available example is the analgesic gel Voltaren, which contains diclofenac as a therapeutic agent.[125-127] The most common route to prepare an emulgel formulation is the emulsification of the oil- and aqueous phase, including the active compound's incorporation, followed by gellification with the gelling agent (**Figure 9a**). Alginate, chitosan, poly(vinyl alcohol), and poly-2-hydroxyethyl methacrylate are often used as the hydrogel component to entrap various oils like mineral, castor, or vegetable oils. Hydrophobic active compounds can partition into the oil phase and thus be incorporated into the emulgel.[125, 127-133] For example, a genipin-cross-linked chitosan hydrogel containing an emulsion of isopropyl myristate can be used to release the poorly water-soluble curcumin (CR) or Nile red (NR) over a period of 10 hours under physiological conditions (**Figure 9b**). It is suggested that the release of curcumin and Nile red is influenced by the crosslinking density, meaning faster release from hydrogels with higher crosslinking density (cross-linked at pH 5.5). Like the release kinetics of drugs from hydrogels, the release of the active agent from an emulgel is a diffusion-controlled and thus, first-order release.[130]
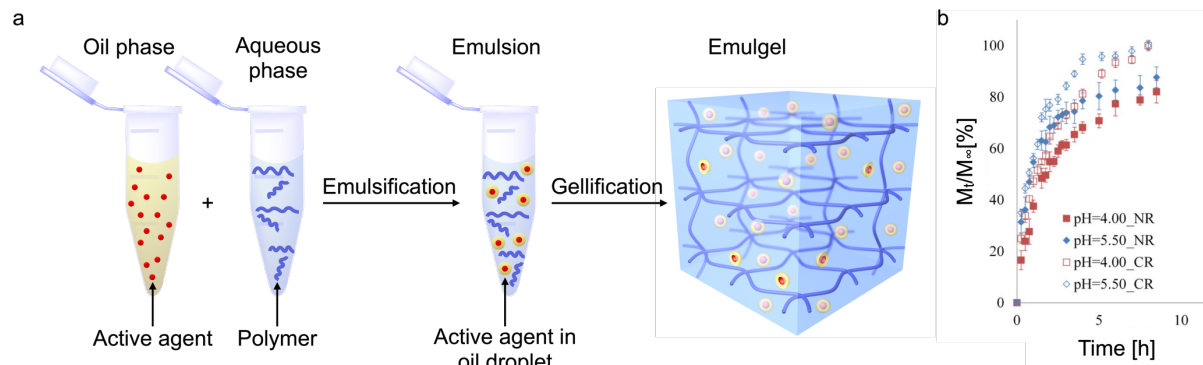
Figure 9: a) Scheme of the preparation of an emulgel. First, the drug is dissolved in the oil phase and the hydrogel-forming polymer is dissolved in the aqueous phase. After emulsification of the oil- and aqueous phase to form the emulsion, the gellification of the polymer is induced to form the final emulgel. **b)** Normalized drug release profile in PBS from genipin-cross-linked chitosan hydrogels crosslinked at pH 4.0 or pH 5.5 that contain an emulsion of isopropyl myristate which is loaded with 0.1 mg/ml Nile red (NR) or 0.4 mg/ml curcumin (CR). Reprinted from reference [128] by permission from Elsevier Ltd., Copyright © 2016.[130]

1.6 Self-protection and zero-order hydrolysis

As Chapter 1.4 described, emulsions and self-emulsifying systems that are stabilized with surfactants, are inert platforms that can be used to deliver especially hydrophobic drugs. In addition to these unreactive oil-in-water emulsions, we can design transient emulsions. Here, the oil droplets have a tunable lifetime and therefore are promising drug delivery platforms.[134-137]

Wanzke *et al.* designed a transient emulsion whose properties are regulated by a chemical reaction cycle. The precursor molecule is converted into a metastable product by the consumption of a carbodiimide fuel (**Figure 10a**). First, the activation reaction of the precursor, a carboxylic acid that is soluble in aqueous solution, irreversibly consumes the fuel (1-ethyl-3-(3-dimethylaminopropyl)carbodiimide (EDC)) and forms a reactive O-acyl urea intermediate. The intermediate reacts with a second intramolecular acid moiety and forms the corresponding anhydride. This activated product is less soluble than the precursor and thus phase-separates into droplets. The anhydride is intrinsically unstable in aqueous solution and spontaneously deactivates *via* hydrolysis. This second chemical deactivation reaction reverts the activated product back to the precursor. Put differently, the emulsion emerges upon fuel addition and can only be maintained with continuous fuel application. When the fuel is fully depleted, the

droplets in this emulsion decay. As a consequence, the so-called active emulsion has a limited lifetime.[136-138]
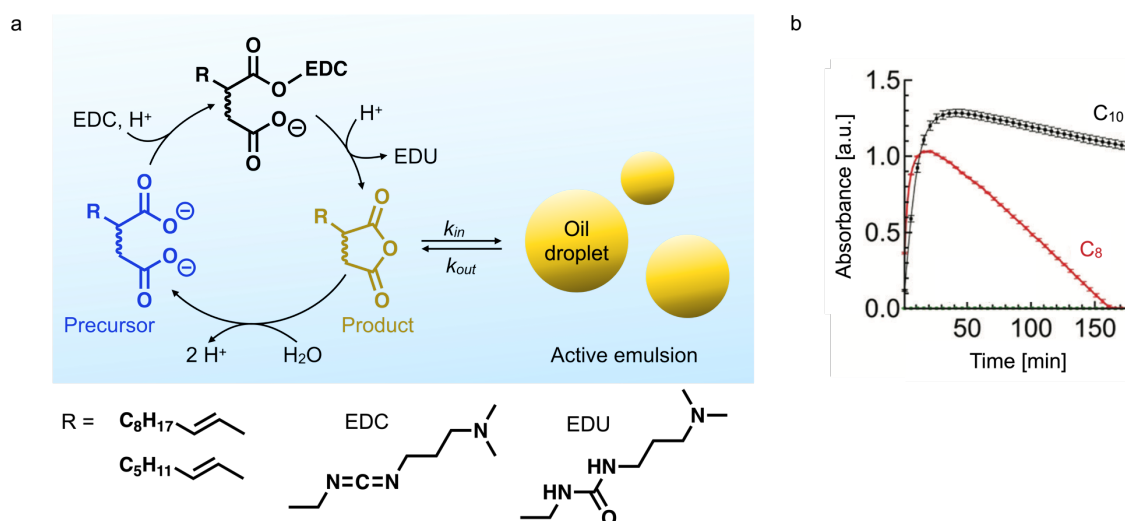
Figure 10: **a)** Scheme of a chemical reaction with a water-soluble carboxylic acid as precursor. The precursor is activated with EDC fuel to form a reactive intermediate which reacts to the activated product. The hydrophobic product can self-assemble into oil droplets and upon hydrolysis reverts back to the original precursor. **b)** Measured absorbance at 500 nm over time from a solution containing 10 mM C_8 acid or 7.5 mM C_{10} acid. Upon EDC addition (10 mM and 7.5 mM, respectively), the absorbance increases indicating the presence of oil droplets. Reprinted from reference [134] by permission from the Royal Society of Chemistry, Copyright © 2020.[136]

Derivatives of succinic acid that contain an unsaturated hydrophobic tail can be used in this reaction cycle, *i.e.,* 2-decen-1-ylsuccinc acid (C_{10} acid) or 2-octen-1-ylsuccinic acid (C_8 acid). The addition of EDC to a C_8 acid solution or C_{10} acid solution, respectively, immediately turned the transparent solution turbid which showed the formation of an emulsion (**Figure 10b**). The measured lifetime of the C_{10} emulsion is 20 hours, approximately 10 times longer than the lifetime of a C_8 emulsion (2 hours). Interestingly, the oil droplets hydrolyze linearly due to the so-called "self-protection" mechanism. Due to anhydride's ability to phase-separate, the major anhydride fraction is physically isolated from the aqueous phase and, therefore, not susceptible to hydrolysis. Thus, hydrolysis can only occur on the fraction of anhydride that remains in the solution, equal to its solubility. Consequently, the hydrolysis rate (v) equals the hydrolysis rate constant (k) multiplied by the anhydride's solubility, which is constant in the presence of oil droplets. This means that the hydrolysis follows zero-order kinetics. Furthermore, the different lifetimes of the C_8 and the C_{10} emulsion can be explained by the "self-protection" mechanism as well. The C_8 anhydride with a solubility of 0.3 mM hydrolyzes

an order of magnitude faster than the C_{10} anhydride with a solubility of 0.03 mM. Thus, the higher the solubility of an anhydride, the faster the hydrolysis.[136, 139]

Moreover, Wanzke *et al.* showed that hydrophobic drugs such as nitrendipine or nimesulide partitioned into the active oil droplets of the emulsion. To immobilize the drug-loaded emulsion, it was embedded in an agar gel. This emulgel was then covered with an aqueous supernatant (2-(N-morpholino) ethane sulfonic acid (MES) buffer, pH 6) and the drug concentration was measured in the supernatant over time. The release of the drug from the active emulsion followed the zero-order hydrolysis kinetics of the anhydride. For example, an active C_{10} emulsion that is loaded with nimesulide achieved a linear drug release over 15 hours (**Figure 11a**). In contrast, the release profile of nimesulide just with C_{10} acid but without the addition of EDC fuel follows first-order kinetics. Furthermore, the amount of the added EDC fuel determines the lifetime of the active emulsion and thus the period of the drug release can be tuned. Meaning the more fuel is available, the longer the oil droplets can be sustained. As a consequence, the t_{50}, the time when half of the initial drug concentration is released, increases (**Figure 11b**). Besides the release period, the release rate of the drug can be tuned by the initial EDC fuel concentration as well. Here a lower initial fuel concentration leads to a higher release rate (**Figure 11c**). For example, the release of nimesulide changed from 2.0 µM/h (5.0 mM EDC) to 0.5 µM/h (20 mM EDC).[136]
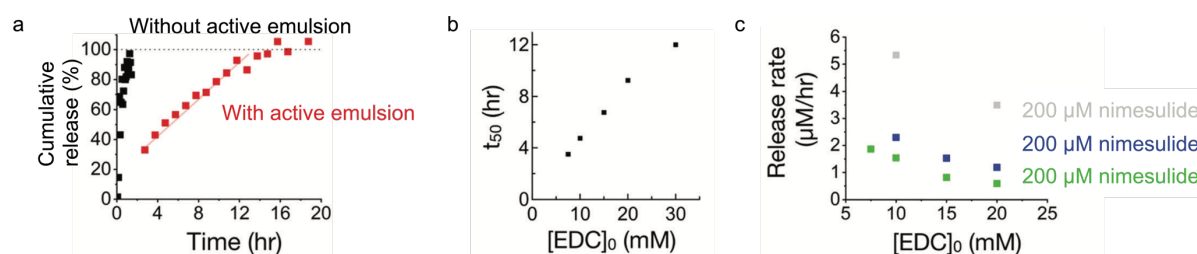
Figure 11: a) Cumulative release of 50.0 µM nimesulide from an agar gel and from an active emulgel comprising agar gel and an emulsion formed by 7.5 mM C_{10} acid and 10 mM EDC. **b)** t_{50}, the time after which 50% (25 mM) nimesulide was released, plotted against the initial EDC concentration used to generate the active C_{10} emulsion. **c)** Release rate of nimesulide in the zero-order regime plotted against initial concentration EDC used to generate the active C_{10} emulsion. Different initial drug concentrations were used.[136]

The linear and tunable release of hydrophobic drugs makes this system a promising candidate as a drug delivery system. As described in Chapter 1.3, zero-order drug delivery systems can positively impact the effectiveness of therapies and patient compliance since they can keep a constant plasma drug concentration and require less frequent administration. However, the biocompatibility of this drug delivery platform is rather low due to the toxicity of the EDC fuel.[140]

Moreover, the *in situ* generation of the active emulsion leads to a complicated and impractical formulation of this system and the platform cannot be stored. This might hurt manufacturing and patient compliance. Additionally, the range of the hydrophobic agents that can be released with this platform is limited to nimesulide and nitrendipine. Other hydrophobic drugs like Acyclovir can only be released with first-order kinetics. This shows that the mechanism of the drug release is not fully understood yet, and a method to predict which hydrophobic compounds can be successfully released with zero-order kinetics is still missing. Overall, the zero-order drug delivery platform based on active emulsions is promising but requires further investigation and optimization.

1.7 Conclusion and Outlook

Great progress has been made in the development of new drug delivery systems. Especially zero-order drug release platforms optimize not only the efficiency and safety of therapies but they also improve patient compliance by achieving a close to constant drug release over long periods. Furthermore, emulsions and emulgels facilitate the delivery of hydrophobic drugs. However, major drawbacks of existing systems, such as high manufacturing costs, narrow their application in clinical settings. Thus, new zero-order drug delivery platforms that are cheap, versatile, and easy to use must be developed.

2 Aim of the Thesis

As outlined in the previous chapter, a major part of pharmaceutical research is developing new and optimizing existing drug delivery platforms. Especially systems that release their active agent with zero-order kinetics became a recent research focus, and several such platforms have been developed. However, the major drawbacks of these systems, discussed in Chapter 1.3, limit their application. One promising platform that has the potential to overcome these limitations is in Chapter 1.6 described active emulgel formulation. The first results of Wanzke *et al.* have already shown the successful zero-order release of the hydrophobic drugs nitrendipine and nimesulide. However, this formulation has still several drawbacks, which are low biocompatibility, complicated preparation of the formulation, no storage possibility, and a limited drug range. Moreover, this system has only been tested in 2-(N-morpholino) ethane sulfonic acid (MES) buffer at pH 6, which is far from physiological conditions. Lastly, the toxicity of the individual compounds of the formulation has not been examined yet.

In light of these insights, this thesis's overreaching goal was optimizing the previously described active emulgel formulation. To ensure the safety and low toxicity of the formulation, the first aim of this work was to improve the system's biocompatibility. Therefore, Chapter 3 focused on obviating the need for a toxic fuel by removing the activation reaction of the chemical reaction cycle. As a consequence, a new, suitable method to generate oil droplets with a sufficient size needed to be established. Furthermore, I aimed to develop a procedure to store the formulation over a long period without changing the release kinetics to guarantee uninterrupted logistics and patient compliance. Another aim of this thesis was to better understand the drug release mechanism. Understanding the underlying processes is important to ensure the platform's predictability and select suitable active compounds.

Next, I explored the versatility of the emulgel drug delivery system in Chapter 4. This chapter aimed to broaden the range of releasable active compounds from hydrophobic drugs to oligonucleotide-based drugs. Moreover, I aimed to combine the release of hydrophobic drugs and oligonucleotide-based drugs, namely cholesterol-conjugated DNA strands, in a dual-release system. Finally, I demonstrated the platform's functionality and the DNA release by using this system to induce the disassembly of gold nanoparticles *via* toehold-mediated strand displacement.

The aim of Chapter 5 was to examine the emulgel system under biorelevant conditions. This includes not only the pH and the temperature but also the physiochemical environment. Thus, I examined the drug release kinetics of the system in the presence of proteins, enzymes, amino acids, and other biological molecules.

Finally, in Chapter 6 I extended the scope of hydrolyzable oils that can be utilized in the drug delivery platform. Here I focused on hydrophobic orthoester and boronic ester compounds, which are less electrophilic and thus more stable in amine-containing media than the hydrophobic anhydrides used in the previous chapters.

In conclusion, this thesis aims to optimize an existing emulgel drug delivery system that releases hydrophobic drugs with zero-order kinetics and investigate the underlying release mechanism. Moreover, I aim to increase the system's versatility by broadening the spectrum of suitable active compounds. Finally, the thesis aims to investigate alternative emulsions that can achieve zero-order drug release.

3 Emulsions of Hydrolyzable Oils for the Zero-Order Release of Hydrophobic Drugs

Abstract

In this work, we optimized the in Chapter 1.6 introduced drug delivery system that can release hydrophobic drugs following zero-order kinetics. This system is based on active oil droplets formed during a carbodiimide-fueled chemical reaction cycle. However, due to the cell toxicity of the fuel, this platform has a low biocompatibility. Furthermore, this formulation has to be prepared *in situ* and cannot be stored. In this chapter, we advanced the existing platform by simplifying the formulation. Our new platform only comprises hydrolyzable oil droplets entrapped in a hydrogel. The oil droplets can incorporate a broad range of hydrophobic drugs, which can be released between three and 50 hours linearly, depending on the initial oil concentration. The drug release rate can be adjusted by varying the initial drug concentration. Furthermore, we can predict the release kinetics of hydrophobic drugs by determining the drug's partition coefficient between the oil and the aqueous phase. Moreover, in this work, we developed a procedure to store the drug delivery formulation at -20°C and demonstrated its biocompatibility. Through these improvements, our emulgel-based drug delivery formulation is a simple, versatile, and cheap platform for the zero-order release of hydrophobic drugs.

This work has been published:

This section states the individual work of each author in the publication above. J. Boekhoven, O. Lieleg, L. Tebcharani, and C. Wanzke designed the experiments. L. Tebcharani and J. Rodon-Fores carried out the experiments. T. Lutz carried out the cell viability studies. L. Tebcharani and J. Boekhoven wrote the manuscript. All authors have given approval to the final version of the manuscript.

Emulsions of hydrolyzable oils for the zero-order release of hydrophobic drugs

Laura Tebcharani [a], Caren Wanzke [a], Theresa M. Lutz [b], Jennifer Rodon-Fores [a], Oliver Lieleg [b], Job Boekhoven [a,*]

[a] Department of Chemistry, Technical University of Munich, Lichtenbergstrasse 4, 85748 Garching, Germany
[b] Center for Protein Assemblies (CPA), Technical University of Munich, Ernst-Otto-Fischer Straße 8, 85748 Garching, Germany

ARTICLE INFO

ABSTRACT

Drug delivery systems that release hydrophobic drugs with zero-order kinetics remain rare and are often complicated to use. In this work, we present a gellified emulsion (emulgel) that comprises oil droplets of a hydrolyzable oil entrapped in a hydrogel. In the oil, we incorporate various hydrophobic drugs and, because the oil hydrolyzes with zero-order kinetics, the release of the drugs is also linear. We tune the release period from three hours to 50 h by varying the initial oil concentration. We show that the release rate is tunable by varying the initial drug concentration. Our quantitative understanding of the system allows for predicting the drug release kinetics once the drug's partition coefficient between the oil and the aqueous phase is known. Finally, we show that our drug delivery system is fully functional after storing it at −20 °C. Cell viability studies show that the hydrolyzable oil and its hydrolysis product are non-toxic under the employed conditions. With its simplicity and versatility, our system is a promising platform for the zero-order release of the drug.

1. Introduction

Conventional drug delivery systems, like hydrogels, emulsions, and emulgels typically deliver their payload with first-order kinetics. Thus, these carriers release their encapsulated drug in a "fast-then-slow" manner, leading to an initial stage with a high plasma drug level, followed by a low plasma drug concentration that may be too low to achieve therapeutic effects. Consequently, these platforms require repeated administration and high dosages to stay within the desired therapeutic window, resulting in poor patient compliance [1–5]. To enhance the effectiveness systems have been developed that regulate drug release, *e.g.*, by sustaining the drug release with matrix tablets, hydrogels, or other release platforms [4,6–10]. Although the release is sustained, it typically remains a diffusion-controlled first-order process following Highuchi's kinetics [1,4,11–14]. In contrast to the above-mentioned examples, drug delivery platforms exist that release their contents with zero-order kinetics, *i.e.*, at a constant rate which does not depend on the amount released. These platforms can result in a desirable constant plasma drug concentration during the entire release period [12,13,15,16]. However, finding systems that achieve such zero-order release remains challenging. Typical examples only work in a limited set of conditions, are complicated to fabricate, and are typically expensive [12,14,15,17–20]. Another challenge is the administration of hydrophobic drugs belonging to the Biopharmaceutics Classification System (BCS) class II, which include Nimesulide, Nitrendipine, and Mebendazole. Drugs in this class are characterized by poor *in vitro* solubility and a high *in vivo* permeability [21]. Due to the low solubility in water, BCS class II drugs have poor bioavailability. These reasons make it difficult to deliver these drugs at a therapeutic level, especially by oral administration [1,2,11].

Emulgels are a promising platform for the release of hydrophobic drugs. These release systems possess the advantages of emulsions as well as hydrogels [21]. Oil-in-water emulsions are known for increasing the water solubility of hydrophobic drugs and thus improving their bioavailability [22–24]. By incorporating the hydrophobic molecules, the oil phase can be used to protect the drugs from premature degradation and precipitation [22,23,25]. Furthermore, hydrogels generally have high biocompatibility due to the high water-content and the physiochemical resemblance to biological tissue. Hydrogels are relatively cheap and are already successfully used for applications such as tissue engineering and drug delivery [14,26–28]. Due to these unique properties, emulgels are emerging drug carriers for hydrophobic drugs,

for example, in topical drug administration [21,29]. However, there are only a few examples of hydrogels that achieve zero-order release [14,17,30,31].

Recently we found that anhydrides that form oil droplets can hydrolyze with zero-order kinetics due to a self-protection mechanism [32,33]. These droplets can be loaded with hydrophobic molecules and loaded into a hydrogel to form a so-called "active emulgel". As the anhydride hydrolyzes with zero-order kinetics, the droplet's total volume also decays with zero-order kinetics. Thus, the active emulgel releases its hydrophobic contents with zero-order kinetics. However, the previously described platform is toxic because we generated the active droplets *in situ* by using 1-ethyl-3-(3-dimethylaminopropyl)carbodiimide [34]. Moreover, the release platform was complicated and impractical to formulate, could not be stored, and showed a limited scope of hydrophobic molecules that could be released. In this work, we simplified the formulation of the drug delivery system. Furthermore, we expanded the scope of the hydrophobic drugs that can be delivered and found a parameter predicting which drugs can be released linearly. Additionally, we examined the drug release under physiological conditions and optimized the formulation so that the platform can be stored. Taken together, we describe the formulation of a drug delivery vehicle that predictably releases a variety of hydrophobic drugs with zero-order kinetics that can be stored and of which the release rate is tunable.

2. Results and discussion

The zero-order release of the drug deliver delivery system we introduce here is based on two components. Firstly, a hydrogel that releases drugs through first-order kinetics into its surrounding medium. Secondly, oil droplets of a hydrolyze oil that hydrolyzes with zero-order kinetics. When these oil-droplets are embedded in the hydrogel, the drug partitions between the oil phase and the aqueous phase, *i.e.*, the hydrogel and the supernatant. Thus, drug with a high partitioning coefficient for the oil, will have a low concentration in the aqueous phase low. As the oil is hydrolyzing with zero-order kinetics, the decreasing oil phase will increase the concentration of the drug in the aqueous phase.

As hydrolyzable oil, we tested two hydrophobic aliphatic anhydrides (Fig. 1a), *i.e.*, C_7C_7 (heptanoic anhydride) and C_{10} (2-decen-1-yl succinic anhydride). These oils have a unique property in that they hydrolyze with zero-order kinetics (Fig. 1b). Due to their ability to phase separate, the major fraction of the oil is physically separated from the water phase, and therefore not susceptible to hydrolysis. Therefore, hydrolysis occurs on the fraction of the oil molecules that remain in the aqueous phase, which is constant and equal to the oil's solubility. The hydrolysis rate is thus equal to the anhydride's rate constant for hydrolysis multiplied by its solubility which is constant as long as droplets are present. We anticipate that the drug molecules that partition in those oil droplets are released with constant kinetics too.
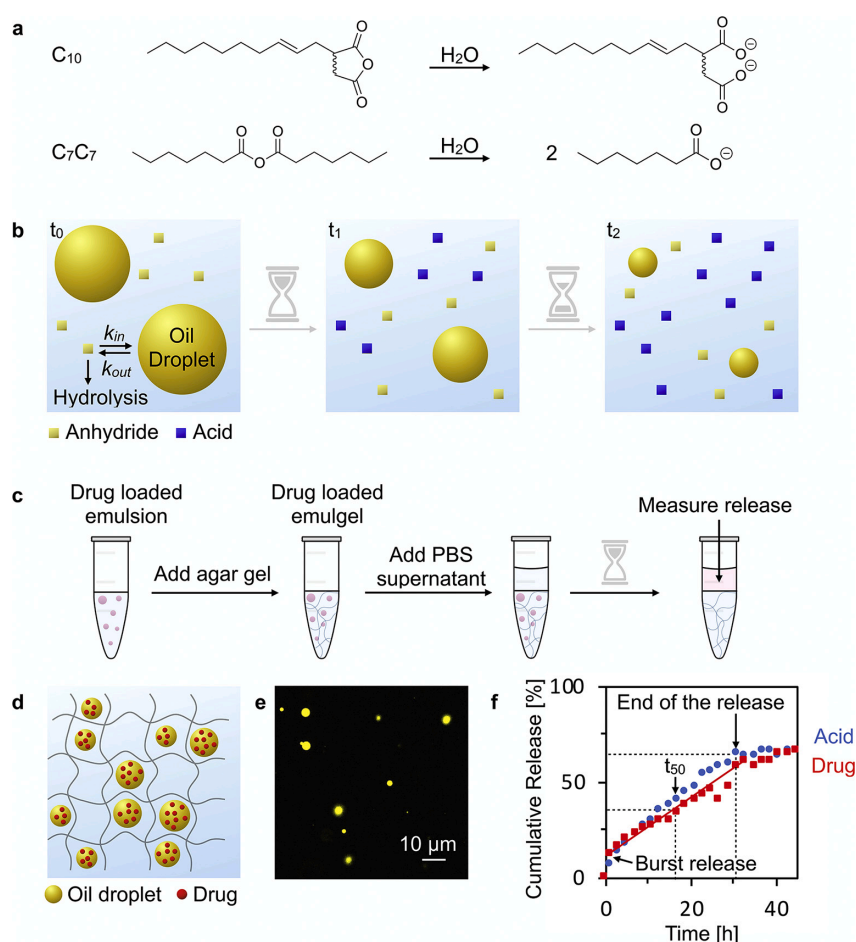
Fig. 1. Composition and release profile of the drug delivery platform. a) Molecular structures of C_{10} and C_7C_7 anhydrides and their corresponding hydrolysis products. b) Phase separation of the anhydride into oil droplets protects it from hydrolysis. Self-protection of the droplets results in a linear decay over time. c) Scheme of the emulgel preparation. The drug-loaded emulsion is gellified by mixing it with agar gel, and, subsequently, the emulgel is covered with PBS. The drug and hydrolysis product release is measured in the supernatant. d) Scheme of an emulgel. The oil droplets are embedded in a hydrogel and loaded with a hydrophobic drug. e) Microscope image of the active emulgel comprising of 3.75 mM C_7C_7, 25.00 µM Nitrendipine and 5 µM Nile red trapped in the 1%-agar gel. f) Cumulative release of 25.00 µM Nitrendipine from a C_7C_7 (3.75 mM) emulgel in 1%-agar gel over 45 h under physiological conditions. (For interpretation of the references to color in this figure legend, the reader is referred to the web version of this article.)

To test the emulgels based on hydrolyzable oils, we sonicated the neat anhydride-based oil and a hydrophobic drug in phosphate-buffered saline (PBS) with a pH of 7.4 (Fig. 1c). Next, the emulsion was gellified by mixing it with an agar gel which yielded a turbid hydrogel loaded with the droplets (Fig. 1d). Confocal microscopy confirmed the presence of the droplets (Fig. 1e). The final composition of the emulgel comprised 1% agar, typically between 2.50 and 7.50 mM of the hydrolyzable oil, and between 12.50 and 100.00 µM of the drug. This means 60 µL of the emulgel, that volume was used for all experiments, contains between 35.70 µg and 107.20 µg hydrolyzable oil and between 169.00 ng and 4.30 µg drug. In the following text the hydrolyzable oil and the drug concentration describes the initial concentration in the emulgel without supernatant. The drug concentration that is measured in the supernatant overtime is not equal to the initial concentration and depends on the supernatant volume. For describing the amount of released drug, we use the cumulative release in percent.

When we incorporated the hydrophobic drug Nitrendipine into this formulation, it showed a linear drug-release profile under physiological conditions (PBS, 37 °C). Specifically, we prepared an emulgel loaded with a final composition of 25.00 µM Nitrendipine in 3.75 mM C_7C_7 and covered it with phosphate-buffered saline (PBS) as supernatant (Fig. 1f). This means 60 µL of the prepared emulgel contains 504.54 ng Nitrendipine and 54.53 µg C_7C_7. We measured the release of the hydrolysis product, *i.e.,* heptanoic acid and Nitrendipine, by analyzing their concentrations in the supernatant by high-performance liquid chromatography (HPLC) (Fig. 1c). We found roughly 70% of the heptanoic acid and Nitrendipine was released after 30 h, after which their concentrations plateaued. Such incomplete release is typical for hydrogel-based formulations [22,35–38]. Roughly 15% of the drug was released in the first hour, *i.e.*, a so-called burst release. Excitingly, after the burst release of the drug, the remainder was released with linear kinetics. We can calculate a drug delivery half-life (t_{50}), *i.e.*, the time point at which 50% of the plateau-value of drugs is released, of 17 h. To examine if the oil droplets are immobilized in the hydrogel, we monitored the drug release experiments of a C_{10} emulgel loaded with Nitrendipine over time (Fig. S1a). The time-lapse video of the experiments shows, that the turbid emulgel slowly becomes transparent while the supernatant is transparent over the whole release period. Additional turbidity measurements have been added to highlight the linear decrease of the turbidity over time (Fig. S1b). This indicates that the oil droplets stay immobilized in the gel and do not diffuse into the supernatant. We can confirm that no hydrolysable oil droplets diffuse into the supernatant by HPLC (Fig. S1c). The HPLC chromatogram shows only a signal for the drug and the C_{10} and C_7C_7 acid, respectively, but no signal for the hydrolysable oils.

From the dataset above, it becomes clear that the release of Nitrendipine and the hydrolysis of the oil are tightly connected. As the volume of the oil droplet is decreasing, the concentration of Nitrendipine in the aqueous environment has to increase provided that the partitioning constant (P) is constant. P in this context describes the distribution of the hydrophobic Nitrendipine between the immiscible aqueous and oil phase (Eq. (1)). Thus, we determined the partitioning coefficient of Nitrendipine in the above-described experiment for several time points in the release trace and found that it is mostly constant (Fig. S2g). Furthermore, we found that the average $logP_{average}$ values were similar and constant when different hydrolyzable oil concentrations were used (Fig. S2h).

$$P = \frac{c(drug)_{oil}}{c(drug)_{aq}} \tag{1}$$

Definition of the partition coefficient P with $c(drug)_{oil}$ as drug concentration in the hydrolyzable oil droplets and $c(drug)_{aq}$ as drug concentration in the aqueous buffer phase.

Excited about the constant release of the drug from the platform, we tested the tunability of the system. Specifically, we varied the initial concentration of the hydrolyzable oil in our emulgels while keeping the initial concentration of Nitrendipine in the emulgel constant and tested how it affected the time after which half of the releasable drug was released (t_{50}) (Fig. 2a). The lowest t_{50} we measured was 8.0 ± 0.1 h (2.50 mM C_7C_7), whereas the longest half-life we found was 23 ± 2.5 h (4.50 mM C_7C_7). To demonstrate the versatility, we performed similar experiments using a different hydrolyzable oil (C_{10}), which also showed a linear release. Its t_{50} ranged from 1.5 ± 0.1 (2.50 mM C_{10}) to 6.5 ± 0.2 h (7.50 mM C_{10}). The combined dataset implies that we can tune the timepoint at which 50% of Nitrendipine is released from 1.5 ± 0.1 h to 23 ± 2.5 h by just changing the initial concentration of the hydrolyzable oil in the emulgel. Noteworthy, all experiments showed linear release over most of the release period (Fig. S3).

Since the initial concentration of the hydrolyzable oil in the emulgel determines the rate at which the drug is released, we assumed that the initial drug concentration in the emulgel and the drug release rate scale linearly too. To test this relation, we chose a formulation with a t_{50} of 1.5 h (2.50 mM C_{10}) and varied the initial concentration of Nitrendipine in the emulgel from 12.50 to 100.00 µM (Fig. 2b), meaning that 60 µL of the emulgel contain between 270.27 ng and 2.16 µg Nitrendipine and 35.70 µg C_{10} initially. Indeed, t_{50} was 1.5 ± 0.1 h in each experiment, but the drug release rate varied depending on the loading. For the lowest loading, we found a release rate of 5.6 ± 0.4 ng/h. Indeed, when we quadrupled the initial drug concentration in the system, the release rate also roughly quadrupled. To examine if the volume of the supernatant influences the release rate, we determined the release rate of an emulgel (60 µL) containing an initial concentration of 5.00 mM C_{10} and 25.00 µM Nitrendipine with supernatant volumes between 120 and 48 µL (Table S1). We found that the release rates are similar and thus the supernatant volume has no influence on the drug release rate.

From the linear relations, we can create a formulation chart (Fig. 2c). Such a chart is effectively a 3D plot from which the user can read the initial concentration of hydrolyzable oil and drug in the emulgel required to obtain a formulation with a desired t_{50} and drug release rate. For example, if a t_{50} of 6.5 h in which Nitrendipine is released with a constant rate of 8.4 ng/h is required, the chart shows that 5.00 mM hydrolyzable oil and 75.00 µM Nitrendipine are required in an emulgel formulation with 60 µL emulgel.

To explore the versatility of the zero-order drug delivery system, we tested the release of different hydrophobic BCS class ɪɪ drugs with a C_{10}-emulgel (5.00 mM C_{10}). We found three types of behaviors in the release profiles:

(1) the drug was released with a small (5–10%) burst and then continue with linear kinetics as desired until all hydrolyzable oil was hydrolyzed, or.

(2) the drug was released with a large (~50%) burst and continued with linear kinetics until all hydrolyzable oil was hydrolyzed, or.

(3) the drug was released with a large (~50%) burst and continued with first-order kinetics until it plateaued.

The desired zero-order release with a small burst was observed for the antiretroviral drug Ritonavir, the antihelminthic drug Mebendazole, and the calcium-channel blocker Nitrendipine (Fig. 3a and S4a, respectively). Nimesulide followed profile 2, *i.e.*, a linear release after a 50% burst (Fig. 3a). Finally, Acyclovir and Piroxicam showed first-order kinetics (Fig. 3a and S4e, respectively). In contrast, all drugs are fully released after 2–3 h with first-order kinetics when no hydrolyzable oil droplets were used (Fig. S4a–f).

To explain the varying release profiles between the drugs, we determined the logP of each drug with C_{10} as oil. We also determined the order of the release kinetics of the drugs by fitting the experimental data with Eq. (2) (Fig. S5a–f). In this equation, when $n = 1$, the drug release follows zero-order kinetics. However, if $n = 0.5$, the release follows first-order kinetics, and if $n \neq 1$, the drug is released by an anomalous mechanism [39]. When the exponent n is plotted against $logP_{average}$, a

31
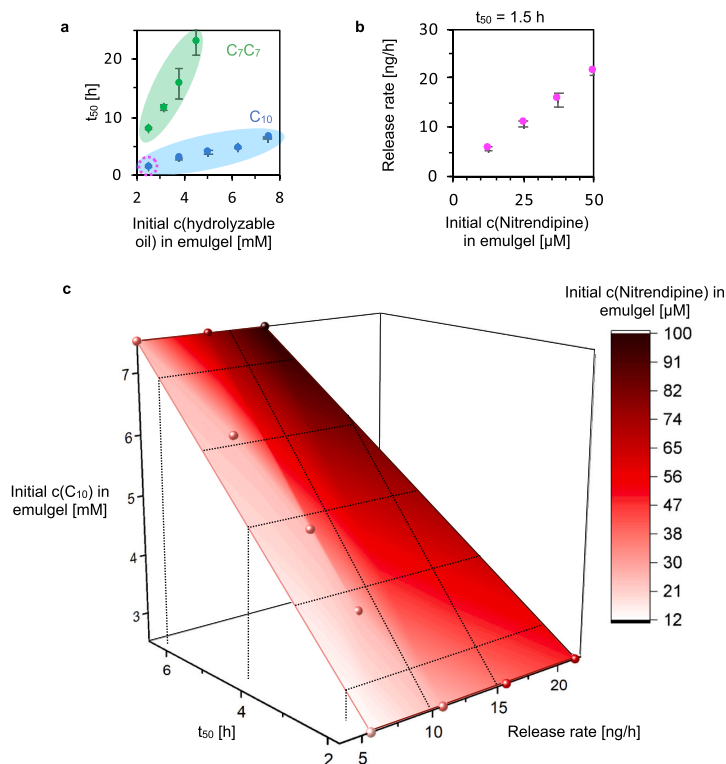
Fig. 2. The tunability of the drug release period and rate. a) t_{50}, the time until 50% of the drug is released, increases with higher C_{10} and C_7C_7 anhydride concentration, respectively. b) The release rate of Nitrendipine by an emulgel containing 2.50 mM C_{10} increases with higher initial Nitrendipine concentrations. c) 3D plot of t_{50}, the release rate, and the initial hydrolyzable oil concentration. The color of the plane corresponds to the initial Nitrendipine concentration in the emulgel.

trend emerges that shows Fig. 3b. We found that when logP was greater than 3.3, the drug partitions into the oil droplets sufficiently such that the release kinetics follow the hydrolysis kinetics of the hydrolyzable oil resulting in desirable zero-order kinetics ($n = 1$, Fig. 3b). A lower logP could still result in a linear release trace (*e.g.,* logP = 3.19 for Nimesulide), but this would also yield a high burst release ($n \neq 1$, Fig. 3b). Finally, when logP was lower than 2.84, first-order kinetics were found ($n = 0.5$, Fig. 3b).

$$c(drug)_{released} = k \bullet t^n + b \qquad (2)$$

c(drug)$_{released}$ is the measured drug concentration in the supernatant (120 µL PBS), k is the release constant, t is the time, n is an exponent characteristic of the mode of transport and b is the concentration of the burst release [39].

With our increased understanding of the zero-order release system, we examined how our system performs under closer to physiological conditions. The human body is not a stationary system. Instead, the fluids around an implanted device are replenished. We thus tested the effect of fluid exchange on our platform. Thus, we simulated the replenishments of the bodily fluids by replenishing the supernatant on top of the emulgel, *i.e.*, the supernatant is removed every hour and replaced by fresh supernatant (Fig. 4a). The cumulative release trace of Nitrendipine from a C_{10} emulgel showed that the fluid replenishment does not influence the release kinetics of the drug (Fig. 4b). We assume that as long as the hydrolysis rate of the hydrolyzable oil molecules in solution is faster than the replenishment rate, the release kinetics are not influenced. Furthermore, we examined the pH of the supernatant over the

whole release period. If the supernatant was not replenished, the pH was decreasing from 7.4 to 6.8 and when the supernatant was replenished, the pH was constant between 7.4 and 7.2 (Table S2). Since both experiments show the same release profile, we conclude that pH fluctuations between pH 7.4 and 6.8 have no influence on the release kinetics.

Moreover, toxicity studies showed that the C_7C_7 anhydride and its corresponding hydrolysis product, C_7 acid, had IC$_{50}$ values of 83.38 mM and 24.47 mM, respectively. These concentrations are far above the maximum concentrations used 2.50 mM C_7C_7 and 4.50 mM C_7 acid used in our experiments. The C_{10} anhydride and its hydrolysis product were more toxic with IC$_{50}$ = 3.31 mM and IC$_{50}$ = 2.46 mM, respectively (Fig. S6c–d). Furthermore, the biocompatibility of the emulgel itself was studied by directly incubating the emulgels containing C_{10} or C_7C_7, respectively, with human epithelial cells (HeLa) (Fig. S6 e–f). The latter experiments demonstrate that C_7C_7 is the preferred hydrolyzable oil from a biocompatibility point of view. At this point, we would like to emphasize that HeLa cells are selected as model cell line to study cytotoxicity of the drug particles *in vitro*. These cells are simple to use in the laboratory, well researched and mainly applied for studies with drug particles. Furthermore, possible applications for our system would be the coating of medical devices, *i.e.*, catheters and hydrogel patches, so human epithelial cells (HeLa) mimic the biological environments for these applications [40,41].

To improve user-friendliness of the material, we examined if the drug delivery system could be stored. The goal here is to demonstrate that ta formulation can be prepared far before usage. A C_7C_7-emulgel (3.75 mM) loaded with 25.00 µM Nitrendipine was prepared and snap-frozen

32
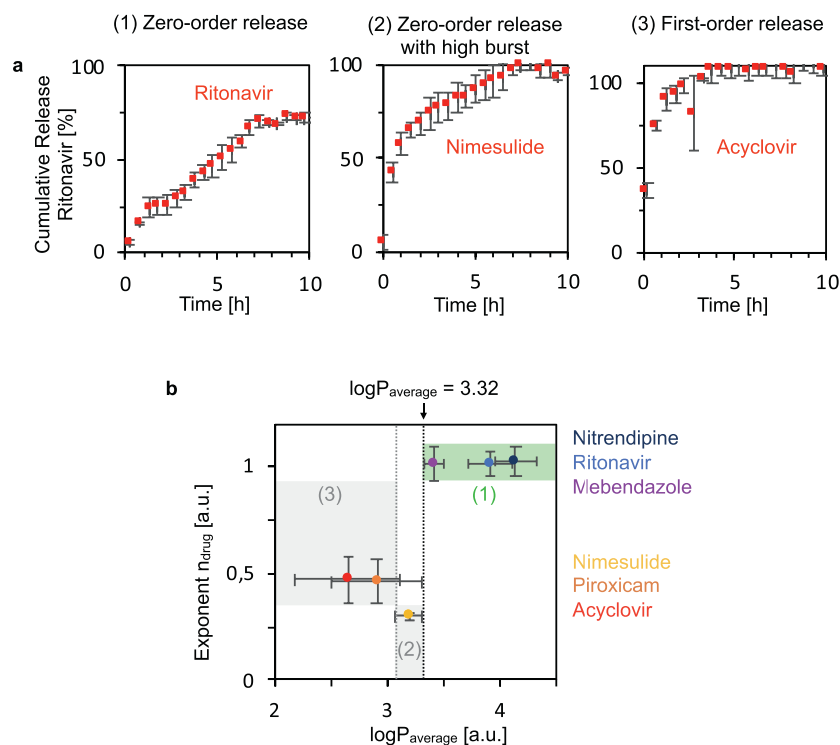
Fig. 3. The release profile of a) Ritonavir with zero-order kinetics and b) Acyclovir with first-order kinetics. c) The exponent n plotted against $logP_{average}$ shows that Nitrendipine, Ritonavir, and Mebendazole with $logP_{average}$ above 3.32 are released with zero-order kinetics ($n = 1$), while Nimesulide, Piroxicam and Acyclovir with $logP_{average}$ below 3.32 are released with high burst-release or not released linearly at all ($n \neq 1$), respectively.
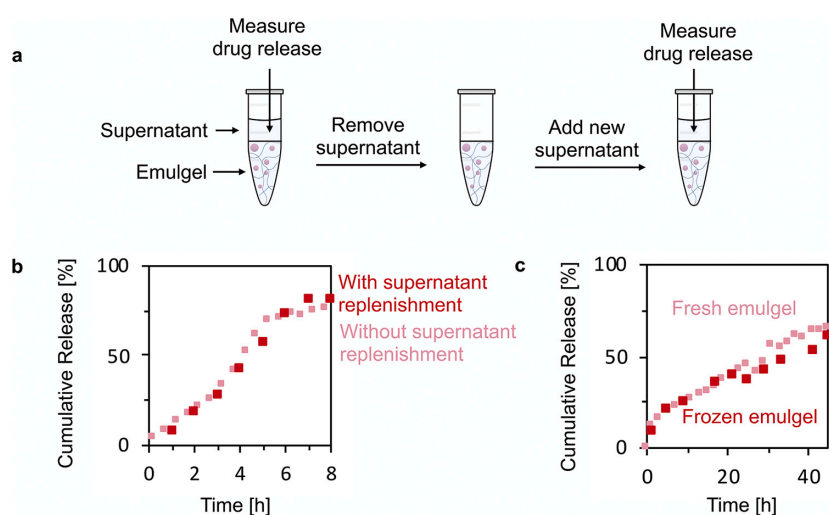
Fig. 4. a) Scheme of the supernatant replenishment: the released drug concentration is measured in the supernatant, and, subsequently the supernatant is fully removed and replaced with fresh supernatant. After one hour, the released drug concentration is measured in the fresh supernatant. The procedure is repeated until the end of the drug release. b) Release profile of 25.00 µM Nitrendipine from a C_{10} emulgel (5.00 mM C_{10}) with and without supernatant replenishment. c) Release profile of 25.00 µM Nitrendipine from a C_7C_7 emulgel (3.75 mM C_7C_7), after freezing it in liquid nitrogen and storing it at −20 °C, and a freshly prepared C_7C_7 emulgel (3.75 mM C_7C_7).

with liquid nitrogen. Subsequently, the sample was stored at −20 °C for 2 weeks. We found that the drug delivery system could be prepared and stored under these conditions without a notable change of the drug release profile (Fig. 4c) or of the droplet size and shape (Fig. S7).

3. Conclusion

In this work, we present a drug delivery system based on entrapped hydrolyzable oils that release hydrophobic drugs with zero-order kinetics. Our system consists of a hydrolyzable oil (C_{10} and C_7C_7, respectively), a hydrogel matrix to immobilize the oil droplets, and the

33

hydrophobic drugs. The linear release of various hydrophobic drugs is a consequence of the zero-order hydrolysis of the oil and can be guaranteed if the logP was higher than 3.3. The t_{50} can be tuned from 1.5 ± 0.1 h to 23 ± 2.5 h which offers a wide release period window. We found that fluid replenishment does not influence the release kinetics. Thus, the formulation is also suitable for applications with bodily fluid fluxes like implants. Moreover, the formulation can be frozen at $-196\ ^\circ$C and subsequently stored at $-20\ ^\circ$C, without changing the release kinetics. Furthermore, especially C_7C_7 and its hydrolysis product is only at concentrations toxic for cells that are far above the used concentrations. In future work, we will investigate how our drug delivery system performs *in vivo*. For example, we are interested in its application as a wound dressing in which the droplets remain immobilized and deliver hydrophobic drugs like anti-inflammatory and antimicrobial agents over their lifetime. Additionally, we aim to immobilize the drug-loaded hydrolyzable oil droplets in various polymer matrices to further optimize the formulation as a coating of the surfaces of medical devices like catheters.

4. Materials and methods

4.1. Materials

We purchased (E/Z)-2-Decen-1-ylsuccinic (C10 anhydride), heptanoic anhydride (C_7C_7), Ritonavir, and Acyclovir from TCI Chemicals. Nile Red, trifluoroacetic acid (TFA), dimethylsulfoxide (DMSO), Nitrendipine, Nimesulide, Mebendazole, Piroxicam, PBS tablets, fetal bovine serum (FBS), L-glutamine, non-essential amino acid solution, Dulbecco's phosphate-buffered saline, tetrazolium (WST-1) solution, Methanol and Minimum Essential Medium Eagle (MEM) were purchased from Sigma-Aldrich. The used Agar-agar was purchased from Carl-Roth. All chemicals were used without any further purification. HPLC grade acetonitrile (ACN) was purchased from VWR. MilliQ-water was received from a Milli-Q®Direct 8 water purification system.

4.2. Sample preparation and drug release experiments

The 5 mM stock solutions of the drugs Nimesulide, Nitrendipine, Ritonavir, and Piroxicam were prepared by dissolving the drug in acetonitrile. For the 5 mM Mebendazole and Acyclovir stock solution dimethylsulfoxide (DMSO) was used as a solvent. All the stock solutions were stored at 8 °C until further use.

The precursor stock solutions were prepared by emulsifying the anhydride in PBS (pH 7.4). For the drug release experiments, 4–200 μL of the drug stock solution was added and the emulsion was sonicated for two minutes with a Branson UltrasonicsTM SonifierTM SFX250 at 25% in an ice bath. These precursor/drug emulsions were prepared freshly for each experiment.

The emulgels were prepared by adding 500 μL of the precursor/drug emulsion to 500 μL of an 2% agar-agar stock in PBS, that was heated to 90 °C. Then 60 μL of this mixture was put on the bottom of a 96 well plate and after the emulgel was cooled off, 120–480 μL PBS was added as supernatant (Fig. 5). The amount of ACN or DMSO that is in contained in

the final emulgel lays between 0.25 and 2%. The cumulative drug and acid release was subsequently measured in the supernatant. All experiments were performed at 37 °C in triplicate.

For the stored samples, the well plate containing the samples was frozen in liquid nitrogen at $-196\ ^\circ$C and subsequently stored at $-20\ ^\circ$C for several weeks. To measure the drug release, the samples were defrosted at room temperature for 10 min, then 120 μL PBS was added and the temperature was set to 37 °C. The cumulative drug and acid release was measured in the supernatant by HPLC.

4.3. Analytical HPLC

The released drug and acid concentrations were determined by analytical high-performance liquid chromatography (HPLC, Thermofisher Dionex Ultimate 3000, Hypersil Gold 250 × 4.8 mm) using a linear gradient of MilliQ-water and acetonitrile, each with 0.1% TFA. All compounds were detected with a UV/Vis detector at 220, 240, and 330 nm. The method we used was programmed to run a H2O:ACN gradient from 98:2 to 2:98 in 13 min (Table 1)

Calibration curves for the drugs (in ACN and DMSO/MeOH respectively) and the carboxylates (in PBS) were conducted with the corresponding method in triplicate.

4.4. Microscopy

Confocal fluorescence microscopy was performed on a Leica TCS SP8 confocal microscope using a 63× water immersion objective. The precursor stock solutions were prepared by emulsifying the anhydride in PBS (pH 7.4) with a Branson UltrasonicsTM SonifierTM SFX250 at 25% in an ice bath and adding 5 mM Nile red dye. The emulgel sample was prepared like previously described. The samples were excited at 552 nm and imaged at 560–650 nm with a HyD detector (pinhole: 1 a.u., laser power: 0.09, gain: 146.7%). The measurements were performed at 25 °C.

4.5. Analysis of the release order

The normalized drug release traces (Fig. S4a–f) were fitted with Eq. (2) with OriginLab to determine the exponent n and thus the order of the

Table 1
Retention time, wavelength and calibration value of all compounds.

Compound	Retention time [min]	Wavelength [nm]	Calibration value	M [g/mol]
C_{10} acid	11.79	220	3.247	238.32
C_7 acid	10.66	220	0.680	242.35
Acyclovir	5.50	240	0.192	225.21
Mebendazole	11.92	330	0.043	295.29
Nimesulide	10.99	330	0.153	308.31
Nitrendipine	11.29	240	0.520	360.36
Piroxicam	9.48	330	0.497	331.35
Ritonavir	10.96	240	0.228	720.90
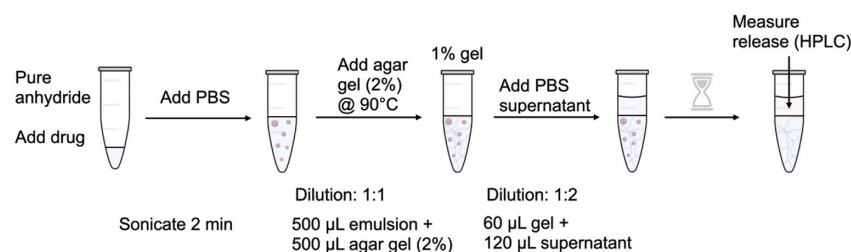
Fig. 5. Preparation of the drug-loaded active emulgel.

drug released. If n = 1, the drug release follows zero-order kinetics, and if n ≠ 1, the drug follows the Fickian- or non-Fickian diffusion mechanism [39].

4.6. Cell viability studies

Human epithelial cells (HeLa) were cultured with Minimum Essential Medium Eagle (MEM) supplemented with 10% (v/v) fetal bovine serum (FBS), 2 mM L-glutamine solution and 1% (v/v) non-essential amino acid solution at 37 °C, 5% CO2, and a humidified atmosphere.

To assess the influence of C_7C_7 and C_7 hydrolyzable oil, as well as of C_{10} and C_{10} acid on the cell viability, first, the cells were seeded in a 96-well plate at a concentration of 15,000 cells per well and incubated for 24 h. Then, the medium was replaced by medium containing different concentrations of the test substances: 1 mM, 2.5 mM, 5 mM, 10 mM, 20 mM, 50 mM, 100 mM, 200 mM C_7C_7 and 0.5 mM, 1 mM, 1.5 mM, 5 mM, 10 mM, 20 mM, 50 mM, 100 mM C_7 acid, 0.000001 mM, 0.00025 mM, 0.00075 mM, 0.001 mM, 0.25 mM, 0.50 mM, 0.75 mM, 1 mM, 7.5 mM and 10 mM C_{10} and C_{10} acid, respectively. Three wells always contain the same concentrations. To study the biocompatibility of the emulgel, the medium was replaced with new medium containing 60 μL emulgel with an initial hydrolyzable oil concentration of 2.5 mM, 5 mM and 7.5 mM C_{10} or 2.5 mM, 3.75 mM and 4.5 mM C_7C_7, respectively. Three wells always contain the same concentrations. In addition, three wells were cultured with 50% (v/v) MeOH (= positive control) or cell culture medium (=negative control). After a further incubation time of 24 h, the cells were washed three times with Dulbecco's phosphate buffered saline. To obtain the cell viability of the treated cells, cell culture medium enriched with 2% water-soluble tetrazolium (WST-1) solution was incubated on the cells for 1 h. Afterward, the metabolized medium was pipetted bubble-free into a fresh well plate and the absorbance of the solutions was measured at an excitation wavelength of 450 nm (Viktor3 plate reader, Perkin Elmer, Rodgaum, Germany).

For biological replicates, the experiments were conducted three times in total. All values obtained were applied for the determination of the half-maximal inhibitory concentration (IC_{50}) of the respective substance (C_7C_7, C_7 acid, C_{10} and C_{10} acid).

4.7. Calculation of logP for each time point of the drug release

The drug concentration c(drug)$_{aq}$ (Fig. S1a) and the heptanoic acid concentration c(C_7 acid)$_{aq}$ (Fig. S1c) in the aqueous buffer phase were measured by HPLC. The amount of drug molecules in the aqueous and the hydrolysable oil phase n(drug)$_{aq}$ and n(drug)$_{oil}$ (Fig. S1b) were calculated from c(drug)$_{aq}$. For calculating the volume of the hydrolysable oil droplets V$_{oil}$ (Fig. S1d) first the hydrolysable oil concentration was calculated from the corresponding heptanoic acid concentration. From this V$_{oil}$ was calculated by using the starting V$_{oil}$. The concentration of the aqueous phase was assumed to be constant because the volume that is added by the hydrolysis product of the hydrolysable oil is neglectable. From V$_{oil}$ and n(drug)$_{oil}$ the drug concentration in the oil phase c(drug)$_{oil}$ (Fig. S1e) was calculated. Finally, logP (Fig. S1g) was obtained. The same procedure was used to obtain the logP values of the C_{10} system with varying drugs (Fig. S4g).

4.8. UV/Vis spectroscopy

The UV/Vis measurements were carried out using a Multiskan FC (ThermoFisher) microplate reader. The samples were prepared the same way as for the HPLC experiments. The temperature was 37 ± 0.5 °C and was set 30 min before starting the measurement. Each experiment was performed at 500 nm and in triplicate.

4.9. Determination of the solubility

To determine the solubility of the drugs in PBS, 5 mg of the drug was stirred in 1 mL PBS at 37 °C. After 24 h, the drug that was not dissolved in the buffer was filtered off. The drug concentration in the PBS was determined by HPLC. The experiments were conducted in triplicate.

Supplementary data to this article can be found online at https://doi.org/10.1016/j.jconrel.2021.10.014.

Declaration of Competing Interest

None.

Acknowledgments

References

[1] J. Li, D.J. Mooney, Designing hydrogels for controlled drug delivery, Nat. Rev. Mater. 1 (12) (2016) 16071.
[2] J. Wang, B. Wang, S.P. Schwendeman, Characterization of the initial burst release of a model peptide from poly(D,L-lactide-co-glycolide) microspheres, J. Control. Release 82 (2002) 289–307.
[3] R. Langer, Drug delivery and targeting, Nature 392 (1998) 5–10.
[4] G. Agarwal, S. Agarwal, P. Karar, S. Goyal, Oral sustained release tablets: an overview with a special emphasis on matrix tablet, Am. J. Adv. Drug Deliv. 5 (2017) 64–76.
[5] I. Joseph, S. Venkataram, Indomethacin sustained release from alginate-gelatin or pectin-gelatin coacervates, Int. J. Pharm. 126 (1) (1995) 161–168.
[6] C. Ma, Y. Shi, D.A. Pena, L. Peng, G. Yu, Thermally responsive hydrogel blends: a general drug carrier model for controlled drug release, Angew. Chem. Int. Ed. 54 (25) (2015) 7376–7380.
[7] W. Fan, Z. Zhang, Y. Liu, J. Wang, Z. Li, M. Wang, Shape memory polyacrylamide/ gelatin hydrogel with controllable mechanical and drug release properties potential for wound dressing application, Polymer 226 (2021) 123786.
[8] C. Lou, X. Tian, H. Deng, Y. Wang, X. Jiang, Dialdehyde-β-cyclodextrin-crosslinked carboxymethyl chitosan hydrogel for drug release, Carbohydr. Polym. 231 (2020) 115678.
[9] H. Zhong, G. Chan, Y. Hu, H. Hu, D. Ouyang, A comprehensive map of FDA-approved pharmaceutical products, Pharmaceutics 10 (4) (2018) 263.
[10] M.J. Naguib, I. Elsayed, M.H. Teaima, Simultaneous optimization of oral and transdermal nanovesicles for bioavailability enhancement of ivabradine hydrochloride, Int. J. Nanomedicine 16 (2021) 2917–2931.
[11] K. Uhrich, S. Cannizzaro, R. Langer, K. Shakesheff, Polymeric systems for controlled drug release, Chem. Rev. 11 (1999) 3181–3198.
[12] Y.N. Zhao, X. Xu, N. Wen, R. Song, Q. Meng, Y. Guan, S. Cheng, D. Cao, Y. Dong, J. Qie, K. Liu, Y. Zhang, A drug carrier for sustained zero-order release of peptide therapeutics, Sci. Rep. 7 (1) (2017) 5524.
[13] Y. Fu, W.J. Kao, Drug release kinetics and transport mechanisms of non-degradable and degradable polymeric delivery systems, Expert Opin. Drug Deliv. 7 (4) (2010) 429–444.
[14] F. van de Manakker, K. Braeckmans, N.E. Morabit, S.C. De Smedt, C.F. van Nostrum, W.E. Hennink, rotein-release behavior of self-assembled PEG-β-Cyclodextrin/PEG-cholesterol hydrogels, Adv. Funct. Mater. 19 (18) (2009) 2992–3001.
[15] A. Gokhale, Achieving zero-order release kinetics using multi-step diffusion-based drug delivery, Pharm. Technol. 38 (5) (2014).
[16] J. Weidner, Drug delivery, Drug Discov. Today 7 (11) (2002) 632.
[17] M.L. Laracuente, M.H. Yu, K.J. McHugh, Zero-order drug delivery: state of the art and future prospects, J. Control. Release 327 (2020) 834–856.
[18] M. Ali, S. Horikawa, S. Venkatesh, J. Saha, J. Hong, M. Byrne, Zero-order therapeutic release from imprinted hydrogel contact lenses within in vitro physiological ocular tear flow, J. Control. Release 124 (3) (2007) 154–162.
[19] L. Zhang, J. Alfano, D. Race, R.N. Davé, Zero-order release of poorly water-soluble drug from polymeric films made via aqueous slurry casting, Eur. J. Pharm. Sci. 117 (2018) 245–254.
[20] A. Grattoni, H. Shen, D. Fine, A. Ziemys, J.S. Gill, L. Hudson, S. Hosali, R. Goodall, X. Liu, M. Ferrari, Nanochannel technology for constant delivery of chemotherapeutics: beyond metronomic administration, Pharm. Res. 28 (2) (2011) 292–300.
[21] Ajazuddin, A. Alexander, A. Khichariya, S. Gupta, R.J. Patel, T.K. Giri, D. K. Tripathi, Recent expansions in an emergent novel drug delivery technology: Emulgel, J. Control. Release 171 (2) (2013) 122–132.
[22] L. Wei, C. Cai, J. Lin, T. Chen, Dual-drug delivery system based on hydrogel/ micelle composites, Biomaterials 30 (2009) 2606–2613.
[23] S. Davis, C. Washington, P. West, L. Illum, G. Liversidge, L. Sternson, R. Kirsh, Lipid emulsions as drug delivery systems, Ann. N. Y. Acad. Sci. (1987) 75–88.

35

[24] V. Patel, H. Kukadiya, R. Mashru, N. Surti, S. Mandal, Development of microemulsion for solubility enhancement of clopidogrel, Iran. J. Pharm. Sci. 9 (4) (2010) 327–334.

[25] A.S. Narang, D. Delmarre, D. Gao, Stable drug encapsulation in micelles and microemulsions, Int. J. Pharm. 345 (1) (2007) 9–25.

[26] L. Serra, J. Domenech, N.A. Peppas, Drug transport mechanisms and release kinetics from molecularly designed poly(acrylic acid-g-ethylene glycol) hydrogels, Biomaterials 27 (31) (2006) 5440–5451.

[27] T.R. Hoare, D.S. Kohane, Hydrogels in drug delivery: progress and challenges, Polymer 49 (8) (2008) 1993–2007.

[28] M. Rizwan, R. Yahya, A. Hassan, M. Yar, A.D. Azzahari, V. Selvanathan, F. Sonsudin, C.N. Abouloula, pH Sensitive hydrogels in drug delivery: brief history, properties, swelling, and release mechanism, material selection and applications, Polymers 9 (4) (2017).

[29] F. Vanpariya, M. Shiroya, M. Malaviya, Emulgel: a review, Int. J. Sci. Res. 10 (2021) 847.

[30] H.J. Chung, Y. Lee, T.G. Park, Thermo-sensitive and biodegradable hydrogels based on stereocomplexed Pluronic multi-block copolymers for controlled protein delivery, J. Control. Release 127 (1) (2008) 22–30.

[31] E.M. Anderson, M.L. Noble, S. Garty, H. Ma, J.D. Bryers, T.T. Shen, B.D. Ratner, Sustained release of antibiotic from poly(2-hydroxyethyl methacrylate) to prevent blinding infections after cataract surgery, Biomaterials 30 (29) (2009) 5675–5681.

[32] M. Tena-Solsona, C. Wanzke, B. Riess, A.R. Bausch, J. Boekhoven, Self-selection of dissipative assemblies driven by primitive chemical reaction networks, Nat. Commun. 9 (1) (2018) 2044.

[33] C. Wanzke, M. Tena-Solsona, B. Rieß, L. Tebcharani, J. Boekhoven, Active droplets in a hydrogel release drugs with a constant and tunable rate, Mater. Horiz. 7 (5) (2020) 1397–1403.

[34] A.B. Moshnikova, V.N. Afanasyev, O.V. Proussakova, S. Chernyshov, V. Gogvadze, I.P. Beletsky, Cytotoxic activity of 1-ethyl-3-(3-dimethylaminopropyl)-carbodii-mide is underlain by DNA interchain cross-linking, Cell. Mol. Life Sci. 63 (2) (2006) 229–234.

[35] B. Jeonga, Y. Baeb, S. Kim, Drug release from biodegradable injectable thermosensitive hydrogel of PEG–PLGA–PEG triblock copolymers, J. Control. Release 63 (2000) 155–163.

[36] W. Zhang, X. Jin, H. Li, R.R. Zhang, C.W. Wu, Injectable and body temperature sensitive hydrogels based on chitosan and hyaluronic acid for pH sensitive drug release, Carbohydr. Polym. 186 (2018) 82–90.

[37] W. Chen, P. Zhong, F. Meng, R. Cheng, C. Deng, J. Feijen, Z. Zhong, Redox and pH-responsive degradable micelles for dually activated intracellular anticancer drug release, J. Control. Release 169 (3) (2013) 171–179.

[38] R. Khullar, D. Kumar, N. Seth, S. Saini, Formulation and evaluation of mefenamic acid emulgel for topical delivery, Saudi Pharm. J. 20 (1) (2012) 63–67.

[39] P. Lee, Kinetics of drug release from hydrogel matrices, J. Control. Release 2 (1985) 277–288.

[40] C. Kimna, T.M. Lutz, H. Yan, J. Song, T. Crouzier, O. Lieleg, DNA strands trigger the intracellular release of drugs from mucin-based nanocarriers, ACS Nano 15 (2) (2021) 2350–2362.

[41] G.-H. Wang, G.-L. Huang, Y. Zhao, X.-X. Pu, T. Li, J.-J. Deng, J.-T. Lin, ATP triggered drug release and DNA co-delivery systems based on ATP responsive aptamers and polyethylenimine complexes, J. Mater. Chem. B 4 (21) (2016) 3832–3841.

Supporting information for

Emulsions of hydrolyzable oils for the zero-order release of

hydrophobic drugs

Laura Tebcharani, Caren Wanzke, Theresa Lutz, Jennifer Rodon-Fores, Oliver Lieleg, Job Boekhoven*

Laura Tebcharani, Dr. Caren Wanzke, Dr. Jennifer Rodon-Fores, Prof. J. Boekhoven, Department of Chemistry, Technical University of Munich, Lichtenbergstrasse 4, 85748 Garching, Germany.

Theresa Lutz, Prof. Oliver Lieleg, Center for Protein Assemblies (CPA), Technical University of Munich, Ernst-Otto-Fischer Straße 8, 85748, Garching, Germany
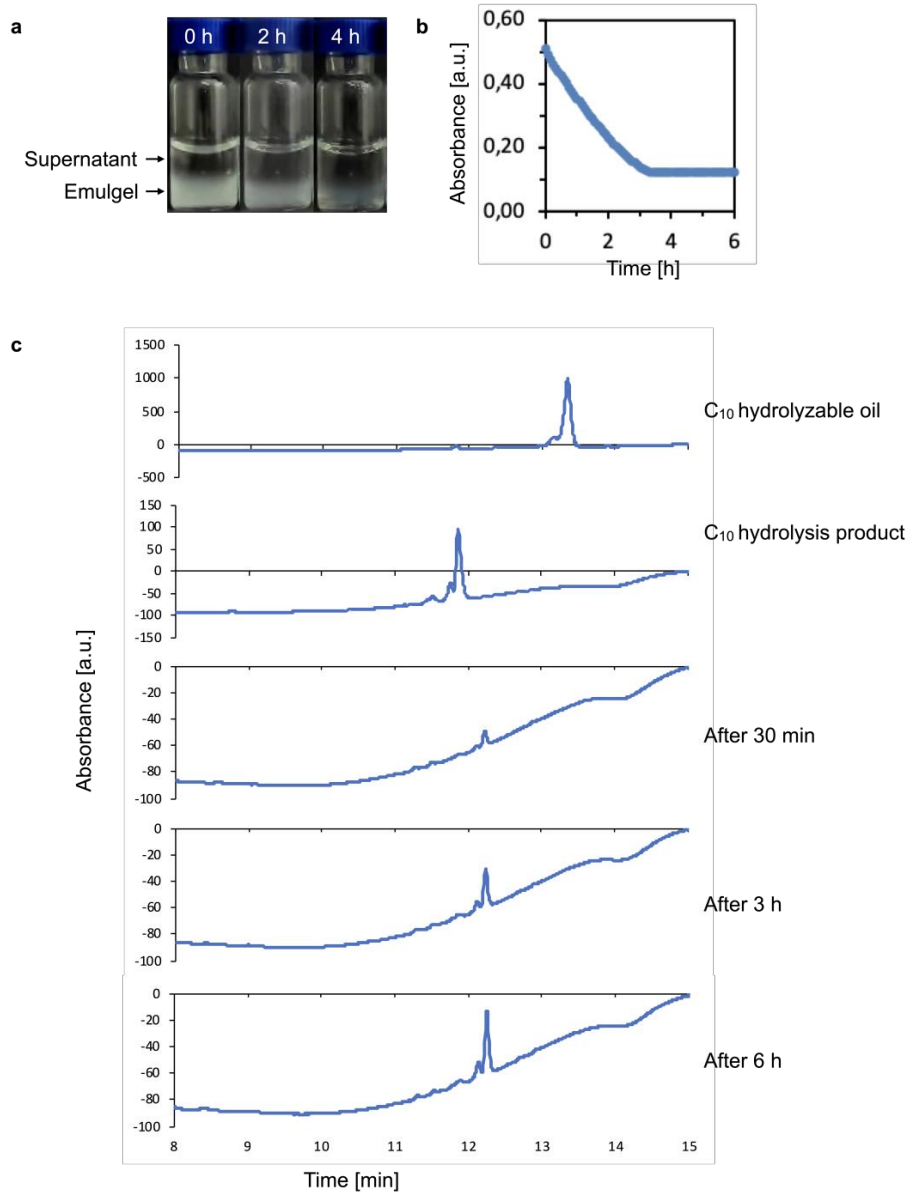
Figure S1: *(a) Photographs of a 2.50 mM C_{10} emulgel loaded with 25.00 µM Nitrendipine and covered with PBS supernatant at 0 h, 2 h and 4 h. (b) Turbidity measurement of of a 2.50 mM C_{10} emulgel loaded with 25.00 µM Nitrendipine and covered with PBS supernatant. (c) HPLC chromatogram at 220 nm of 5 mM C_{10} hydrolyzable oil (C_{10} anhydride), 5 mM C_{10} hydrolysis product (C_{10} acid) and of the supernatant of an emulgel containing 5 mM C_{10} hydrolyzable oil and 25 µM Nitrendipine after 30 min, 3 h and 6 h.*

2
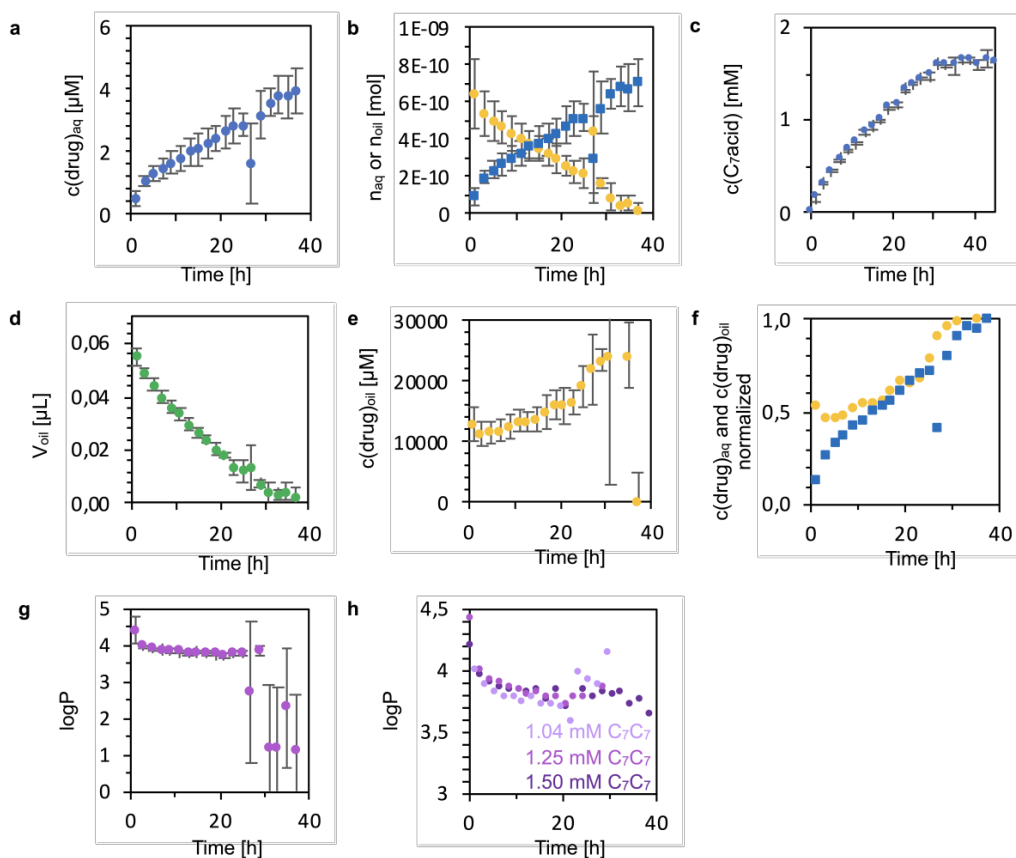
Figure S2: *a-g) The concentration drug (a), the number of mols in the aqueous (blue) or oil (yellow) phase (b), the concentration heptanoic acid (c), the volume of the oil phase (d), the concentration drug in the oil phase (e), the concentration drug in the oil phase and the normalized concentration drug in the oil (yellow) and aqueous phase (blue) (f) plotted against the time for an C_7C_7 emulgel (3.75 mM) loaded with 25.00 μM Nitrendipine. These values are used to calculate logP against time (g). h) LogP of C_7C_7 emulgels with different hydrolysable oil concentration (3.13 mM, 3.75 mM and 4.50 mM) and 25.00 mM Nitrendipine over time.*

3
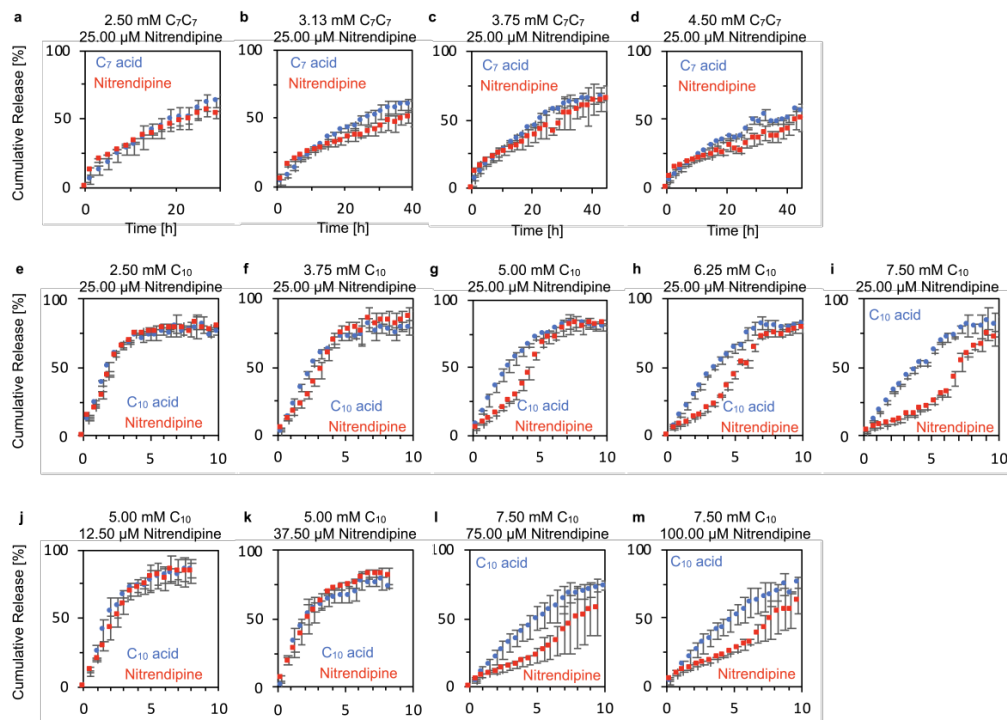
Figure S3: *a-d) Cumulative release of 25.00 µM Nitrendipine from a C_7C_7 emulgel with different hydrolysable oil concentrations (2.50 mM, 3.13 mM, 3.75 mM and 4.5 mM). e-i) Cumulative release of 25.00 µM Nitrendipine from a C_{10} emulgel with different hydrolysable oil concentrations (5.00 mM, 3.75 mM, 5.00 mM, 6.26 mM and 7.50 mM). j-m) Cumulative release of different Nitrendipine concentrations (12.50 µM, 37.50 µM, 75.00 µM and 100.00 µM) from a C_{10} emulgel (2.50 mM and 7.50 mM).*
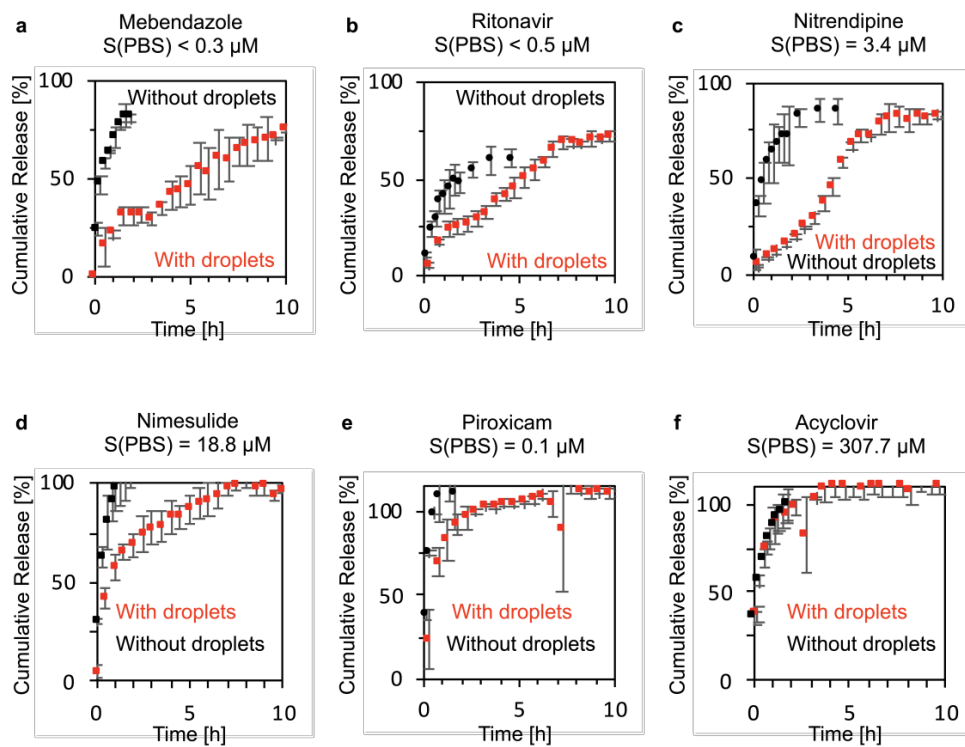
Figure S4: *a-f) Solubility in PBS and release profile of the drugs Mebendazole, Ritonavir, Nitrendipine, Nimesulide, Piroxicam and Acyclovir, respectively, with (red) and without (black) a C_{10}-emulgel (5.00 mM C_{10}).*

5
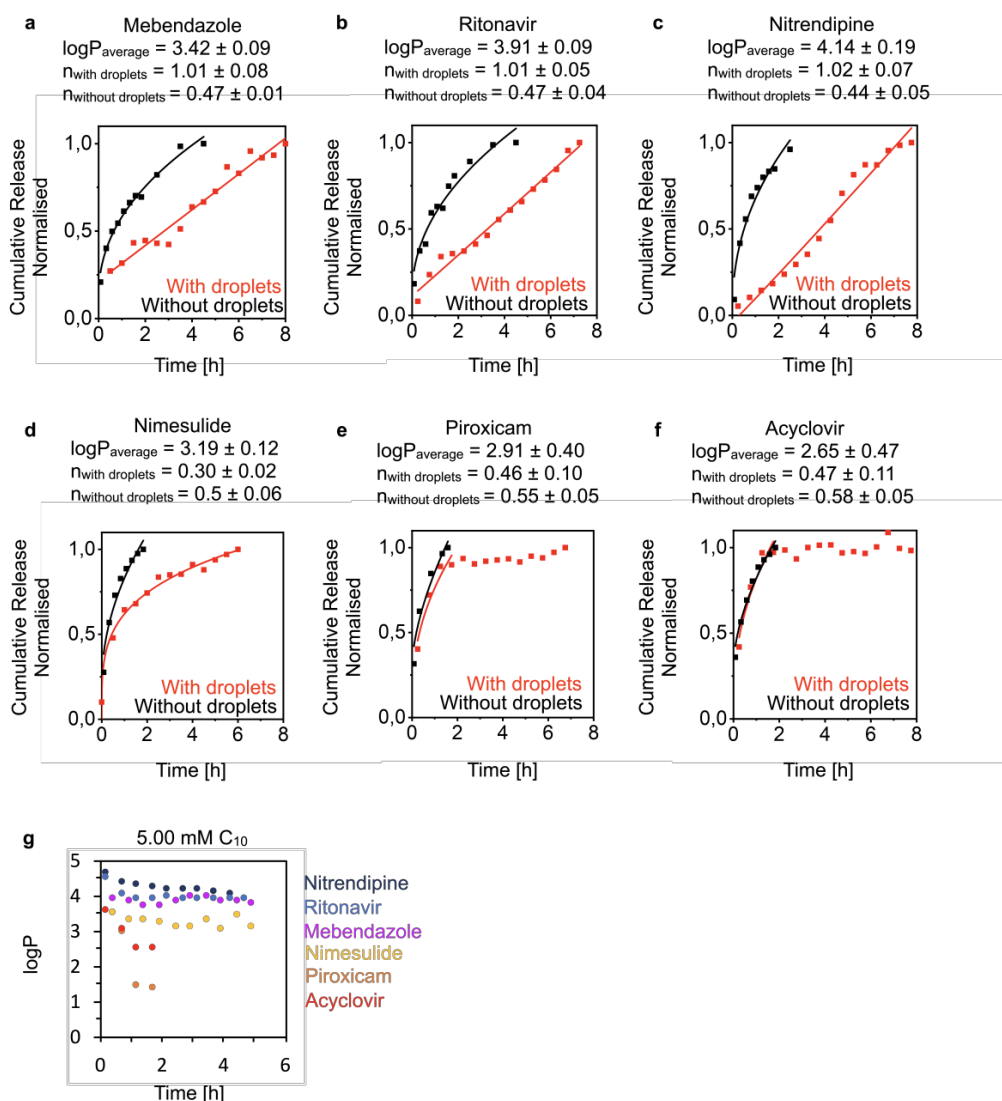
Figure S5: *a-f) logP$_{average}$, exponent n$_{with\ droplets}$ and n$_{without\ droplets}$ and normalized release profiles of 25.00 µM Mebendazole, Ritonavir, Nitrendipine, Nimesulide, Piroxicam and Acyclovir, respectively, with (red) and without (black) a C$_{10}$-emulgel (5.00 mM C$_{10}$) and fitted graphs for the experimental data with equation 2. g) logP over time of Mebendazole, Ritonavir, Nitrendipine, Nimesulide, Piroxicam and Acyclovir with a C$_{10}$-emulgel (5.00 mM C$_{10}$).*
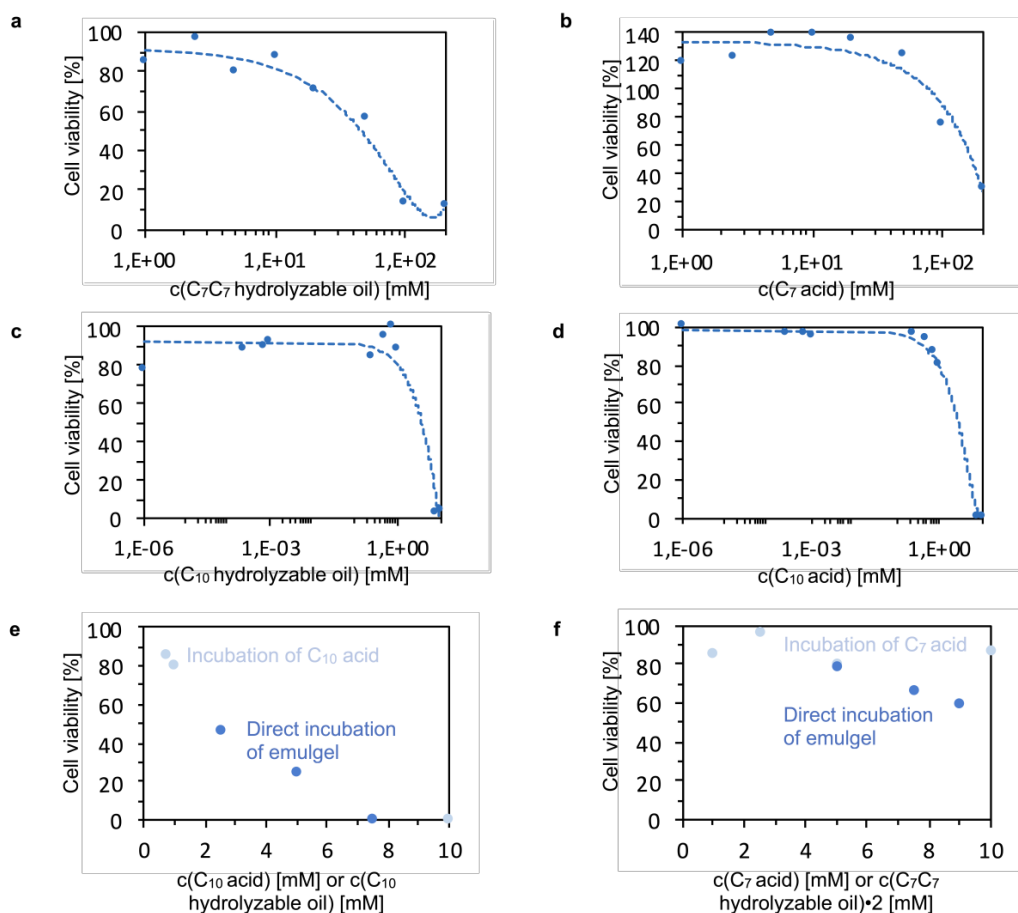
Figure S6: *Cell viability of the hydrolyzable oils (C_7C_7 and C_{10}) and the corresponding acids with human epithelial cells (HeLa). a) 1 mM, 2.5 mM, 5 mM, 10 mM, 20 mM, 50 mM, 100 mM, 200 mM C_7C_7 and b) 0.5 mM, 1 mM, 1.5 mM, 5 mM, 10 mM, 20 mM, 50 mM, 100 mM C_7 acid and c-d) 0.000001 mM, 0.00025 mM, 0.00075 mM, 0.001 mM, 0.25 mM, 0.50 mM, 0.75 mM, 1 mM, 7.5 mM and 10 mM C_{10} and C_{10} acid, respectively. e) Comparison of the cell viability of 0.75 mM, 1 mM, 5 mM and 10 mM C_{10} acid with human epithelial cells (HeLa) and the cell viability of an emulgel system containing an initial concentration of 2.5 mM, 5 mM and 7.5 mM C_{10} hydrolyzable oil, that is directly incubated with the HeLa cells. f) Comparison of the cell viability of 1 mM, 2.5 mM and 10 mM C_7 acid with human epithelial cells (HeLa) and the cell viability of an emulgel system containing an initial concentration of 2.5 mM, 3.75 mM and 4.5 mM C_7C_7 hydrolyzable oil, that is directly incubated with the HeLa cells. Since one C_7C_7 hydrolyzable oil molecule forms two molecules of corresponding C_7 acid molecules that leave the emulgel, the cell viability was here plotted against the initial C_7C_7 hydrolyzable oil concentration times two.*
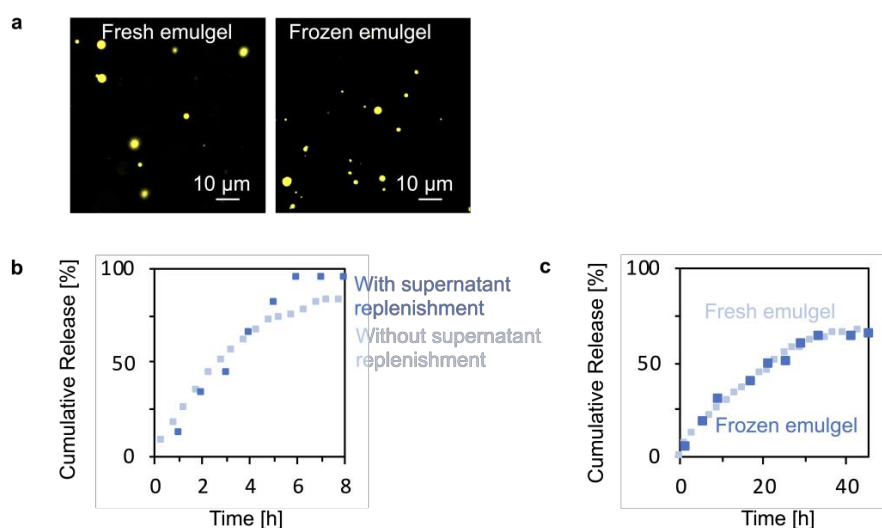
Figure S7: *a) Confocal microscope picture of a freshly prepared C_7C_7 emulgel (3.75 mM C_7C_7) and one that was frozen in liquid nitrogen and stored at 20°C. Nile red was added to both emulgels for imaging. b) Release profile the C_{10} acid 25.00 µM Nitrendipine from a C_{10} emulgel (5.00 mM C_{10}) loaded with Nitrendipine (25.00 µM) with and without supernatant replenishment. c) Release profile of C_7C_7 acid from a C_7C_7 emulgel (3.75 mM C_7C_7) loaded with Nitrendipine (25.00 µM), after freezing it in liquid nitrogen and storing it at -20°C, and a freshly prepared C_7C_7 emulgel (3.75 mM C_7C_7).*

Table S1: *release rates in ng/h for different combinations of initial C_{10} and Nitrendipine concentrations in the emulgel and different supernatant volumes. The volume of the emulgel was 60 µL for all experiments. The volume of the supernatant was 120, 240, 360 and 480 µL, respectively.*

Initial c(C_{10}) in the emulgel [mM]	Initial c(Nitrendipine) in the emulgel [µM]	Total volume of the emulgel and supernatant [µL]	Release rate [ng/h]
2.50	12.50	180	5.61
2.50	25.00	180	10.77
2.50	37.50	180	15.70
2.50	50.00	180	21.51
3.75	25.00	180	8.77
5.00	25.00	180	6.97
5.00	25.00	300	5.61
5.00	25.00	420	6.68
5.00	25.00	540	6.75
6.25	25.00	180	5.39
7.50	25.00	180	3.47
7.50	75.00	180	8.40
7.50	100.00	180	12.64

8

Table S2: *pH values of the supernatant of 2.50, 5.00 and 7.50 mM initial concentration of C_{10} and 25.00 µM initial Nitrendipine with and without supernatant replenishment, respectively.*

Time [h]	pH of 2.50 mM initial C_{10} in the emulgel	pH of 5.00 mM initial C_{10} in the emulgel	pH of 7.50 mM initial C_{10} in the emulgel	pH of 5.00 mM initial C_{10} in the emulgel with supernatant replenishment
0	7.40	7.40	7.40	7.40
1	7.21	7.20	7.18	7.20
2	7.14	7.05	6.97	7.17
3	7.11	7.07	6.90	7.24
4	7.12	7.00	6.85	7.24
5	7.12	6.90	6.83	7.22
6		6.85	6.71	7.25
7		6.88		7.32
8		6.79		7.35
24			6.71	

9

4 Hydrolyzable Emulsions as Dual Release Platform for Hydrophobic Drugs and DNA

Abstract

In the previous chapter, I showed an emulgel-based drug delivery platform that can release hydrophobic drugs with zero-order kinetics. Thus, BCS II drugs with a low bioavailability can be released with a constant and tunable rate within a narrow therapeutic window over an adjustable period. The formulation comprises hydrophobic oil droplets that can incorporate a hydrophobic therapeutic agent and is subsequently immobilized in a hydrogel. In this work, we demonstrated that this formulation can also be used to control the onset of the release of oligonucleotides. Here, short cholesterol-conjugated DNA strands accumulate on the surface of the hydrolyzable oil droplets embedded in a hydrogel. When the hydrolysis of the oil droplets is completed, the DNA is released from the hydrogel within four hours. Tuning the lifetime of the hydrolyzable oil allows control over the onset of the cholesterol-conjugated DNA release. This could help to improve the short circulatory half-life and stability of nucleic acid-based therapeutics, *i.e.,* due to degradation by serum nucleases. Furthermore, we combined this formulation into a dual-release platform to release a hydrophobic drug with zero-order kinetics, followed by a rapid release of cholesterol-conjugated DNA. Moreover, we could show the functionality of our platform and the released cholesterol-conjugated DNA by using these DNA strands to induce the disassembly of gold nanoparticles *via* toehold-mediated strand displacement.

This work has been published:

This section states the individual work of each author in the publication above. J. Boekhoven, L. Tebcharani, J. Gibbs, and O. Lieleg designed the experiments. L. Tebcharani carried out the experiments. N. Akter synthesized the DNA strands as well as the DNA-conjugated gold nanoparticles. D. Fan carried out the cell viability studies. L. Tebcharani and J. Boekhoven wrote the manuscript. All authors have given approval to the final version of the manuscript.

ROYAL SOCIETY
OF CHEMISTRY

rsc.li/chemcomm

COMMUNICATION

Hydrolyzable emulsions as dual release platform for hydrophobic drugs and DNA

Laura Tebcharani[a], Nahida Akter[b], Di Fan[c, d], Oliver Lieleg[c, d], Julianne M. Gibbs[b], Job Boekhoven[a]

Several challenges need to be overcome when applying nucleic acids as therapeutic agents. We developed a new way to control the onset of the release of cholesterol-conjugated oligonucleotides with a simple, versatile, and cheap platform. Moreover, we combine the platform into a dual-release system that can release a hydrophobic drug with zero-order kinetics, followed by a rapid release of cholesterol-conjugated DNA.

Over the last years, nucleic acids have become more in focus as therapeutic agents. Especially small oligonucleotides such as antisense oligonucleotides and small interfering RNA (siRNA) have enormous potential in treating diseases. These short single-stranded DNA and double-stranded RNA sequences, respectively, can modulate the expression of target genes by interfering with the translation or transcription.[1-7] One major challenge in DNA and RNA-based therapeutics is the stability of nucleic acid oligomers due to degradation by serum nucleases.[1, 8, 9] Short oligonucleotides' stability and circulatory half-life can be improved through chemical modification. For example, modifying the nucleic acid backbone with phosphorothioate or adding functional groups like cholesterol can enhance the pharmacological properties of siRNA *in vivo* and *in vitro*. While unmodified siRNA strands are degraded within one minute, cholesterol-conjugated siRNA could be detected in rats after 24 hours.[4, 10-13] Other approaches for targeted oligonucleotide delivery include polymeric microparticles and micelles like PEG-poly(aspartic acid) copolymers or nanoparticles such as gold nanoparticles.[1, 14, 15] However, these delivery systems only allow the spatial control of the oligonucleotide delivery. Platforms with temporal release control over oligonucleotide release are rare.[14-16] In this work, we developed a formulation that controls the onset of the release of cholesterol-conjugated oligonucleotides. Moreover, we combine this into a dual-release system that releases a hydrophobic drug with zero-order

kinetics, followed by a rapid release of DNA. The modular design of the platform allows a free selection of the drug and DNA sequence as well as the release period and onset. Thus, our platform is simple, versatile, and cheap to produce.

The formulation is based on an emulsion of oil droplets embedded in an emulgel (Scheme 1a). The droplets are made of a hydrolyzable oil that hydrolyzes with zero-order kinetics. When a hydrophobic drug with a high partition coefficient for the oil is added, the drug partitions into the oil droplets (Scheme 1b (t_0)). Cholesterol-tagged DNA strands accumulate at the surface of the oil droplets (Scheme 1b (t_0)). As the oil droplets hydrolyze, the hydrophobic drug is released with zero-order kinetics (Scheme 1b (t_1), c). Only when the droplets are completely hydrolyzed is the DNA rapidly released (Scheme 1b (t_2), c).
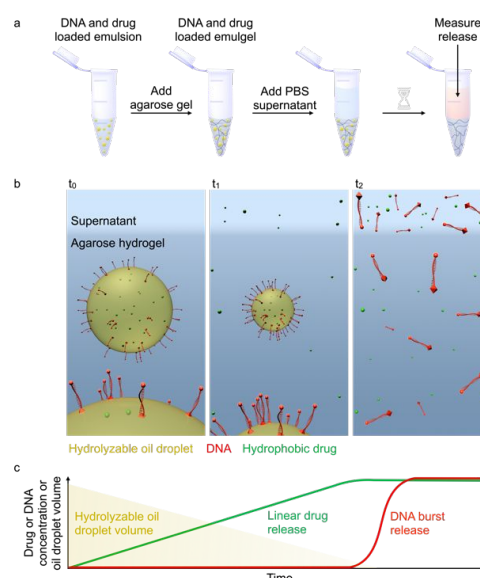
Scheme 1. a) Preparation of the DNA and drug-loaded emulgel. b) Design of the release platform. b) Expected evolution of the volume of the hydrolyzable oil droplets, the drug release, and the DNA.

a. *Department of Chemistry, Technical University of Munich, Lichtenbergstrasse 4, 85748 Garching, Germany.*

b. *Department of Chemistry, University of Alberta, Edmonton T6G 2G2, Canada.*

c. *Center for Protein Assemblies (CPA), Technical University of Munich, Ernst-Otto-Fischer Straße 8, 85748 Garching, Germany*

d. *Department of Materials Engineering, School of Engineering and Design, Technical University of Munich, Boltzmannstraße 15, 85748 Garching, Germany*

COMMUNICATION

The dual-release drug delivery system comprises oil droplets from hydrolyzable oil embedded in a 0.6% agarose gel. As hydrolyzable oil, we used hexanoic anhydride (C_6C_6), heptanoic anhydride (C_7C_7), or decenylsuccinic anhydride (C_{10}). Moreover, as a model for the oligonucleotide-based drugs, we added fluorescently labeled, cholesterol-tagged DNA, specifically chol-T_{15}-cy5 (table S1). We assumed the hydrophobic cholesterol partitions into the hydrolyzable oil droplet while the negatively charged DNA strand remains in an aqueous solution.[17] Thus, the chol-DNA-cy5 accumulates at the droplet surface (Scheme 1a). As a model for the hydrophobic drug, we added the hydrophobic dye BODIPY 493/503, assuming the hydrophobic dye partitions well into the oil droplets. Finally, by confocal microscopy, we confirmed the partitioning of the hydrophobic dye in the droplets and the DNA at the interface of the droplets (Fig. 1a, Fig. S1).

The DNA-containing qualified emulsion (emulgel) was covered with PBS. As a function of time, the concentration of the released compounds in the supernatant was measured by fluorescence spectroscopy. The release profile of chol-T_{15}-cy5 shows that the droplets can delay the DNA release by several hours (Fig. 1b). Specifically, without the oil droplets, the measured DNA concentration reaches 100% after as little as 4.0 ± 0.0 hours. In contrast, we measured a minor burst release of $17 \pm 9\%$ with the oil droplets, after which the concentration stayed constant for a long time. Then, after 10.0 ± 0.8 hours, the chol-T_{15}-cy5 concentration increases rapidly until $110 \pm 16\%$ is released after 13 ± 0.2 hours. From these data, we conclude that the affinity of the cholesterol for the oil droplets is so high that the chol-T_{15}-cy5 is set free only after the oil droplets are fully hydrolyzed (Scheme 1a).

Thus, the lifetime of the hydrolyzable oil droplets should determine when the DNA is released. The initial hydrolyzable oil concentration in the hydrogel can tune this lifetime.[18] We first determined the lifetime of the droplets of varying C_6C_6 concentrations by measuring the turbidity over time (Fig. 1c, Fig. S2a). In line with previous work, this lifetime increases linearly with the concentration of C_6C_6 (Fig. S2b and Fig. 1d).[18, 19] We determined the timepoint where the DNA burst release starts by measuring the concentration in the supernatant for different hydrolyzable oil concentrations (Fig. S2c). Fig. 1d shows that the onset of DNA burst release matches the lifetime of the hydrolyzable oil droplets. In other words, the onset of the burst release can be tuned by varying the initial oil concentration. For example, an initial C_6C_6 concentration of 2.50 mM leads to the release of the DNA strands after 4.6 ± 0.5 hours, while the DNA is released after 22.3 ± 0.5 hours for 10 mM initial C_6C_6 concentration.

We determined the ranges of possible DNA release for this system by comparing the lifetimes of different hydrolyzable oils and found a range from 4 to 150 hours (Fig. 1e). While the symmetric anhydride C_6C_6 and the asymmetric anhydride C_{10} can reach lifetimes between 0 and 23.5 ± 0.4 and 26.5 ± 0.4, respectively, the symmetric anhydride C_7C_7 can have a lifetime up to 147.0 ± 3.1 hours (Fig. S2d-e). As previously reported, the varying lifetime is a consequence of the oil's solubilities.[18, 19] As the anhydride in the oil droplets is protected from hydrolysis, hydrolysis only takes place on the fraction

that remains in solution which is equal to the anhydride's solubility. Thus, the higher the solubility, the faster the hydrolysis[3] therefore, the more soluble C_6C_6 has a shorter lifetime than the less soluble C_7C_7. As for the C_6C_6 droplets, we found that the cholesterol-conjugated oligonucleotides accumulate on the surface of C_{10} and C_7C_7 oil droplets (Fig. S3a-b). We also found that chol-T_{15}-cy5 release can be delayed by an emulgel containing C_{10} oil droplets (Fig. S3c). Next, we investigated the influence of the length of DNA strand on the release kinetics by comparing the release of 15, 25, or 35 thymine nucleobases in the sequence chol-T_n-cy5 from an emulgel containing 2.50 mM C_6C_6 oil droplets (Fig. 1f). For all three DNA lengths, the release starts after 4.0 hours and is completed after 6.5 ± 1.0 hours. In addition, the release of a cholesterol and cy5-modified DNA strand with a sequence containing all nucleobases was also delayed by 4 hours. Taken together, the jellified emulsion of hydrolyzable oil can delay the release of DNA for up to 150 hours.

The linear decay of the C_6C_6-based emulgel is in line with our previous work.[18, 19] Since the significant fraction of the anhydride forms oil droplets, it is physically separated from the aqueous phase and therefore protected from hydrolysis (Fig. 2a). Thus, hydrolysis only occurs on the oil molecules that remain in the water phase which is equal to the solubility of the oil and thus constant. Therefore, as long as droplets are present, the hydrolysis rate is equal to the hydrolysis rate constant multiplied by the solubility of the anhydride. Since both are constant, the total volume of the oil droplets decreases linearly, which can be quantified by measuring the turbidity as a function of time (Fig 2b). We further confirmed the linear decay by measuring the evolution of the released C_6 acid by HPLC (Fig. S4a). While an initial concentration of 2.50 mM C_6C_6 is fully hydrolyzed after 4.58 ± 0.1 hours, the lifetime can be doubled to 10.33 ± 0.9 hours by doubling the initial concentration to 5.00 mM C_6C_6 or quadrupled to 23.5 ± 0.4 hours if 10.00 mM C_6C_6 is used.
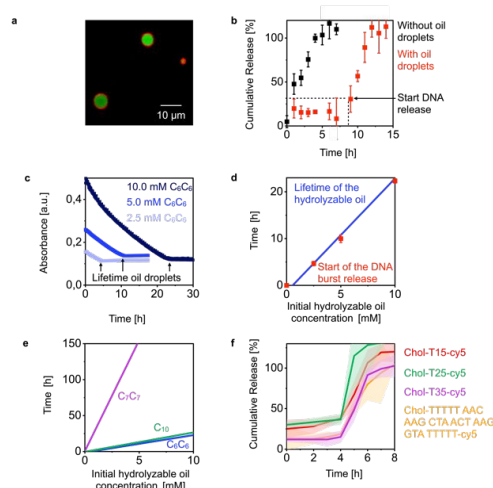
Fig. 1. a) Confocal microscope image of C_6C_6 oil droplets embedded in an agarose gel. BODIPY 493/503 dye (green) is incorporated into the droplets, and chol-T_{15}-cy5 (red) is accumulated on the droplet surfaces. b) Release profile of chol-T_{15}-cy5 from a hydrogel gel without and with C_6C_6 oil droplets. c) Linear hydrolysis profiles of C_6C_6

Journal Name   COMMUNICATION

oil droplets in an agarose gel. d) The lifetime of the hydrolyzable oil is directly proportional to the initial oil concentration embedded in the hydrogel and corresponds to the onset of the chol-T_{15}-cy5 release. e) The emulsion's lifetime against the hydrolyzable oil's initial concentration. f) The release profile of DNA from an emulgel.

Next, we tested the release of hydrophobic drugs from these emulsions of hydrolyzable oils. As the hydrophobic drug molecules partitioning is nearly constant over time, the drug is released linearly from the oil droplets as their total volume decreases linearly with time. To examine the release profiles of a dual-release system that releases a hydrophobic drug and cholesterol-tagged DNA, we measured the release of 25.00 µM Nitrendipine and 30.00 nM chol-T_{15}-cy5 a 0.6% agarose gel containing 5.00 mM C_6C_6 oil droplets (Fig. 2c). As predicted, the hydrophobic drug is first released with zero-order kinetics as a consequence of the linear hydrolysis of the hydrolyzable oil. During this period, the DNA concentration in the supernatant stays constant after a minor burst release of 0.10 nM. After 9 hours, the hydrophobic drug is completely released as the oil droplets are fully hydrolyzed. It is followed by the DNA burst release, during which the DNA is set free rapidly in four hours. Control experiments show that the DNA and the drug release do not influence by each other's release profile (Fig. S4b-e).

We determined when the drug is fully released and when DNA burst release starts from agarose gels containing different hydrolyzable oil concentrations (Fig. 2d). Both time points correspond to the lifetime of thy hydrolyzable oil, which was determined by measuring the absorbance at 500 nm over time. This means that the rapid DNA release always starts immediately after the hydrophobic drug is fully released. While the burst of the DNA release always lasts four hours, the regime of the linear drug release can be tuned to last between 5 and 23 hours.
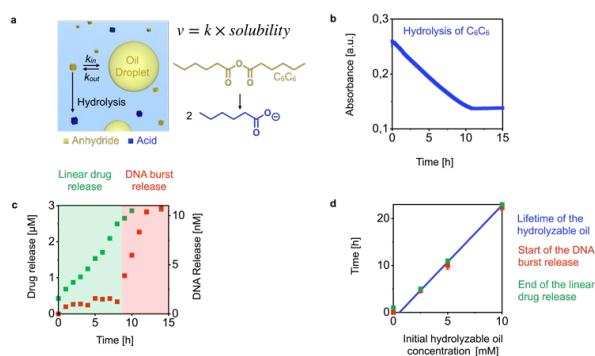
Fig. 2. a) *Self-protection mechanism of the droplets results in constant hydrolysis. b) Linear hydrolysis profiles of C_6C_6 emulgel. c) Dual-release profile of Nitrendipine (green) and chol-T_{15}-cy5 (red) from an emulgel. d) The lifetime of the oil droplets corresponds with the onset of the DNA release and the end of the drug release.*

Furthermore, to show that the released cholesterol-tagged DNA remains functional, we designed a method to use the released DNA to delay the disassembly of gold nanoparticle aggregates. Gold nanoparticles functionalized with DNA-strand A* aggregates with gold nanoparticles with DNA-strand B* when mixed with a linker

DNA strand complementary to A* and B* (table S1).[21] The linker DNA forms a nicked duplex with the A* and B* DNA strands of the nanoparticles resulting in the aggregation of the nanoparticles (Fig. 3a). The linker strand has a toehold and an overhang of 5 adenine nucleotides on both ends that do not participate in the hybridization with the DNA-AuNPs. The nanoparticle aggregate disassembly is induced via toehold-mediated strand displacement by adding a target DNA strand. The target strand is complementary to the linker strand, including a complementary thymine nucleotide sequence on both ends. It forms a more stable complete duplex with the linker strand (Fig. 3a). After adding the target strand, the aggregates dissociate within 10 minutes.
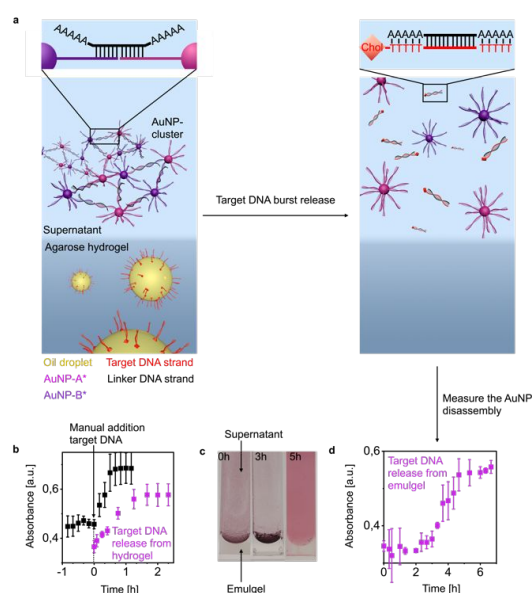
Fig. 3. *a) The design of the DNA-AuNP-system. b) The disassembly of gold nanoparticle aggregates induced manually and by releasing target DNA from an agarose gel, respectively. c) Photographs of target DNA-loaded emulgel covered with a supernatant containing AuNP aggregates. d) The disassembly of the AuNP aggregates can be delayed by 3 hours if the target DNA is released from an emulgel.*

We predict that the disassembly of the nanoparticle aggregates can be delayed by combining them with our emulgel to yield a DNA nanoparticle release system. First, the emulgel is prepared by loading the hydrolyzable oil droplets with the cholesterol-conjugated target DNA strand and embedding the loaded droplets in a hydrogel (Fig. 3a). Subsequently, the linker-DNA-AuNP aggregates are suspended in the supernatant that covers the emulgel. Because the oil droplets with the cholesterol-tagged target strands are trapped in the hydrogel, hybridizing the target and linker strands is impossible. When the target DNA is released into the supernatant due to the oil droplet hydrolysis, hybridization of the target and the linker strand and subsequent aggregate disassembly is induced (Fig. 3a). As the release of the cholesterol-modified target DNA strand depends on the lifetime of the hydrolyzable oil droplets, the timepoint of th target strand release and hence the timepoint of the disassembly of the aggregates can be tuned freely.

We first examined the ability of the cholesterol-tagged target DNA strand to induce the disassembly of gold nanoparticle aggregates consisting of 1.50 pmol A*-AuNPs, 1.50 pmol B*-AuNPs and 60.00 pmol linker DNA in PBS containing 3.00 mM magnesium chloride. The experimentally determined melting temperature of the duplex-linked aggregates (T_m) is 45.5°C (Fig. S5a). Thus, all experiments were carried out at 37 °C, *i.e.*, in the operational window $T = T_m − 2.0°C$ and $T = T_m − 10.0°C$ for a toehold system with an overhang of 5 adenine nucleobases on both ends of the linker strand.[23] The absorbance of the suspension is monitored over time by UV/Vis absorbance spectroscopy at the surface plasmon resonance wavelength of the DNA-AuNP colloid at λ_{max} = 525 nm. After equilibrating the aggregates for 50 min, 120.00 pmol cholesterol conjugated target strand is added. Upon target DNA addition, the absorbance of the suspension increases rapidly due to the changes in the surface plasmon resonance that correspond with the disassembly of gold nanoparticle aggregates (Fig. 3b).[21] Additionally, we confirmed that the target and the linker strand hybridize by measuring the melting curve of the linker-target duplex (Fig. S5b).

Next, we tested whether DNA strands released from the gel could induce DNA nanoparticle disassembly. To do so, 120.00 pmol cholesterol-conjugated target DNA was embedded in a hydrogel and subsequently covered with a suspension of the gold nanoparticle aggregates in PBS. The sample was incubated at 37°C, and the absorbance at 525 nm was measured over time. The absorbance immediately increases, showing the disassembly of the AuNPs induced by the released target DNA (Fig. 3b). The disassembly with the target strand released from a hydrogel was slower compared to the manual target strand addition, which we explain by the diffusion of the cholesterol-tagged DNA out of the agarose gel that takes 3.0 ± 1.0 hours. As 120.00 pmol target DNA is released in total from the emulgel, the required amount to complete the disassembly in 2 ± 1.0 hours is 60.00 pmol.

With the confirmation that the target DNA strands released from a hydrogel can induce disassembly and that the timepoint of the burst release of such DNA can be tuned, we studied the delayed disassembly of the aggregates. The target strands were released from an emulgel containing 5.00 mM C_6C_6 oil droplets with a 3.0 ± 0.1 hours lifetime at 37°C in PBS (Fig. S5c). A photograph of the system shows the turbid droplet containing gel on the bottom of the cuvette covered by a dark layer of gold nanoparticle aggregates (Fig. 3c). After 3 hours, the disappearance of the oil droplets is visible, meaning a now transparent gel can be observed. This marks the start of the target strand burst release. After 5 hours, the supernatant turned bright red, indicating that the nanoparticles started disassembling. To quantify the evolution of the disassembly, we measured the absorbance of the supernatant over time (Fig. 3d). The absorbance was constant during the first 3 hours, followed by a rapid increase which further confirms the gold nanoparticle aggregates disassembly can be delayed by 3 hours. Finally, we showed that the C_6C_6 oil has a good biocompatibility, which is in line with the previously studied anhydrides, and that the cholesterol conjugated DNA is sensitive to degradation by DNase (Fig. S6-S7).[18]

Conclusions

This work shows a dual-release drug delivery formulation that can release DNA and hydrophobic drugs. Hydrolyzable oil droplets can release the DNA strands from a hydrogel in a delayed-burst fashion. Moreover, hydrophobic drug molecules within the oil droplets are released with linear kinetics because of the self-protection mechanism of the oil droplets. Since the lifetime of the hydrolyzable oil can be tuned, the time at which the DNA is released can be tuned between 3 to 150 hours. Finally, we demonstrated the functionality of our system and released DNA that induces the disassembly of gold nanoparticle aggregates by toehold-mediated strand displacement.

In future work, we aim to extend the oligonucleotide library with more nucleotide sequences, different chemical modifications, and double-stranded oligonucleotides like siRNA. Additionally, we will replace the agarose gel with different hydrogel matrices that have desirable properties such as biodegradability. We plan to examine the degree of protection from enzymatic degradation given by the oil droplets and the hydrogel. Recent research shows that increasing the size of DNA-conjugated nanoparticles protects the DNA strands better from enzymatic degradation than smaller nanoparticles.[25] We hypothesize that the hydrolyzable oil droplets with a 100 times bigger diameter compared to these nanoparticles can prevent or reduce the degradation of oligonucleotides by enzymes as well. Finally, we plan to test the dual release system *in vivo*, i.e., the downregulation of *β*-galactosidase expression in *Escherichia coli*.[13]

Conflicts of interest

There are no conflicts to declare.

Notes and references

1. Fattal, E., and Barratt, G., *Br. J. Pharmacol.,* 2009, **157**, 179-194.
2. Kim, Y. J., and Krainer, A. R., *Mol. Cell,* 2023, **46**, 10-20.
3. Scharner, J., *et al.*, *Nucleic Acids Res.,* 2020, **48**, 802-816.
4. Gao, S., *et al.*, *Mol. Ther.,* 2009, **17**, 1225-1233.
5. de Martimprey, H., *et al.*, *Eu J Pharm Biophar,* 2009, **71**, 490-504.
6. Hu, B., *et al.*, *Signal Transduct. Target. Ther.,* 2020, **5**, 101.
7. Kuijper, E. C., *et al.*, *J. Inherit. Metab. Dis.,* 2021, **44**, 72-87.
8. Pouton, C., Seymour, L., *Adv. Drug Deliv. Rev.,* 2001, **46**, 187-203.
9. Sepp-Lorenzino, L., Ruddy, M., *Clin. Pharmacol. Ther.,* 2008, **84**, 628-632.
10. Braasch, D., *et al.*, *Bioor. Med. Chem. Lett.,* 2004, **14**, 1139-1143.
11. Geary, R. S., *et al.*, *Curr. Opin. Invetig. Drugs.,* 2001, **2**, 562-573.
12. Soutschek, J., *et al.*, *Nature,* 2004, **432**,173-178.
13. Lorenz, C., *et al.*, *Bioor. Med. Chem. Lett.,* 2004, **14**, 4975-4977.
14. Krebs, M. D., and Alsberg, E., *Chem. Eur. J.,* 2011, **17**, 3054-3062.
15. Pissuwan, D., *et al.*, *J. Control. Release,* 2011, **149**, 65-71.
16. Lee, S. E., *et al.*, *Nano Lett.,* 2009, **9**, 562-570.
17. Jahnke, K., *et al.*, *Adv. Funct. Mater.,* 2019, **29**, 1808647.
18. Tebcharani, L., *et al.*, *J. Control. Release,* 2021, **339**, 498-505.
19. Wanzke, C., *et al.*, *Mater. Horiz.,* 2020, **7**, 1397-1403.
20. Lam, M. K., *et al.*, *Langmuir,* 2016, **32**,1585-1590.
21. Mirkin, C. A., *et al.*, *Nature,* 1996, **382**,607-609.
22. Hsiao, J. C., *et al.*, *Nanoscale,* 2021, **13**,4956-4970.
23. Spoelstra, W. K., *et al.*, *Langmuir,* 2020, **36**,1956-1964.

Supporting Information for:

Title: Hydrolyzable emulsions as dual release platform for hydrophobic drugs and DNA

Authors: Laura Tebcharani[a], Nahida Akter[b], Di Fan[c, d], Oliver Lieleg[c, d], Julianne M. Gibbs[b], Job Boekhoven[a]

Affiliations:

[a] Department of Chemistry, Technical University of Munich, Lichtenbergstrasse 4, 85748 Garching, Germany.

[b] Department of Chemistry, University of Alberta, Edmonton T6G 2G2, Canada.

[c] Center for Protein Assemblies (CPA), Technical University of Munich, Ernst-Otto-Fischer Straße 8, 85748 Garching, Germany

[d] Department of Materials Engineering, School of Engineering and Design, Technical University of Munich, Boltzmannstraße 15, 85748 Garching, Germany

Supporting Figures
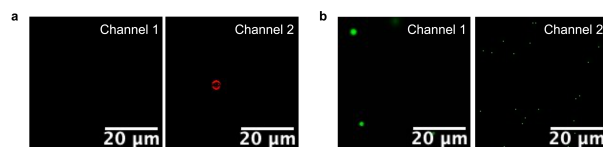
Figure S1: a) Confocal image of 5.00 mM C_6C_6 oil droplets loaded with 30.00 nM chol-T_{15}-cy5 embedded in a 0.6% agarose gel. The sample is excited at 488 nm and imaged at 500 -520 nm (Channel 1) as well as 638 nm and 650 - 750 nm (Channel 2), respectively. Chol-T_{15}-cy5 is only visible in channel 2, confirming that the DNA only accumulates on the droplet surface. b) Confocal image of 5.00 mM C_6C_6 oil droplets loaded with 10.00 μM BODIPY 493/503 embedded in a 0.6% agarose gel. The sample is excited at 488 nm and imaged at 500 - 520 nm (Channel 1) as well as 638 nm and 650 - 750 nm (Channel 2), respectively. BODIPY 493/503 is only visible in channel 1, confirming that the dye partitions into the oil droplets.
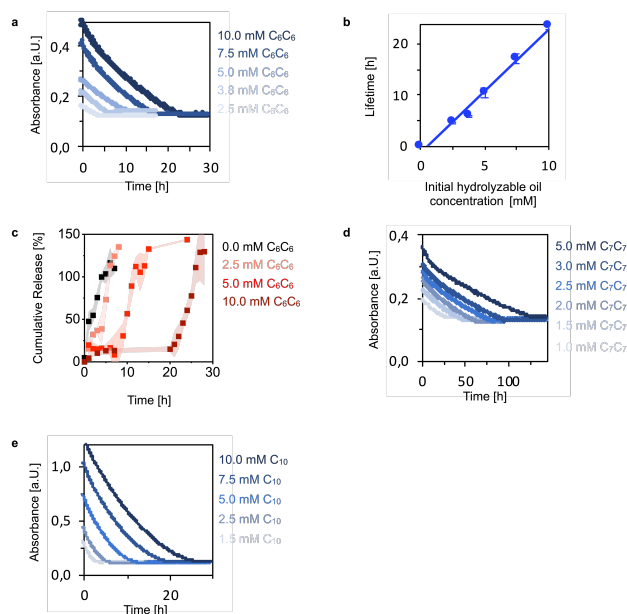
Figure S2: a) UV/Vis measurement showing the hydrolysis of 10.00, 7.50, 5.00, 3.80 and 2.50 mM C_6C_6 oil droplets embedded in a 0.6% agarose gel over time. b) The lifetime of the hydrolyzable oil is directly proportional to the initial oil concentration

that is embedded in the hydrogel. To determine the lifetimes, the absorbance was measured at 500 nm over time for 2.50, 3.75, 5.00, 7.50 and 10.00 mM C_6C_6. c) Release profile of 30.00 nM chol-T_{15}-cy5 released from an agarose gel containing 2.50, 5.00, 10.00 mM C_6C_6 droplets (red), as well as no oil droplets (black), respectively. d) UV/Vis measurement showing the hydrolysis of 5.00, 3.00, 2.50, 2.00, 1.50 and 1.00 mM C_7C_7 oil droplets embedded in a 0.6% agarose gel over time. e) UV/Vis measurement showing the hydrolysis of 10.00, 7.50, 5.00, 2.50 and 1.50 mM C_{10} oil droplets embedded in a 0.6% agarose gel over time. All experiments were performed at 25°C in PBS in triplicate.
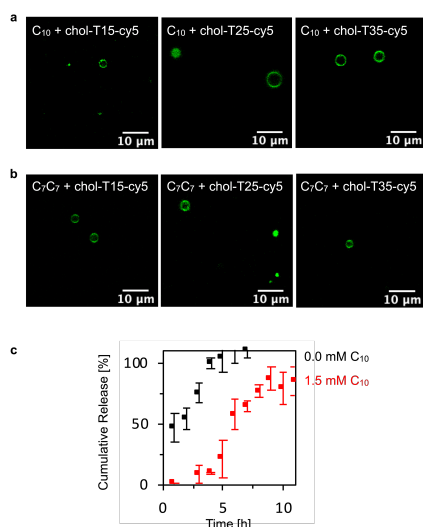
Figure S3: a) Confocal images of 30.00 nM chol-T_{15}-cy5, chol-T_{25}-cy5 and chol-T_{35}-cy5, respectively, in 10.00 mM C_{10} oil droplets embedded in a 0.6% agarose gel. b) Confocal images of 30.00 nM chol-T_{15}-cy5, chol-T_{25}-cy5 and chol-T_{35}-cy5, respectively, in 10.00 mM C_7C_7 oil droplets embedded in a 0.6% agarose gel. c) release of 10.00 nM chol-T_{15}-cy5 from an emulgel containing 1.50 mM C_{10} oil droplets (red) and from a pure agarose gel (black), respectively.
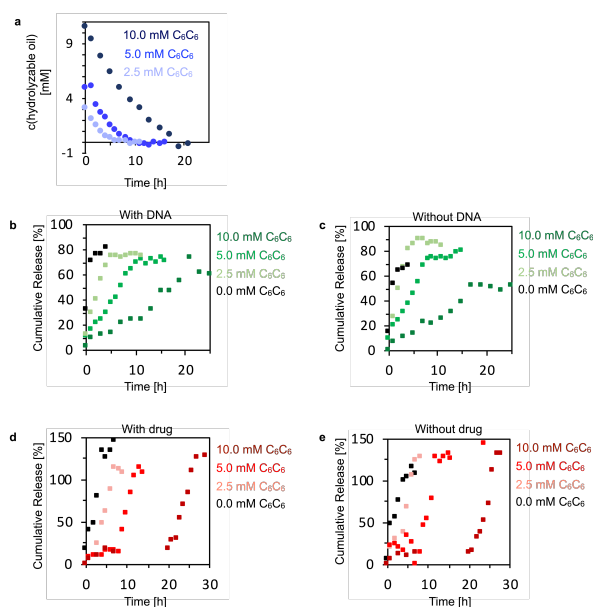
Figure S4: a) Evolution of the hydrolyzable oil concentration over time for emulgels containing initial concentrations of 10.00, 5.00 and 2.50 mM C_6C_6. The oil concentration was calculated by subtracting the measured hydrolysis product concentration of the initially used hydrolyzable oil concentration. The value is then divided by 2 and multiplied by 3, to take into account

that one anhydride molecule hydrolyses to two corresponding acid molecules and the dilution through the supernatant addition (emulgel/supernatant = 1/2). b) Release profile of 25.00 µM Nitrendipine from an emulgel containing 10.00, 5.00, 2.50 and 0.00 mM C_6C_6 oil droplets, respectively, as well as 30.00 mM chol-T_{15}-cy5. c) Release profile of 25.00 µM Nitrendipine from an emulgel containing 10.00, 5.00, 2.50 and 0.00 mM C_6C_6 oil droplets, respectively, without any DNA strands. d) Release profile of 30.00 nM chol-T_{15}-cy5 from an emulgel containing 10.00, 5.00, 2.50 and 0.00 mM C_6C_6 oil droplets, respectively, as well as 25.00 µM Nitrendipine. e) Release profile of 30.00 nM chol-T_{15}-cy5 from an emulgel containing 10.00, 5.00, 2.50 and 0.00 mM C_6C_6 oil droplets, respectively, without any hydrophobic drug.
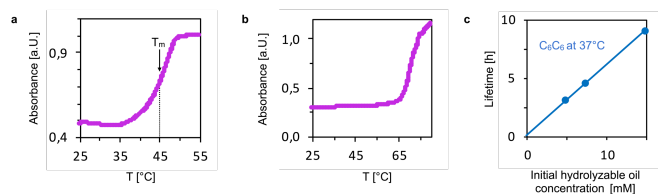
Figure S5: a) Melting curve of DNA-AuNP aggregates formed with 1.50 pmol A*-AuNPs, 1.50 pmol B*-AuNPs and 60.00 pmol linker in PBS containing 3.00 mM $MgCl_2$, 0.01%SDS and 0.05% NaN_3. b) Melting curve of the linker-target duplex. c) Lifetime of 5.00, 7.50 and 15.00 mM C_6C_6 droplets embedded in 0.6% agarose gel with a PBS supernatant containing 3.00 mM $MgCl_2$ at 37°C.

Table S1: Sequence of the used DNA strands.

DNA	DNA sequence
Chol-T_{15}-cy5	5'-(CholTEG) TTT TTT TTT TTT TTT cy5-3'
Chol-T_{25}-cy5	5'-(CholTEG) TTT TTT TTT TTT TTT TTT TTT TTT T cy5-3'
Chol-T_{35}-cy5	5'-(CholTEG) TTT TTT TTT TTT TTT TTT TTT TTT TTT TTT TTT TT cy5-3'
A* for AuNP-A*	5'-(HS) AAAAAAAAAA ATG GAA TCA-3'
B* for AuNP-B*	5'-ATC GAA CAA AAA AAA AAA A(SH)-3'
Linker DNA	5'-AAAAA TTG TTC GAT TGA TTC CAT AAAAA-3'
Target DNA	5'-(CholTEG) TTTTT ATG AAG TCA ATC AAG CAA TTTTT-3'
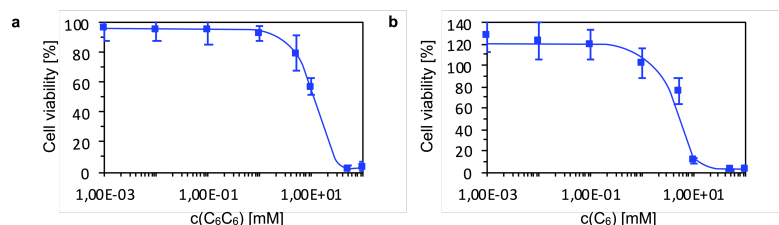
Figure S6: Cell viability of a) the hydrolyzable oil C_6C_6 with an IC_{50} value of 14.00 mM and b) the corresponding acid C_6 with an IC_{50} value of 6.25 mM with Human epithelial cells (HeLa). For both compounds, the tested concentrations were 0.001 mM, 0.01 mM, 0.10 mM, 1.00 mM, 5.00 mM, 10.00 mM, 50.00 mM and 100.00 mM.
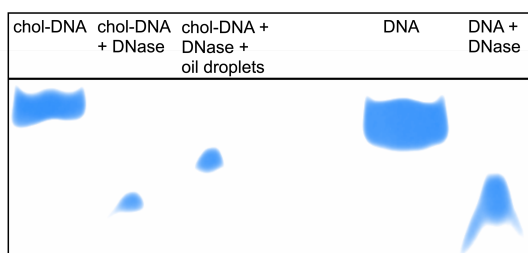
Figure S7: Polyacrylamide gel image of 1.00 nmol cholesterol-conjugated DNA and 1.00 nmol cholesterol-conjugated DNA incubated with 20 U DNase I with and without 2.50 mM C_6C_6 oil droplets as well as 1.00 nmol DNA of the same sequence without cholesterol modification with and without DNase I incubation. The gel image indicates the complete degradation of all DNA strands in the presence of DNase I. All samples were incubated for 30.00 min at 37°C and analyzed by gel electrophoresis with a 25% polyacrylamide gel and stained with methylene blue.

Methods

1. Materials

We purchased (E/Z)-2-Decen-1-ylsuccinic (C_{10} anhydride) and heptanoic anhydride (C_7C_7 anhydride) from TCI Chemicals. Hexanoic (C_6C_6 anhydride), Difluoro(2-[1-(3,5-dimethyl-2H-pyrrol-2-ylidene-N)ethyl]-3,5-dimethyl-1H-pyrrolato-N)boron (BODIPY 493/503), Poly(vinyl alcohol) (PVA, Mw = 89.000-98.000), trifluoroacetic acid (TFA), Nitrendipine, PBS tablets and Gold(III)-chloride solution (HAuCl4) were purchased from Sigma-Aldrich. The agarose powder (TopVision low melting point) was purchased by Thermo Scientific. Chol-T_{15}-cy5, chol-T_{25}-cy5, chol-T_{35}-cy5, chol- TTTTT AAC AAG CTA ACT AAG GTA TTTTT-cy5 and chol-target were synthesized by Merck KgAa. All chemicals were used without any further purification. HPLC grade acetonitrile (ACN), ethanol and PES filter units (pore size: 0.45 µm) were purchased from VWR. MilliQ-water was received from a Milli-Q®Direct 8 water purification system. DNase I (RNase free) was purchased from Thermo Fischer.

The DNA strands for the gold nanoparticles, the linker DNA strands, and the gold nanoparticles were synthesized. All chemicals used for the DNA and the DNA-AuNP synthesis as well as the Glen-Pak Cartridges were purchased by Glen Research. PD-10 columns were purchased from GE Healthcare.

2. Emulgel sample preparation and release experiments

The DNA release experiments were performed in PVA-passivated microtubes. The passivation was performed with a 5% w/v PVA solution in water following a protocol by L. Reese and coworkers.[1]

The 100.00 µM and 5.00 µM stock solutions of the cholesterol-conjugated DNA (chol-T_{15}-cy5, chol-T_{25}-cy5, chol-T_{35}-cy5, chol-TTTTT ATG AAG TCA ATC AAG CAA TTTTT-cy5) were prepared by dissolving the DNA in MilliQ-water and stored at -20°C. The 5.00 mM hydrophobic drug stock solution was prepared by dissolving the Nitrendipine in acetonitrile and stored at 8°C until further use.

The precursor stock solutions were prepared by emulsifying the anhydride (C_6C_6, C_7C_7, C_{10}) in PBS (pH 7.4) through sonication with a Branson UltrasonicsTM SonifierTM SFX250 at 25% for two minutes in an ice bath. These precursor emulsions were prepared freshly for each experiment.

The emulgels were prepared by adding 6.00 µL of the 5.00 µM DNA stock solution and 2.50 µL of the 5.00 mM drug stock solution, respectively, or both to 250.00 µL of the precursor stock solution (Scheme 1a). 250.00 µL of a 1.2% agarose stock, that was heated to 60°C, was added to the mixture and 100.00 µL of this emulgel was put on the bottom of a PVA-passivated microtubes. Subsequently, the emulgel was covered with 200.00 µL PBS and the cumulative DNA and drug release were measured in the supernatant by fluorescence spectroscopy and HPLC, respectively. All experiments were performed at 25°C in triplicate.

3. Synthesis of the DNA strands and the DNA-conjugated gold nanoparticles

The DNA strands A* and B* used for the modification of the gold nanoparticles were synthesized by solid-phase synthesis with an Applied Biosystems Model 392 DNA/RNA Synthesizer. All bases used to synthesize DNA were standard nucleotide phosphoramidites. Additionally, Thiol-Modifier C6 and 3' Thiol-Modifier C3 S–S CPG were used to synthesize thiolated strands. Once the synthesis was done, overnight deprotection of the strands was performed with 1.00 mL of ammonium hydroxide (NH_4OH) followed by purification using the DMT-On procedure with Glen-Pak Cartridge. The purified DNA was lyophilized before placing in the freezer (−20°C) for future use.

Concentration calculations and kinetic and thermal denaturation experiments were conducted with an µDrop™ on a Multiskan FC microplate reader (ThermoFisher) or a HP 8453 diode- array spectrophotometer equipped with a HP 89090A Peltier temperature controller. All DNA concentrations were determined from their absorbance at a wavelength of 260 nm with an extinction coefficient determined by Oligocalc.[2] All samples, buffers, and solutions were dissolved in Milli-Q water.

Gold nanoparticles with 13.00 nm diameters were synthesized following the established Turkevich Synthesis.[3-5] Briefly, all glassware used in the synthesis was soaked in aqua regia, rinsed multiple times with Milli-Q water and then oven-dried at 100°C. Gold(III)-chloride solution ($HAuCl_4$, 0.085 g, 0.25 mmol) was dissolved in Milli-Q water (250.00 mL) and heated to reflux. After 20 min, an aqueous solution of trisodium citrate (25.00 mL, 38.80 mM) was added. This mixture was allowed to reflux for another 10 min followed by cooling and filtering through a PES filter unit with a pore size of 0.45 µm. The nanoparticles were stored in a plastic container in the dark at room temperature. The nanoparticles were characterized by UV/Vis absorbance spectroscopy revealing the characteristic peak at $\lambda = 519$ nm of citrate capped 13.00 nm AuNPs.

The loading of thiolated DNA A* and B*, respectively, onto the AuNPs followed a modified procedure of Hurst et al.[6] Briefly, by reacting the disulfide terminated DNA strand A* or B* at room temperature with a dithiothreitol (DTT) solution (0.10 M DTT, 0.18 M phosphate buffer (PB), pH 8) for 2 h, then purifying through a PD-10 column with buffer (50.00 mM PB, 0.05% SDS, 2.5% NaN_3, pH 7), the thiolated DNA was generated. All fractions with thiolated DNA were combined and the concentrations were determined based on the absorbance at 260 nm using OligoCalc.[2] Then 15.00 nmol of the thiolated DNA was added to 1.00 mL of AuNPs in 3.00 mL water. Elution buffer was added to reach a total volume of 5.00 mL. After 20 min the thiolated DNA and gold nanoparticle mixture was salted up to 0.05 M NaCl with a salt solution containing 10.00 mM PB, 0.01% SDS and 0.5% NaN_3 (pH 7) and leaving it overnight. The next day, we further salted up to 0.70 M NaCl by adding 0.01 M NaCl solution in increments while maintaining the buffer concentration until the desired salt concentration was reached.

The purification of the DNA-AuNP A* and B* were performed as outlined by Hurst et al. with few modifications.[6] Briefly, the AuNP probes were centrifuged at 20000 RCF for 20 min and the supernatant was removed. The AuNPs were resuspended in 0.10 M NaCl buffer (0.10 M NaCl, 10.00 mM PB, 0.01% SDS, 0.5% NaN_3, pH 7). These steps were repeated 3 times. Finally, the DNA-AuNPs were resuspended in 0.10 M NaCl buffer (0.10 M NaCl, 10.00 mM PB, 0.01% SDS, 0.5% NaN_3, pH 7). The concentration of gold nanoparticles was determined via UV–visible absorbance spectroscopy at a wavelength of 525 nm with a molar coefficient ε of 2.4×108 $M^{-1}cm^{-1}$.[7]

4. Preparation of the gold nanoparticle aggregates

The DNA-AuNP A*-B*-aggregates were freshly prepared for every experiment by adding 1.50 pmol AuNP-A*, 1.50 pmol AuNP-B* and 60.00 pmol linker DNA to a 10.00 mM PBS containing 0.01% SDS, 0.5% NaN_3 and 3.00 mM magnesium chloride to get a total volume of 1.00 mL. After 1 day incubation at room temperature, the gold nanoparticle aggregates are formed and were used in experiments.

5. Fluorescence spectroscopy

The concentration of the released cholesterol-conjugated and cy5-tagged DNA in the supernatant was determined by fluorescence spectroscopy with Jasco Spectrofluorometer FP-8300. The samples were excited at 600 nm and the emission was measured at 665 nm at 25°C in triplicate. Calibration curves for all DNA strands were performed with the same method in PBS in triplicate.

6. Microscopy

Confocal fluorescence microscopy was performed on a Leica TCS SP8 confocal microscope using a 63× water immersion objective. 1.00 µL BODIPY 493/503 or 1.50 µL cholesterol-conjugated DNA or both was added to the freshly prepared hydrolyzable oil emulsion. The emulgel samples were prepared as previously described. The samples were excited at 638 nm and imaged at 650 – 750 nm with a HyD detector (pinhole: 1 a.u., laser power: 0.03, gain: 150.0%) for chol-T_n-cy5. For the BODIPY 493/503 dye the samples were excited at 488 nm and imaged at 500 – 520 nm with a PMT detector (pinhole: 1 a.u., laser power: 1.00, gain: 400.0%). The measurements were performed at 25°C.

7. Analytical HPLC

The released drug and acid concentrations were determined by analytical high-performance liquid chromatography (HPLC, Thermo- fisher Dionex Ultimate 3000, Hypersil Gold 250 × 4.8 mm) using a linear gradient of MilliQ-water and acetonitrile, each with 0.1% TFA. All compounds were detected with a UV/Vis detector at 220 and 240 nm. The method we used was programmed to run a H2O:ACN gradient from 98:2 to 2:98 in 13 min (Table 1). Calibration curves for the drug (in ACN) and the carboxylate (in PBS) were conducted with the corresponding method in triplicate. All experiments were performed at 25°C in triplicate.

Table S2: Chemical compounds and the in the HPLC measured retention time, the wavelength at which the compound was detected, the calibration value and molar mass.

Compound	Retention time [min]	Wavelength [nm]	Calibration value	M [g/mol]
Nitrendipine	11.29	240	0.52	360.36
C_{10} acid	11.79	220	3.25	238.32

8. UV/Vis-spectroscopy

A Multiskan FC microplate reader (ThermoFisher) was used for UV/vis measurements. The emulgels were pipetted on the bottom of a 96-well-plate (tissue culture plate non-treated) and subsequently covered with PBS to measure the turbidity over time. The measurements were performed at a wavelength of 500 nm at 25°C in triplicate.

To measure the absorbance of the gold nanoparticle aggregates over time, 1.00 mL gold nanoparticle aggregate suspension was pipetted into quartz glass cuvette. The absorbance at a wavelength of 525 nm was measured every 10 min at 37°C. Before and after measurements the sample was mixed carefully to prevent precipitation of the aggregates. When the target DNA was released from the emulgel, the samples were prepared as previously described and 100.00 µL of the emulgel was pipetted on the bottom of the quartz glass cuvette. Subsequently, the emulgel was covered with the gold nanoparticle aggregate suspension. The absorbance was measured at 525 nm at 37°C and the supernatant was mixed carefully to prevent precipitation of the aggregates before and after measurements. When the target DNA strand was added manually, the DNA was added after 50 min to make sure that the nanoparticle aggregate solution was equilibrated and the disassembly only starts after the target addition. All experiments were performed in triplicate.

9. Cell viability studies

Human epithelial cells (HeLa) were cultured in minimum essential medium (MEM; Sigma-Aldrich) containing 10% (v/v) fetal bovine serum (FBS; Sigma-Aldrich), 2 mM L-glutamine (Sigma-Aldrich), and 1% (v/v) of a non-essential amino acid solution (Sigma-Aldrich), and 100 U/mL penicillin-streptomycin (Sigma-Aldrich) at 37 °C in a humidified atmosphere with 5% CO2.

The viability of HeLa cells after incubation with the hydrolyzable oil C6C6 and the corresponding acid C_6 was assessed by a WST-1 assay (5015944001, Sigma-Aldrich). First, 5,000 cells were seeded into each well of a 96-well plate and incubated for 24 h. Then, the medium was replaced by a medium containing different concentrations of C_6C_6 or C_6, respectively: 0.001 mM, 0.01 mM, 0.10 mM, 1.00 mM, 5.00 mM, 10.00 mM, 50.00 mM, and 100.00 mM. Cells incubated with a cell culture medium were used as a negative control group. Cells incubated with 50% (v/v) methanol were used as a positive control group. After a further incubation time of 24 h, the cells were washed twice with Dulbecco's phosphate-buffered saline (D-PBS, Sigma-Aldrich). To determine the cell viability of the treated cells, a cell culture medium enriched with 2% (v/v) water-

soluble tetrazolium (WST-1) solution was incubated with the cells for 1 h. Afterward, the metabolized medium was pipetted bubble-free into a fresh well plate and the absorbance of the solutions was measured at 450 nm with a plate reader (SpectraMax ABS Plus, Molecular Devices, San José, USA). Finally, the cellular viability was calculated by normalizing the absorbance value of a test group to those of the negative control group. Each group has 6 replicates of independent samples. All values obtained were used for the determination of the half-maximal inhibitory concentration (IC_{50}) of C_6C_6 or C_6.

10. DNA degradation by DNase I

1.00 nmol of cholesterol-conjugated DNA or 1.00 nmol DNA of the same sequence but without cholesterol modification were incubated with 20 U DNase I (RNase free) in a reaction buffer containing $MgCl_2$. Additionally, 2.5 mM C_6C_6 oil droplets were added to some samples. The reaction mixtures were incubated for 30 min at 37°C and subsequently frozen at -20°C and lyophilized. To analyze the samples via gel electrophoresis, the samples were diluted with 2.00 µL MQ water and 0.6 µL 6x running dye (0.25% (w/v) bromophenol blue and 40% (w/v) sucrose). The samples were loaded into a 25% polyacrylamide gel. After 50 min gel electrophoresis at 250V, the gels are stained with 0.02% methylene blue staining solution for 30 min and imaged with a GelDoc EZ Imager (BioRad).

Bibliography

1. Spoelstra, W. K.*, et al.*, *Langmuir,* 2020, **36**, 1956-1964.

2. Kibbe, W. A., *Nucleic Acids Research,* 2007, **85**, W43-W46.

3. Storhoff, J. J.*, et al.*, *Journal of the American Chemical Society,* 1998, **120**, 1959-1964.

4. Enustun, B. V., and Turkevich, J., *Journal of the American Chemical Society,* 1963, **85**, 3317-3328.

5. Kimling, J.*, et al.*, *The Journal of Physical Chemistry B,* 2006, **110**, 15700-15707.

6. Hurst, S. J.*, et al.*, *Analytical Chemistry,* 2006, **78**, 8313-8318.

7. Stoeva, S. I. L., J. S.; Thaxton, C. S.; Mirkin, C. A., *Angew. Chem.,* 2006, **45**, 3303-3306.

5 Hydrolyzable Emulsions as Biomaterials

Abstract

In Chapters 3 and 4, I described a simple, versatile, and cheap drug delivery platform that comprises hydrolyzable oil droplets that are embedded in a hydrogel. This emulgel is subsequently covered with a PBS supernatant. The oil droplets can incorporate various hydrophobic drugs, which can be released linearly with a tunable release rate and period. Furthermore, cholesterol-conjugated oligonucleotide strands can accumulate on the oil droplets' surface. This gives control over the oligonucleotide's release onset. Moreover, this formulation allows the dual release of a hydrophobic drug with zero-order kinetics and a subsequent rapid release of cholesterol-conjugated DNA. In this chapter, I examined the performance of our drug delivery platform under physiological conditions. This means that the PBS supernatant is replaced with media that have a similar composition as human blood plasma. Hydrolysis studies of C_7C_7 or C_{10} containing emulgels in different media showed that the hydrolysis rate is increasing if primary amines are present. As a consequence, a drastically decreased oil lifetime could be observed, which is not sufficient for the constant and linear release of drugs.

5.1 Introduction

When developing a drug delivery platform, it is important to investigate the in vitro drug release, as described in Chapter 3, and *in vivo*. Studying drug release in animals is a crucial step before a developed drug delivery platform ever reaches human clinical trials and is eventually put on the market.[141] However, developing animal models and conducting such experiments, *i.e., in vivo* toxicity tests, is expensive and time-consuming. For example, testing new pharmaceutical agents using rodents can cost between $2 and $4 million and add 4 to 5 years until all required studies are completed.[142, 143] Therefore, a drug delivery system must be tested under conditions that are as close as possible to physiological conditions. This includes temperature, pH, body fluid exchanges, and the platform's performance in a biological medium. As described in Chapter 3, the hydrolyzable emulsion-based drug delivery system can release hydrophobic drugs linearly at body temperature (37°C) and a physiological pH value of 7.4. We measured the drug release in phosphate-buffered saline, which has an osmolarity and ion concentration that match the human body's. We found that this does not influence the order of the release. Moreover, in previous studies, Wanzke *et al.* showed that a change in the temperature did not change the order of the release; only the release period and rate increased with temperature. We showed in Chapter 3 that simulated body fluid exchanges do not influence the release kinetics. Therefore, this drug delivery platform can also be applied to body parts with high fluid turnover.

Previously we have studied our drug delivery platform in biorelevant conditions. Yet they did not reflect the complexity of the composition of body fluids. For example, human blood plasma contains various proteins, ions, and other organic molecules like amino or fatty acids.[144-147] Since future applications of our formulation are located in or close to the human body*, i.e.,* as hydrogel wound dressing that contains an anti-inflammatory drug or as catheter coating, it is crucial to simulate such conditions as precisely as possible. Therefore, we have tested our emulgel drug delivery platform in pure fetal bovine serum (FBS), which has a composition that is similar to human blood plasma and is commercially available.

5.2 Hydrolyzable emulsions in different media

We followed the hydrolysis kinetics over time in different aqueous media to examine our emulgel drug delivery platform under close to physiological conditions. This means the PBS supernatant, in which the drug is being released from the emulgel, was replaced by an FBS supernatant (**Figure 12a**). Pure FBS was chosen as supernatant since it has a similar

composition to human blood serum. Subsequently, the absorbance at 500 nm of an emulgel comprising 10.0 mM C_7C_7 and 7.50 mM C_{10} oil droplets, respectively, as a measure of the presence of oil droplets, was followed over time (**Figure 12b-c**). **Figure 12b-c** shows that the lifetime of C_7C_7 and C_{10} oil droplets in FBS is drastically reduced compared to that in PBS. While in PBS, the oil droplets hydrolyze over 90 hours for C_7C_7 and 5 hours for C_{10}, the lifetime in FBS is decreased by 96% and 84%, respectively. This indicates that the FBS milieu sped up the hydrolysis kinetics of the oil droplets.
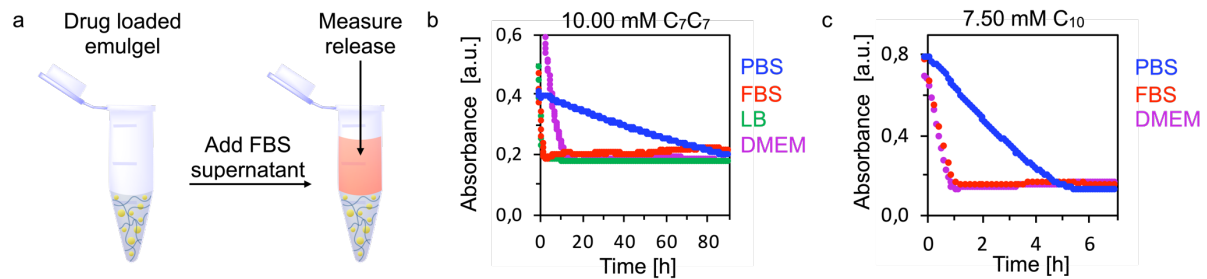
Figure 12: a) Scheme of drug-loaded emulgel, which is subsequently covered with pure FBS. Hydrolysis of **b)** 10.00 mM C_7C_7 oil droplets and **c)** 7.50 mM C_{10} oil droplets embedded in a 0.6% agar gel that is covered with a PBS supernatant (blue), an FBS supernatant (red), an LB supernatant (green), or a DMEM supernatant (purple). The preparation of the emulgel was still conducted with PBS as an aqueous solution.

Furthermore, Dulbecco's Modified Eagle Medium (DMEM) and PBS-buffered lysogeny broth (LB), used to support mammalian cells' growth and bacteria, respectively, were used as supernatant. In contrast to FBS, these media have a known concentration of ingredients and similar salt concentrations as PBS and are not subjected to reproducibility issues (**Table 1**).[148-150] The hydrolysis profile of both 10.00 mM C_7C_7 and 7.50 mM C_{10} oil droplets embedded in a hydrogel and covered with LB and DMEM as supernatant, respectively, showed the same decrease in the lifetime as with the FBS supernatant (**Figure 12b-c**). This suggests that pure LB and pure DMEM contain the same or similar compounds that drastically increase anhydride hydrolysis and, thus, the lifetime of the oil.

Table 1: Composition PBS, FBS, LB, and DMEM. Only the compounds, *i.e.,* salts and amino acids, with the highest concentrations are listed in this table. For FBS, the average concentrations are used because of the varying concentrations of each FBS batch.[148-154]

Compound	PBS	LB	DMEM	FBS
NaCl [mM]	137.0	137.0	109.0	142.0 mM Na^+
KCl [mM]	2.7	2.7	5.0	155.5 mM Cl^-
Na_2HPO_4 [mM]	8.0	8.0	1.6	8.0 mM K^+
KH_2PO_4 [mM]	2.0	2.0	-	2.3 mM PO_4^{3-}
$NaHCO_3$ [mM]	-	-	44	1.1 mM Mg^{2+}
$CaCl_2$ [mM]	-	-	2.0	3.0 mM Ca^{2+}
Glucose [mM]	-	-	24.0	7.0
Amino acids [mM] (total concentration)	-	-	13.1	5.4
Lysine [mM]	-	-	8.0	0.2
Other	-	1.0% (w/v) tryptone 0.5% (w/v) yeast extract	0.16 mM vitamins	38.0 mg/mL proteins 0.35 mM BSA
pH	7.4	7.0	7.4	7.5

As described in Chapter 1.6, the oil droplets' hydrolysis rate (v) is equal to the hydrolysis rate constant (*k*) multiplied by the anhydride's solubility, which is constant in the presence of oil droplets. Consequently, the hydrolysis rate could change if the anhydride solubility changes due to the varying supernatants. Furthermore, if the hydrolysis rate constantly changes, *i.e.,* due to changes in the pH value, the hydrolysis rate would also change.[136, 155, 156] Moreover, the reaction of the anhydride molecules in solution or in the oil droplets with a compound present in FBS but not PBS could lead to different lifetimes of the emulsion. As previous work showed, the pH influences the hydrolysis rate, with higher pH leading to faster hydrolysis. However, the difference between the lifetime at, *i.e.*, pH 6 and pH 7.4 is minimal.[136] This means

that the different pH of the used supernatants between 7.0 and 7.5 does not cause a more than 84% shorter lifetime.

As shown in **Table 1**, the salt and ion concentrations in the used supernatants are very similar, with high concentrations of sodium chloride or sodium and chloride ions, respectively, and low concentrations of other ions. However, PBS has no further additives, while FBS, LB, and DMEM have various additional compounds. For example, FBS and DMEM contain high levels of glucose. To test if the glucose concentration leads to short droplet lifetimes, we covered an emulgel containing an initial concentration of 10.00 mM C_7C_7 or 7.50 mM C_{10} oil droplets with a PBS supernatant containing 7.00 mM and 24.00 mM glucose. Subsequently, the absorbance at 500 nm was monitored over time (**Figure 13a**). The hydrolysis profiles of emulgels covered with a glucose-containing PBS supernatant are similar to the hydrolysis in pure PBS. The lifetime of a C_{10} emulgel can even be extended by 3 hours if a glucose-containing PBS is used as supernatant. However, **Figure 13** indicates that D-glucose (**Figure 13b**) has minimal to no influence on the hydrolysis kinetics of the anhydride oil droplets.
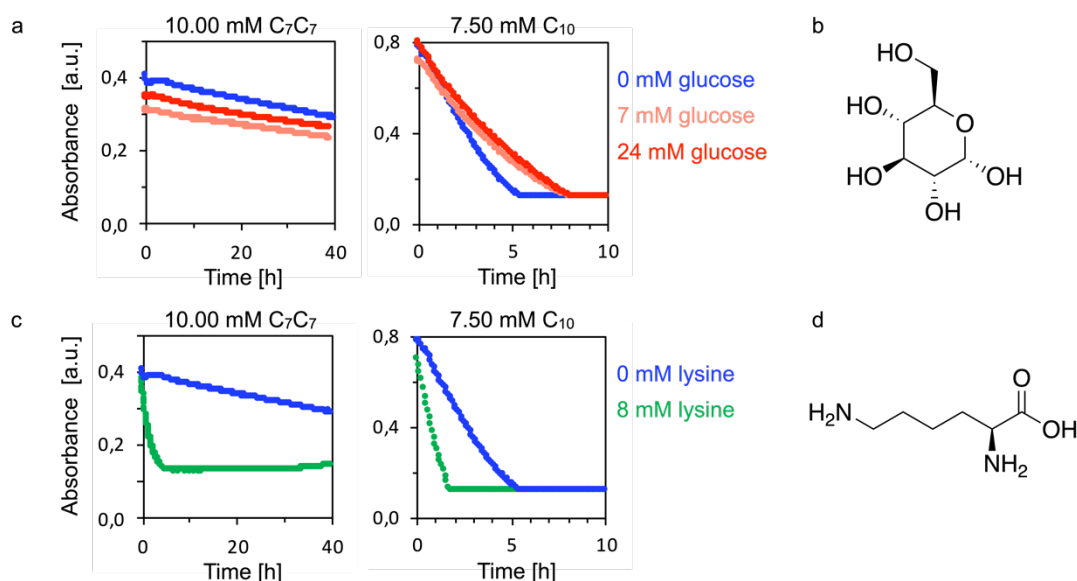
Figure 13: a) Measured absorbance at 500 nm of an emulgel containing 10.00 mM C_7C_7 or 7.50 mM C_{10} oil droplets, respectively, that is covered with a PBS supernatant that contains 7.00 mM and 24.00 mM D-glucose, respectively. **b)** Molecular structure of D-glucose. **c)** Measured absorbance at 500 nm of an emulgel containing 10.00 mM C_7C_7 or 7.50 mM C_{10} oil droplets, respectively, that is covered with a PBS supernatant that contains 8.00 mM L-lysine. **d)** Molecular structure of L-lysine.

Another group of additives that are present in FBS, DMEM, and LB are amino acids. While PBS contains no amino acids, the average total amino acid concentration of FBS is 5.4 mM

(**Table 1**). The total amino acid concentration of DMEM is even higher (13.1 mM), while LB has undefined levels of free amino acids that may be part of the yeast extract. Also, human blood plasma contains, on average, 2.9 mM free amino acids.[147] To determine the influence of amino acids on the hydrolysis kinetics, 8.00 mM L-lysine (**Figure 13d**) was added to the PBS supernatant to represent the free amino acids in FBS, DMEM, and LB. **Figure 13c** shows that when lysine was added to the supernatant, the hydrolysis was faster, and the lifetime of the emulgel decreased from 90.0 hours to 4.0 hours for C_7C_7 and from 5.0 hours to 1.5 hours for C_{10}. The hydrolysis profile aligns with the hydrolysis profiles performed in FBS, DMEM, and LB, indicating that lysine and potentially other amino acids are speeding up the hydrolysis of the anhydride. Presumably, the amino acids' primary amine moieties react with the hydrolyzable oil's anhydride moiety. Since amines are better nucleophiles than water, it is possible that the amine moiety of the amino acid reacts faster with the anhydride molecules and therefore results in faster depletion of the oil droplets.[157] This prevents the self-protection mechanism and, thus, the zero-order hydrolysis of the anhydride.

Besides amino acids, proteins and enzymes are also present in the blood plasma, FBS and LB. For example, the blood plasma of a healthy adult male contains, on average, 0.65 mM human serum albumin that contains 585 amino residues, including 59 lysine moieties. The primary amine groups of the lysine residues can also react with the hydrolyzable oil.[147, 158] As shown in Chapter 3, the hydrolyzable oil droplets stay immobilized in the hydrogel. Thus the hydrolysis and the reaction of the anhydride with primary amines take place in the hydrogel. To prevent the human serum albumin from diffusing into the hydrogel, the drug delivery platform could be encapsulated by a membrane with a pore size that is smaller than 66.4 kDa.[159] However, this is not a sufficient strategy to prevent the diffusion of amino acids and their reaction with the anhydride.

5.3 Conclusion and Outlook

In this chapter, we have shown that physiological media such as FBS have a detrimental effect on the drug release profile. We have demonstrated that the reason for this is the fast reaction of primary amine moieties with the anhydride molecules, due to the high nucleophilicity of amines. This reaction is faster than the hydrolysis of the anhydride with water, therefore preventing the self-protection mechanism. These primary amine groups can be found as part of free amino acids of proteins in all physiological media. While it may be possible to physically separate proteins and enzymes from the emulgel by a membrane with suitable pore size, this is not adequate for free amino acids.

However, since all human body fluids can contain free amino acids or proteins with reactive amino moieties, our emulgel drug delivery system is not sufficient yet to linearly release drugs *in vivo*. Thus, our formulation needs to be further optimized before it can be applied in the medical field. One approach to overcome this challenge is to use hydrolyzable emulsions that are less electrophilic and thus not susceptible to reaction with primary amines. For example, boronic esters or orthoesters could be suitable candidates. These compounds are already researched for medical applications, *i.e.,* boronic acids as glucose sensors to treat diabetes mellitus.[160-164]

6 Alternative Hydrolyzable Oils

Abstract

In Chapter 5, I demonstrated the limitations of our formulation, which comprises a hydrophobic anhydride that forms oil droplets and is susceptible to hydrolysis aqueous solution. The presence of amine moieties in human body fluids increases the droplets' hydrolysis rate and thus drastically decreases the formulation's lifetime. Since all human body fluids can contain free amino acids or proteins with reactive amino moieties, our formulation is insufficient for clinical applications. Thus, I replaced the hydrophobic anhydride with orthoesters and boronic esters susceptible to hydrolysis. These compounds, which form oil droplets in an aqueous solution and can incorporate hydrophobic compounds *i.e.,* Nile red, are less electrophilic and therefore do not react with amine moieties. However, sufficient hydrolysis of the synthesized orthoesters (tributyl orthoformate) only occurs at pH 6 or lower. Thus, zero-order at physiological pH is not possible. However, this formulation could deliver drugs in low-pH environments, *i.e.,* malignant tumors. Like the orthoesters, the synthesized boronic esters are also unsuitable to release drugs under physiological conditions linearly. This is because, at pH values higher than the boronic acid's pKa value, the esterification process is favored over the hydrolysis. Thus the synthesized boronic ester is favored over the boronic acid and the diol at pH 7.4. However, I suggest that this limitation could be overcome by choosing a boronic acid with a pKa value higher than the physiological pH of 7.4 for the boronic ester synthesis.

6.1 Introduction

As concluded in Chapter 5, we have shown that anhydride-based hydrolyzable emulsions as drug delivery systems have one major drawback: the high reactivity of anhydride moiety with primary amine groups that are part of free amino acids and proteins. These compounds are present in all human body fluids, therefore we need to develop a hydrolyzable oil that resists primary amines. We tested two different classes of molecules, which are less electrophilic than the previously used hydrophobic anhydrides, as hydrolyzable emulsions: boronic esters and orthoesters.

6.2 Boronic Esters

One class of hydrolyzable reagents that does not react with amines are boronic esters. Boronic esters and their corresponding boronic acids are widely studied as materials for biomedical applications. It has already been shown that these compounds display good biocompatibility *in vitro* and *in vivo*.[165] Furthermore, many examples of boronic esters and acids are already incorporated into various materials to facilitate drug delivery.[165-168] For example, PEG-dendritic copolymers that are functionalized with peripheral boronic acid can optimize the delivery of the chemotherapeutic gemcitabine. Upon addition of the diol catechol the polymer self-assembles into micelles, that can encapsulate gemcitabine.[169] Since most boronic esters are stable at neutral pH and only hydrolyze at mildly acidic pH, they can also be incorporated into polymers to gain pH-responsive materials.[166] Importantly, boronic esters can be easily synthesized from commercial boronic acids and diols.[170]

We designed our emulgel so that the boronic ester is thermodynamically less favored than the boronic acid and the diol, thus showing a sufficient hydrolysis profile. Furthermore, the boronic ester should form oil droplets to incorporate a hydrophobic drug and achieve zero-order hydrolysis *via* the self-protection mechanism. Lastly, reactions with compounds containing amine moieties that are present in the human should not take place with the boronic ester.

We synthesized a library of different boronic esters BE1 – BE5 (**Scheme 5a**). The molecular structures of these boronic esters are displayed in **Scheme 5b**.
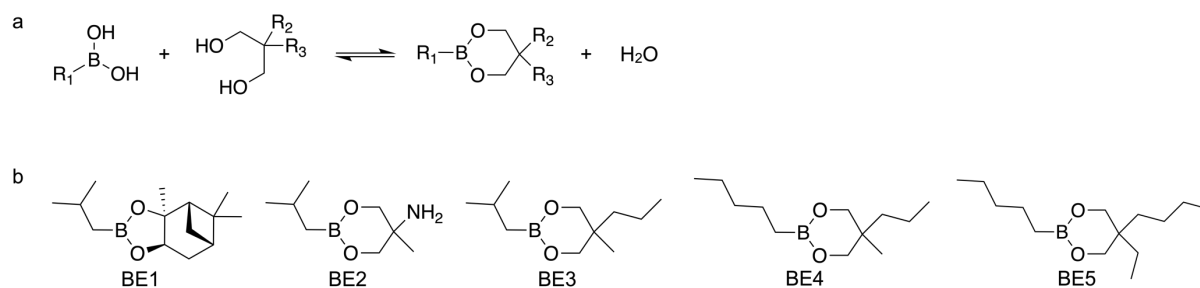
Scheme 5: a) Reaction scheme of a boronic acid with a diol to form a boronic ester. **b)** Scheme of the synthesized boronic esters BE1 – BE5.

All synthesized boronic esters were transparent oils, that form oil droplets upon sonication in an aqueous solution such as PBS (**Figure 14a-e (middle)**). As the boronic ester droplets incorporated the hydrophobic dye Nile red, we assume that hydrophobic drugs can be incorporated as well. We examined if the boronic ester emulsion hydrolyses by monitoring the absorbance at 500 nm over time as a measure of the turbidity and thus the presence of oil droplets (**Figure 14a-e (bottom)**). The turbidity profiles in **Figure 14b-e** show a linear decrease in the absorbance over time for BE2, BE3, BE4, and BE5. This indicates that these boronic ester droplets hydrolyze following zero-order kinetics. Moreover, the lifetimes of the boronic ester emulsions differ. While BE5 has the longest lifetime of 25.00 hours at the lowest concentration of 25.00 mM, 50.00 mM BE2 and BE3 have shorter lifetimes of 0.75 and 1.50 hours. In between is BE4 with a lifetime of 6.00 hours when an emulgel containing 35.00 mM oil droplets is used. We assume that the different lifetimes are a consequence of varying solubilities in aqueous solution, meaning that less soluble boronic esters like BE5 would hydrolyze slower than more soluble boronic esters such as BE2 and BE3. In contrast to BE2 to BE5, BE1 shows a constant absorbance over time, suggesting that this boronic ester does not hydrolyze and is stable in PBS at pH 7.4. Here, the boronic ester is favored over the boronic acid and the diol.
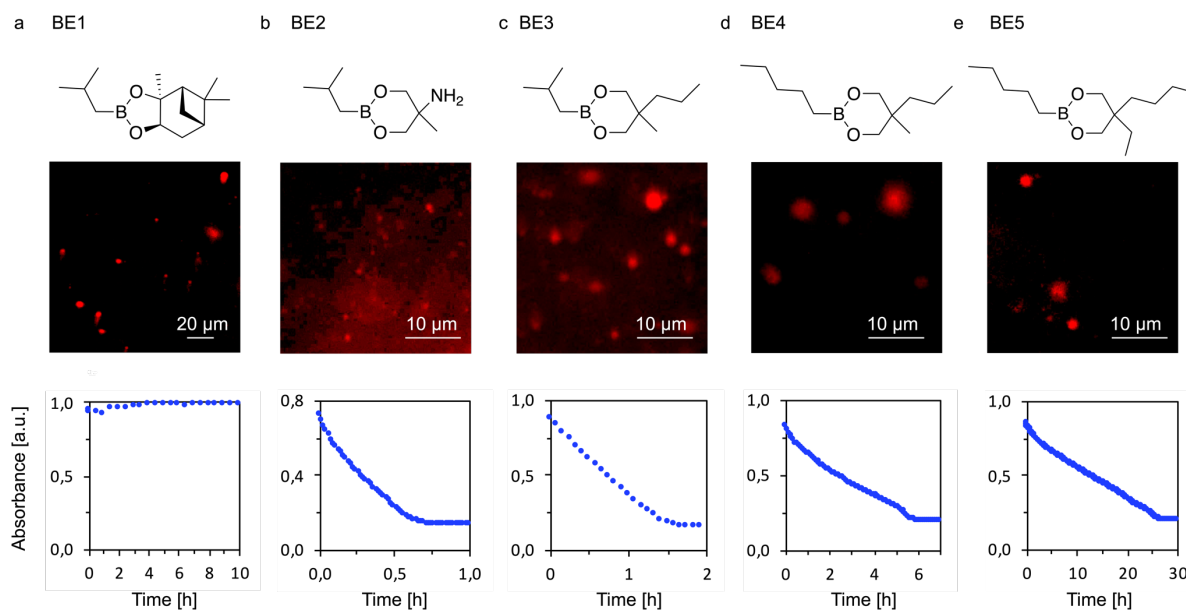
Figure 14: Molecular structure, fluorescence microscope image of boronic ester oil droplets with 5.00 µM Nile red dye and absorbance profile of **a)** 1.50 mM BE1 b) 50.00 mM BE2 c) 50.00 mM BE3 d) 35.00 mM BE4 and e) 25.00 mM BE6 trapped in a 0.6% agar gel. The absorbance was measured at 500 nm over time at 37.0°C with a PBS supernatant in triplicate.

Since BE5 has the longest lifetime, this boronic ester is the most suitable compound for a drug delivery platform and therefore was used in these experiments. Next, the influence of different physiological media is examined by monitoring the turbidity of boronic ester emulgels containing 50.00 mM BE5. Here, different physiological supernatants were used to cover the emulgel such as FBS, LB, and DMEM (**Figure 15a**). Especially the hydrolysis kinetics in FBS are important to examine due to the similarity of FBS to human blood plasma. **Figure 15** shows, that the absorbance profile in FBS, DMEM, and LB are in line with the profile in PBS. This indicates that different concentrations of various amino acids, proteins, ions, as well as other compounds, do not influence the hydrolysis kinetics of BE6. Moreover, if a PBS supernatant with a defined concentration of L-lysine or D-glucose is used, no changes in the turbidity profile are visible (**Figure 15b**).
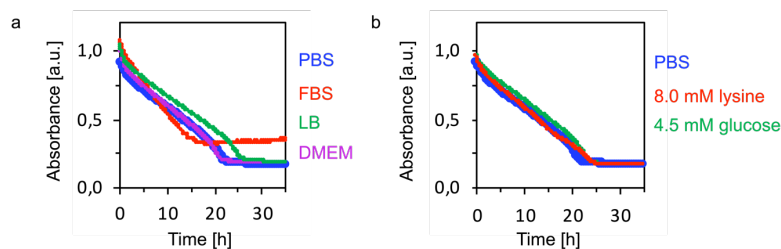
Figure 15: Measured absorbance over time of emulgels containing 25.00 mM BE5 oil droplets that are covered with **a)** PBS, FBS, LB, and DMEM supernatants and **b)** with a PBS supernatant containing either 8.00 mM L-lysine or 4.50 mM D-glucose, as well as pure PBS. The experiments were performed at 37°C in triplicate.

Next, 25.00 µM of different hydrophobic drugs, namely ritonavir, nitrendipine, mebendazole, and lopinavir were incorporated into a boronic ester emulgel to study the drug release kinetics. **Figure 16a-d** shows the cumulative release profiles of these drugs from 25.00 mM BE5 oil droplets that were embedded in a hydrogel, as well as the release profile of the drugs from a pure hydrogel. As already described in Chapter 3, the release of the drugs from the hydrogel is a diffusion-controlled process and thus follows first-order kinetics (**Figure 16a-d** (black)). However, if the drugs are released from the boronic ester emulgel, the release kinetics also show a first-order profile rather than a zero-order release profile (**Figure 16a-d** (red)). The release of ritonavir and nitrendipine reaches approximately 75.0% total cumulative release for the boronic ester emulgel as well as the pure hydrogel system. In addition, the release kinetics of both systems are close to identical. This indicates, that these drugs may not partition into the boronic ester droplets and hence diffuse from the hydrogel into the surrounding supernatant. The total cumulative release of mebendazole and lopinavir from a boronic ester emulgel only reaches 50.0 to 60.0%, in contrast to 80.0 to 100.0% release from the pure hydrogel. The incomplete release indicates that a part of the drug remains in the hydrogel. However, this requires the presence of oil droplets, even though the turbidity profile of a BE5 emulgel indicates the complete hydrolysis of the droplets.

One explanation for these observations is, that the boronic ester is in equilibrium with the boronic acid and the diol (**Figure 16e**). If the boronic ester is favored at the chosen conditions (37°C and pH 7.4), the boronic ester may hydrolyze to its boronic acid and diol which can then revert back to the boronic ester. Phase separation leads to the formation of a boronic ester phase in either the hydrogel or the supernatant followed by partitioning of the hydrophobic drug molecules into these newly formed phases. Especially if the boronic ester phase is formed as a layer on top of the supernatant it would be invisible in the turbidity profile. Indeed, the measurement of the BE5, the 2-butyl-2-ethyl propane-1,3-diol, and the N-Pentylboronic

acid concentration in PBS at 37°C reveals that 70.0% BE5 and 30.0% diol and boronic acid are present in the equilibrium at these conditions. Furthermore, the spontaneous formation of oil droplets can be observed under the microscope if 25.00 mM N-Pentylboronic acid is added to a solution comprising 25.0 mM 2-butyl-2-ethyl propane-1,3-diol in PBS (**Figure 16f**). As the esterification process is favored if the pH is higher than the boronic acids' pKa value, selecting a boronic acid with a pKa value that is higher than the physiological pH of 7.4 could overcome the limitations of BE1 – BE5.[165, 169] For example boronic acids with phenyl moieties can have pKa values up to 9.9.[171]
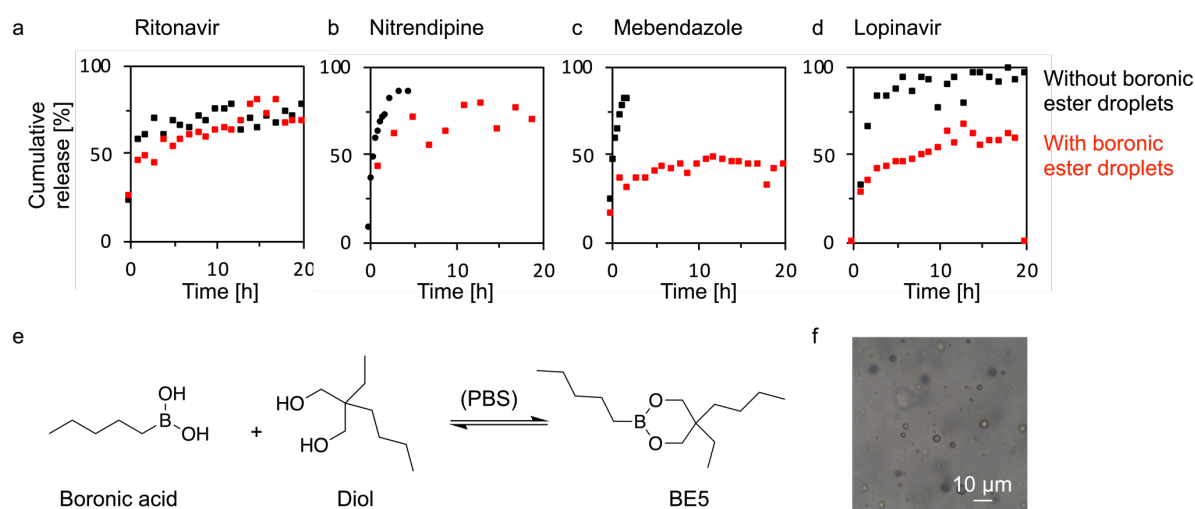
Figure 16: Cumulative release profile of 20.00 μM **a)** ritonavir, **b)** nitrendipine, **c)** mebendazole, and **d)** lopinavir from an emulgel comprising 25.00 mM BE5 oil droplets in 0.6% agar gel (red) and from a 0.6% agar gel that does not contain oil droplets (black). The experiments were performed at 37°C in triplicate. **e)** Equilibrium of the boronic acid, the diol, and boronic ester BE5. **f)** Brightfield microscope image of 25.00 mM N-Pentylboronic acid and 25.00 mM 2-butyl-2-ethyl propane-1,3-diol spontaneously forming oil droplets in PBS at 37°C.

6.3 Orthoesters

A second functional group that should be explored is the orthoesters, which can be hydrolytically cleaved into one formate and two alcohol molecules. Orthoesters also been widely researched for medical applications.[164, 172] For example, block-copolymer micelles that are modified with orthoester side chains can incorporate the anticancer drug doxorubicin into the hydrophobic core. Due to the hydrolysis of the orthoester chains, the micelles can disassemble at low pH and release the encapsulated agent.[173] Furthermore, orthoesters show a high level of stability towards strong nucleophiles such as amines, especially in physiological conditions. The formation of orthoamides through the reaction of an orthoester with an amine requires high temperatures and often a catalyst.[174, 175]

To study if orthoesters are suitable hydrolyzable oils for the delivery of hydrophobic drugs, we tested tripropyl orthoformate (TPO) and tributyl orthoformate (TBO), both commercially available (**Figure 17a**). First, an emulsion of 12.50 mM TPO or TBO, respectively, was prepared and mixed with 5.00 µM Nile red and gellified with a hydrogel to examine the ability of the orthoesters to form oil droplets that can incorporate a hydrophobic compound. **Figures 17b** and **c** show both the TPO and the TBO can form Nile red-loaded oil droplets in PBS. Next, the hydrolysis profiles of both orthoester compounds were examined by measuring the turbidity of an emulgel containing 12.50 mM TPO or TBO oil droplets, respectively, over time (**Figure 17d**). While both compounds show a linear decrease in absorbance, the lifetime of the oil droplets differs enormously. TPO oil droplets have a lifetime of 2.00 hours, which is insufficient for a prolonged zero-order drug delivery platform. In contrast, TBO may be a suitable hydrolyzable oil because it lasts 60.00 hours.

Consequently, TBO was chosen for further experiments. **Figure 17e**, which displays the first 20 hours of the absorbance profiles of TBO emulgels covered with different supernatants, shows that neither FBS nor PBS that contains 8.00 mM L-lysine influences the hydrolysis kinetics. This makes TBO ideal for application in biological fluids.
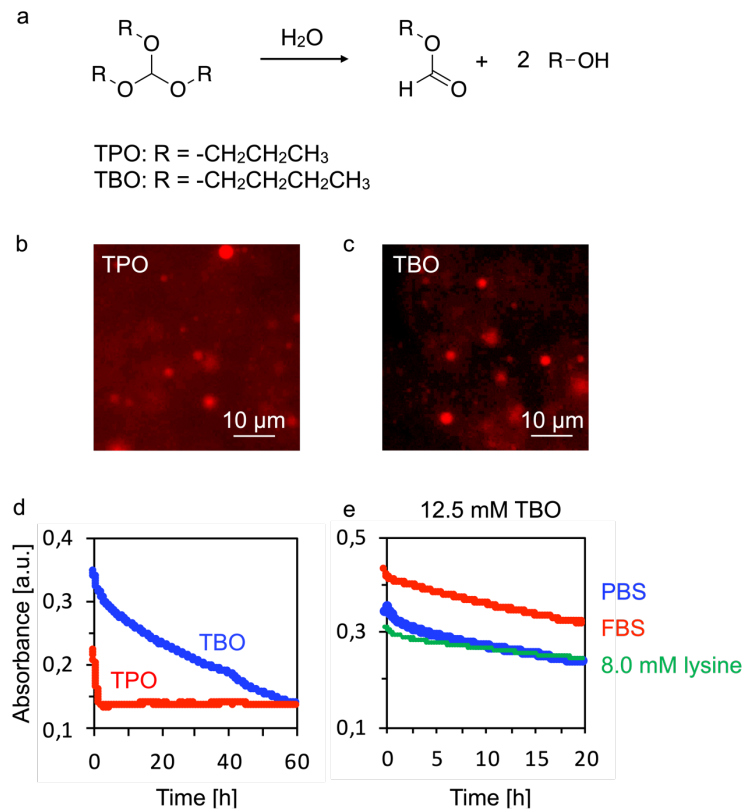
Figure 17: a) Reaction scheme of the hydrolysis of an orthoester to its corresponding formate and alcohol. **b)** Fluorescence microscope image of 12.50 mM TPO droplets with 5.00 µM Nile red incorporated into a 0.6% agar gel. **c)** Fluorescence microscope image of 12.50 mM TBO droplets with 5.00 µM Nile red incorporated into an agar gel. **d)** Absorbance measured at 500 nm over time of an emulgel containing 12.50 mM TPO (red) or TBO (blue), respectively. **e)** Absorbance profile of the first 20 hours of a 12.50 mM TBO emulgel covered with a PBS supernatant (blue), a PBS supernatant containing 8.00 mM L-lysine, or an FBS supernatant, respectively. All absorbance measurements were performed at 37°C in triplicate.

Next, 25.00 µM of the hydrophobic model drug nimodipine was incorporated in 12.50 mM TBO oil droplets and subsequently entrapped in a hydrogel to study the drug release. **Figure 18a** shows that under physiological conditions at pH 7.4 and at 37°C, only 20.0% nimodipine is released after 60.0 hours. However, the absorbance profile of this emulgel shows no presence of oil droplets after 60.0 hours (**Figure 18b** (blue)). Although, without the presence of oil droplets, at least 60.0% of the drug should diffuse out of the gel into the supernatant, only 20.0% drug is released (**Figure 18a (black)**). One explanation is that at pH 7.4 TBO does not fully hydrolyze, but the oil droplets might diffuse out of the gel and form a phase on top of the supernatant. As a consequence, a decrease in the absorbance can be observed, while only a low drug concentration is detected in the supernatant. An NMR measurement of 10.00 mM TBO incubated in PBS at pH 7.4 at 37°C shows that only 40.0% of the orthoester is hydrolyzed

in 6 days (**Figure 18c**). In contrast, 50.0% nimodipine is released from a TBO emulgel at pH 6 (**Figure 18a (red)**). The release profile shows a linear release over the total release period of 14.0 hours, which aligns with the measured absorbance profile (**Figure 18b (red)**). The composition measurement of 10.00 mM TBO incubated in PBS at pH 6.4 as well as pH 5.3 at 37°C reveals 70.0% and 93.0% of the orthoester is hydrolyzed (**Figure 18c**). This indicates that only the hydrolysis at pH 6 or lower is sufficient to achieve zero-order drug release.
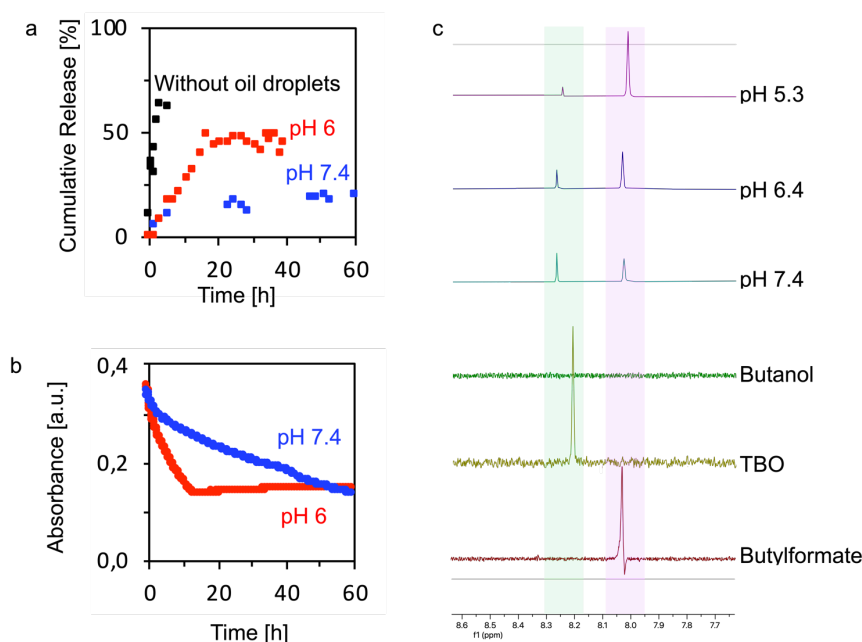
Figure 18: a) Cumulative release profile of 25.00 µM Nimodipine from a pure hydrogel at pH 7.4 (black), from an emulgel containing 12.50 mM TBO oil droplets at pH 7.4 (blue) as well as at pH 6 (red). **b)** Absorbance measured at 500 nm of an emulgel containing 12.50 mM TBO at pH 7.4 (blue) and pH 6 (red). **c)** Stacked NMR spectra of 10.00 mM butylformate, 10.00 mM TBO, 10.00 mM butanol as well as NMR spectra of 10.00 mM TBO incubated in PBS at pH 7.4, pH 6.4, and pH 5.3 for 6 days at 37°C. The spectra are displayed from 7.7 to 8.6 ppm and show the characteristic signals of TBO at δ = 8.25 ppm (green) and of butylformate at δ = 8.04 ppm (purple). The ratio of the characteristic TBO signal and the butylformate signal show that at pH 7.4 only 40.0%, at pH 6.4 70.0%, and at pH 5.3 93.0% TBO is hydrolyzed to butylformate. The spectrum of TBO was recorded in DMSO-d_6, and all other spectra were recorded in PBS with water suppression and an insert containing 50.00 mM hydroquinone in D_2O.

6.4 Conclusion and Outlook

In this chapter, the suitability of hydrophobic boronic esters and orthoesters as hydrolyzable oil was explored. The synthesized boronic esters BE1 – BE5 could form oil droplets in an aqueous solution and incorporate the hydrophobic dye Nile red as a model drug. However, a linear drug release could not be achieved, because under the chosen physiological conditions the boronic ester is favored over the boronic acid and the diol. This means that the boronic ester may hydrolyze and revert back to the boronic ester. Phase separation of the boronic ester in the hydrogel or on top of the aqueous supernatant may then incorporate a major part of the hydrophobic drug and prevent its release. Thus, the selected boronic ester compounds are not suitable as a zero-order drug delivery platform. However, this limitation may be overcome by choosing a boronic acid with a pKa value that is higher than the physiological pH of 7.4 for the boronic ester synthesis. At pH values that are higher than the boronic acid's pKa value, the esterification process is favored over the hydrolysis. Scientists have shown that high pKa values up to 9.9 can be achieved by *i.e.,* functionalizing the boronic acid with a phenyl group.[165, 169, 171] Thus, boronic esters formed by a phenylboronic acid should easily hydrolyze at physiological pH and therefore may achieve zero-order drug release. In the future, these boronic esters should be further explored.

Of the studied orthoesters, tripropyl orthoformate (TPO) and tributyl orthoformate (TBO) as hydrolyzable oils, TBO is suitable to achieve zero-order drug release. However, sufficient hydrolysis of the orthoester only takes place at pH 6 or lower. As a consequence, the hydrophobic drug nimodipine can only be fully released at pH 6, while under physiological pH only 20% of the drug is released. This means a TBO emulgel would be a suitable drug delivery system for environments with low pH, *i.e.,* the urinary tract with a pH between 4.5 and 7.8.[176] One example of its application could be the coating of urinary catheters with an anti-bacterial drug containing TBO emulgel to prevent biofilm formation and thus infections of the urinary tract.[177] However, determining the correct drug release rate and period may be challenging due to the broad range of urine pH of different patients. Furthermore, pH fluctuations in the patient's urine may lead to an unpredictable drug release that may change over time. Another low-pH environment where a TBO emulgel may be suitable is tumor tissue. For example, malignant tumors have an acidic microenvironment with a pH of 5.6 to 6.8 which would be ideal for the application of a TBO emulgel.[178] In contrast to boronic esters, future studies of the orthoester drug delivery systems should focus on the applications in low-pH environments.

7 Conclusion and Outlook

This thesis aims to build a simple, versatile, cheap drug delivery platform that can release hydrophobic drugs with zero-order kinetics. As described in Chapter 1, these linear release systems create a constant plasma drug concentration within the therapeutic window. As a result, adverse side effects are decreased while simultaneously the therapy's effectiveness and patient compliance are improved.

Our designed drug delivery system is based on two cheap commercially available components: first, a hydrolyzable oil that forms oil droplets in an aqueous solution and that can incorporate a hydrophobic drug. The second component is a hydrogel that functions as a matrix to immobilize the oil droplets. Specifically, the biocompatible agar gel or agarose gel were used for our drug delivery platform. Of the different hydrolyzable oils that were examined, symmetric or asymmetric hydrophobic anhydrides such as heptanoic anhydride (C_7C_7), hexanoic anhydride (C_6C_6), or 2-decen-1-ylsuccinic anhydride (C_{10}) are most suitable for achieving zero-order drug release. As shown in Chapter 3, a range of hydrophobic drugs can be released linearly with hydrophobic anhydride droplets, which the partition coefficient of the drug between the oil and the aqueous phase can predict. Here, the release period and the release rate can be tuned by adjusting the initial hydrolyzable oil and the initial drug concentration, respectively. Furthermore, cholesterol-conjugated oligonucleotides can also be released from this emulgel platform as demonstrated in Chapter 4. In contrast to the hydrophobic drug, the cholesterol-conjugated DNA accumulates on the oil droplet's surface and is only released if the oil is fully hydrolyzed. This creates a unique dual-release platform that can linearly release a hydrophobic drug which is followed by a rapid DNA burst release. We found that our emulgel platform, especially if C_7C_7 is used, has a low cell toxicity and therefore is suitable for biomedical applications. Moreover, the formulation can be frozen at -196°C and stored at -20°C without changing the release kinetics. However, as explained in Chapter 5, this hydrophobic anhydride-based formulation cannot achieve zero-order drug release in biological media. We found that this is caused by the fast reaction of the highly nucleophilic amine moieties of amino acids and proteins with the anhydride.

To overcome this limitation, we introduced hydrophobic boronic ester and orthoester as hydrolyzable emulsions in Chapter 6. These compounds are less electrophilic and thus not susceptible to reaction with primary amines. While the boronic esters and the orthoesters show no reactivity with primary amine moieties, zero-order drug release can only be partly achieved. The equilibrium favors the synthesized boronic esters over the boronic acid and diol at

physiological conditions. As a result, the hydrophobic drug remains in the boronic ester phase and thus cannot be released linearly. Similarly, the hydrolysis of the chosen orthoester TBO is only sufficient at a pH lower than 6. Consequentially, drug release follows zero-order kinetics only at pH 6 or lower, while at a physiological pH of 7.4, only an incomplete drug release can be observed.

For future research, boronic esters particularly show high potential. Overcoming the limitations of the selected boronic esters may be achieved by adjusting the pKa values of the used boronic acids. The esterification process is favored at pH values higher than the boronic acid's pKa value. Thus, choosing a boronic acid with a pKa value higher than pH 7.4 as a boronic ester precursor may result in sufficient hydrolysis at physiological pH. For example, phenyl moieties can be introduced to increase the boronic acid's pKa value to 9.9. [165, 169, 171] Furthermore, different applications of the orthoester-based drug delivery system should be explored. As zero-order drug release can only be achieved at a slightly acidic pH value, formulations for environments with low pH, such as the urinary tract or tumors, should be developed.[176, 178]

.

8 Materials and Methods

8.1 Materials

8.2 Emulgel preparation and release experiments

Stock solutions (5.00 mM) of the drugs nimesulide, nitrendipine, ritonavir, and piroxicam were prepared by dissolving the drug in acetonitrile. For the mebendazole and acyclovir stock solutions (5.00 mM) dimethylsulfoxide was used as a solvent. All the stock solutions were stored at 8°C until further use.

The precursor stock solutions were prepared by emulsifying the anhydride, the orthoester, or the boronic ester, respectively, in PBS (pH 7.4). For the drug release experiments, 4.00–200.00 µL of the drug stock solution was added and the emulsion was sonicated for two minutes with a Branson UltrasonicsTM SonifierTM SFX250 at 25% in an ice bath. These pure precursor or precursor/drug emulsions were prepared freshly for each experiment.

The emulgels were prepared by adding 500.00 µL of the precursor/drug emulsion to 500.00 µL of a 2% agar-agar stock in PBS, which was heated to 90°C (**Scheme 6**). Then 60.00 µL of this mixture was put on the bottom of a 96-well plate and after the emulgel was cooled off, 120.00 µL PBS, DMEM, FBS, or LB, respectively, was added as supernatant. The cumulative drug and acid release were subsequently measured in the supernatant. All experiments were performed at 37°C in triplicate.
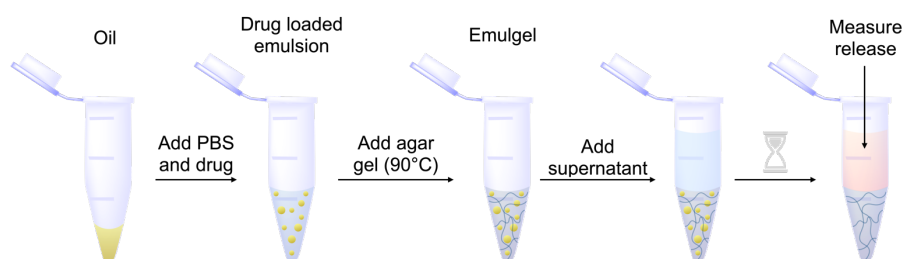
Scheme 6: Preparation of the drug delivery formulation.

8.3 Analytical HPLC

The released drug and acid concentrations were determined by analytical high-performance liquid chromatography (HPLC, Thermo-fisher Dionex Ultimate 3000, Hypersil Gold 250 × 4.8

mm) using a linear gradient of MilliQ-water and acetonitrile, each with 0.1% trifluoroacetic acid. All compounds were detected with a UV/Vis detector at 220, 240, and 330 nm. The method we used was programmed to run an H2O:ACN gradient from 98:2 to 2:98 in 13 min. Calibration curves of all compounds were conducted with the corresponding method in triplicate.

8.4 UV/Vis spectroscopy

The UV/Vis measurements were carried out using a Multiskan FC (ThermoFisher) microplate reader. The samples were prepared the same way as for the HPLC experiments. The temperature was 37.0 ± 0.5°C. Each experiment was performed at 500 nm and in triplicate.

8.5 Microscopy

Confocal fluorescence microscopy was performed on a Leica TCS SP8 confocal microscope using a 63× water immersion objective. The precursor stock solutions were prepared by emulsifying the anhydride, the othoester, or the boronic ester in PBS (pH 7.4) with a Branson UltrasonicsTM SonifierTM SFX250 at 25% in an ice bath and adding 5 mM Nile red dye. The emulgel sample was prepared as previously described. The samples were excited at 552 nm and imaged at 560–650 nm with a HyD detector (pinhole: 1 a.u., laser power: 0.09, gain: 146.7%). The measurements were performed at 25°C.

8.6 NMR spectroscopy

The ^{1}H nuclear magnetic resonance (NMR) spectra were recorded with a Bruker AV-III-300 spectrometer at 20°C. The NMR spectroscopic chemical shifts δ are reported in ppm. For concentration measurements, emulgel samples were prepared as described previously. The aqueous supernatant was placed in an NMR tube with an insert containing a solution of 50.00 mM hydroquinone in D_2O. The NMR spectra were recorded using a water-suppression method. Calibrations of all compounds were recorded with the same method and used to calculate the concentrations in the supernatant.

8.7 Synthesis of the boronic esters

The general synthesis of the boronic esters BE1 – 5 followed a modified method of Bernardini *et al.* from the boronic acid and a diol.[170]

(1S,2S,6R,8S)-4-Isobutyl-2,9,9-trimethyl-3,5-dioxa-4-boratricyclo[6.1.1.0*2,6*]decane (BE1)

Yield 90%. ^{1}H-NMR (DMSO-d_6) δ 0.68 (d, 2H, J = 7.27 Hz, BC**H₂**CH), 0.82 (s, 3H, CHCC**H₃**), 0.90 (d, 6H, J = 6.61 Hz, CH2CH(C**H₃)₂**), 1.01 (d, 1H, J = 10.58 Hz, CHC**H₂**CH), 1.25 (s, 3H, CHCC**H₃**), 1.30 (s, 3H, OCC**H₃**), 1.67 (m, 1H, OCHC**H₂**CH), 1.79 (m, 1H, CH₂C**H**(CH₃)₂), 1.87 (m, 1H, CC**H**CH₂), 1.99 (m, 1H, CC**H**C), 2.18 (m, 1H, CHC**H₂**CH), 2.27 (m, 1H, OCHC**H₂**CH), 4.28 (dd, 1H, J_1 = 8.73 Hz, J_2 = 2.03 Hz, OC**H**CH₂).

2-Isobutyl-5-methyl[1,3,2]dioxaborinan-5-ylamine (BE2)

Yield 87%. ^{1}H-NMR (DMSO-d_6) δ 0.55 (d, 2H, J = 7.18 Hz, BC**H₂**CH), 0.87 (m, 6H, CH₂CH(C**H₃)₂**), 0.98 (s, 3H, NCC**H₃**), 1.73 (dq, 1H, J_1 = 13.41 Hz, J_2 = 6.61 Hz, CH₂C**H**(CH₃)₂), 3.51 (m, 4H, OC**H₂**C), 7.35 (s, 2H, N**H₂**).

2-isobutyl-5-methyl-5-propyl-1,3,2-dioxaborinane (BE3)

Yield 90%. ^{1}H-NMR (DMSO-d_6) δ 0.55 (d, 2H, J = 7.08 Hz, BC**H₂**CH), 0.85 (m, 12H, CH₂CH(C**H₃)₂**, CC**H₂**CH₂C**H₃**, CC**H₃**), 1.22 (m, 4H, CC**H₂**CH₂CH₃), 1.74 (dt, J_1 = 13.50 Hz, J_2 = 6.80 Hz, BCH₂C**H**(CH₃)₂), 3.57 (q, 4H, J = 10.67 Hz, OC**H₂**C).

5-methyl-2-pentyl-5-propyl-1,3,2-dioxaborinane (BE4)

Yield 89%. ^{1}H-NMR (DMSO-d_6) δ 2.25 (t, 2H, J = 7.41 Hz, BC**H₂**CH), 2.86 (m, 9H, C**H₃**), 4.17 (m, 10H, BCH₂(C**H₂)₃**CH₃, C(C**H₂)₂**CH₃), 5.23 (q, 4H, J = 10.67 Hz, OC**H₂**C).

5-butyl-5-ethyl-2-pentyl-1,3,2-dioxaborinane (BE5)

Yield 93%. ^{1}H-NMR (DMSO-d$_6$) δ 0.57 (t, 2H, *J* = 7.51 Hz, BC**H₂**CH), 0.82 (m, 9H, C**H₃**), 1.22 (m, 14H, BCH$_2$(C**H₂**)**₃**CH$_3$, C(C**H₂**)**₃**CH$_3$, CC**H₂**CH$_3$), 3.60 (s, 4H, OC**H₂**C).

9 Acknowledgments

I am thanking Job Boekhoven for giving me the opportunity to pursue a doctorate at his chair and for supporting my research along this way. I learned a lot of new skills and not only grew as a scientist but also as a person. I appreciate that your door was always open for me and that you took time for all the group meetings, sub-group meetings and writing sessions.

My sincere gratitude also goes to Julianne Gibbs who welcomed me into her group during my research stay at the University of Alberta and supported me on my DNA-based project. I also want to thank Nahida for being a great collaboration partner and making me feel at home at the University of Alberta.

I would also like to give a big thanks to my collaboration partners Oliver Lieleg, Theresa, and Di for helping me with my *in vivo* experiments. Thank you for all of your contributions.

Thank you to all the members and former members of the Boekhoven Lab: Caren, Martha, Rapha, Benno, Schnitti, Padi, Carsten, Kun, Michi, Alex, Jennifer, Xiaoyao, Judit, Michele, Fabi, Brigitte, Christine, Anna-Lena, Monika, Simone, Oleksii, Hector, and Pablo. You created a wonderful atmosphere to work in and I enjoyed all the science and non-science discussions at our lunch and coffee breaks and during our creative workshops. It was a pleasure to work with you. I especially want to thank Caren for supervising me during my master's thesis and for initiating this interesting project that became my Ph.D. thesis. Thank you to Jennifer and Hector for proofreading my thesis and thank you Ruth and Corina for handling all the administrative things. I am also extremely grateful to have shared an office with my friends and colleagues Judit, Jennifer, Xiaoyao, and of course Savänni, the best lab-puppy ever. I had so much fun with you, I learned so much from you and I appreciate that I could share all the ups and downs of my Ph.D with you. I also want to thank Fabi "the boss babe", without you the lab would be less fun (and without a peptide synthesizer).

I am also very grateful for having so many amazing friends far too many to list everyone here. Especially thank you, Tami and Anna, we made it together through our Bachelor's and Master's studies and even though we ended up in different labs and universities for our doctorates you were still always there for me.

Of course, this would not be complete without thanking my family: Mama, Papa, Franca, Alex, Evelyne, and Johannes. So, thank you for your endless support, unconditional love and always believing in me, no matter what. This thesis would not have been possible without you!

10 Literature

[1]   K. K. Jain, Drug Delivery Systems - An Overview. In *Drug Delivery Systems*, Jain, K. K., Ed. Humana Press: Totowa, NJ, 2008; pp 1-50.

[2]   J. Li; D. J. Mooney, *Nat. Rev. Mater.* **2016**, *1*, 16071.

[3]   A. K. Nayak; S. A. Ahmad; S. Beg; T. J. Ara; M. S. Hasnain, 12 - Drug delivery: Present, past, and future of medicine. In *Applications of Nanocomposite Materials in Drug Delivery*, Inamuddin; Asiri, A. M.; Mohammad, A., Eds. Woodhead Publishing: 2018; pp 255-282.

[4]   A. K. Shah; S. A. Agnihotri, *Journal of Controlled Release* **2011**, *156*, 281-296.

[5]   Y. Zhang; H. F. Chan; K. W. Leong, *Advanced Drug Delivery Reviews* **2013**, *65*, 104-120.

[6]   R. Verma; S. Garg, *Pharmaceutical Technology On-Line* **2001**, *2*, 1–14.

[7]   G. Tiwari; R. Tiwari; B. Sriwastawa; L. Bhati; S. Pandey; P. Pandey; S. K. Bannerjee, *Int J Pharm Investig* **2012**, *2*, 2-11.

[8]   D. Paolino; P. Sinha; M. Fresta; M. Ferrari, Drug Delivery Systems. In *Encyclopedia of Medical Devices and Instrumentation*, 2006.

[9]   K. K. Jain, An Overview of Drug Delivery Systems. In *Drug Delivery Systems*, Jain, K. K., Ed. Springer New York: New York, NY, 2020; pp 1-54.

[10]   S. Adepu; S. Ramakrishna, *Molecules* **2021**, *26*.

[11]   M. K. Miah; I. H. Shaik; F. G. Feturi; A. Ali; R. Venkataramanan, Chapter 29 - Clinical Pharmacokinetics. In *Clinical Pharmacy Education, Practice and Research*, Thomas, D., Ed. Elsevier: 2019; pp 409-424.

[12]   M. Sabyasachi; S. Kalyan Kumar, Introductory Chapter: Drug Delivery Concepts. In *Advanced Technology for Delivering Therapeutics*, Sabyasachi, M.; Kalyan Kumar, S., Eds. IntechOpen: Rijeka, 2017; p Ch. 1.

[13]   J. Wang; B. Wang; S. P. Schwendeman, *J. Control. Release* **2002**, *82*, 289-307.

[14]   W. J. Goh; S. Zou; W. Y. Ong; F. Torta; A. F. Alexandra; R. M. Schiffelers; G. Storm; J.-W. Wang; B. Czarny; G. Pastorin, *Scientific Reports* **2017**, *7*, 14322.

[15]   K. Uhrich; S. Cannizzaro; R. Langer; K. Shakesheff, *Chem. Rev.* **1999**, *11*, 3181–3198.

[16]   G. Agarwal; S. Agarwal; P. Karar; S. Goyal, *Am. J. Adv. Drug Deliv.* **2017**, *5*, 64-76.

[17]   M. M. Cheng; R. Alfonso; J. H. Best; L. P. Garrison; D. Bruhn; D. L. Veenstra, *Journal of Medical Economics* **2010**, *13*, 193-202.

[18]   I. M. Ram; S. N. Ajit, *Pharmaceutical Dosage Forms and Drug Delivery : Revised and Expanded*. CRC Press: Boca Raton, 2017; Vol. Third edition.

[19]   J. Kim; O. D. Jesus Medication Routes of Administration. (accessed 20.02.2023).

[20]   E. T. L. Lau; K. J. Steadman; J. A. Y. Cichero; L. M. Nissen, *Advanced Drug Delivery Reviews* **2018**, *135*, 75-84.

[21]   B. Homayun; X. Lin; H. J. Choi, *Pharmaceutics* **2019**, *11*.

[22]   P. Viswanathan; Y. Muralidaran; G. Ragavan, Chapter 7 - Challenges in oral drug delivery: a nano-based strategy to overcome. In *Nanostructures for Oral Medicine*, Andronescu, E.; Grumezescu, A. M., Eds. Elsevier: 2017; pp 173-201.

[23]   V. F. Patel; F. Liu; M. B. Brown, *Journal of Controlled Release* **2011**, *153*, 106-116.

[24]   K. N. Means; A. E. Gentry; T. T. Nguyen, *West J Emerg Med* **2018**, *19*, 417-422.

[25]   M. L. Laracuente; M. H. Yu; K. J. McHugh, *J. Control. Release* **2020**, *327*, 834-856.

[26]   B. Homayun; X. Lin; H.-J. Choi, *Pharmaceutics* **2019**, *11*, 129.

[27]   L. Shargel; S. Wu-Pong; A. B. C. Yu, Chapter 17. Modified-Release Drug Products. In *Applied Biopharmaceutics & Pharmacokinetics, 6e*, The McGraw-Hill Companies: New York, NY, 2012.

[28]   R. Langer, *Nature* **1998,** *392*, 5-10.

[29]   A. H. P. Paes; A. Bakker; C. J. Soe-Agnie, *Diabetes Care* **1997,** *20*, 1512-1517.

[30]   M. Gupta; B. Ray, *International Journal of Therapeutic Applications* **2012,** *8*, 18 - 23.

[31]   Y. Hattori; Y. Haruna; M. Otsuka, *Colloids and Surfaces B: Biointerfaces* **2013,** *102*, 227-231.

[32]   T. R. Dash; P. K. Verma, *International Journal of Pharma Research & Review* **2013,** *2013*.

[33]   J. Siepmann; F. Siepmann, *Journal of Controlled Release* **2012,** *161*, 351-362.

[34]   P. Colombo, *Advanced Drug Delivery Reviews* **1993,** *11*, 37-57.

[35]   R. Censi; T. Vermonden; M. J. van Steenbergen; H. Deschout; K. Braeckmans; S. C. De Smedt; C. F. van Nostrum; P. di Martino; W. E. Hennink, *Journal of Controlled Release* **2009,** *140*, 230-236.

[36]   D. Klose; F. Siepmann; K. Elkharraz; S. Krenzlin; J. Siepmann, *International Journal of Pharmaceutics* **2006,** *314*, 198-206.

[37]   C. Cai; S. Mao; O. Germershaus; A. Schaper; E. Rytting; D. Chen; T. Kissel, *Journal of Microencapsulation* **2009,** *26*, 334-345.

[38]   A. Turek; E. Olakowska; A. Borecka; H. Janeczek; M. Sobota; J. Jaworska; B. Kaczmarczyk; B. Jarząbek; A. Gruchlik; M. Libera; A. Liśkiewicz; H. Jędrzejowska-Szypułka; J. Kasperczyk, *Pharmaceutical Research* **2016,** *33*, 2967-2978.

[39]   B. Y. S. Ong; S. H. Ranganath; L. Y. Lee; F. Lu; H.-S. Lee; N. V. Sahinidis; C.-H. Wang, *Biomaterials* **2009,** *30*, 3189-3196.

[40]   K. W. Leong; B. C. Brott; R. Langer, *Journal of Biomedical Materials Research* **1985,** *19*, 941-955.

[41]   Y. Tabata; S. Gutta; R. Langer, *Pharmaceutical Research* **1993,** *10*, 487-496.

[42]   J. Hanes; M. Chiba; R. Langer, *Biomaterials* **1998,** *19*, 163-172.

[43]   Y. N. Zhao; X. Xu; N. Wen; R. Song; Q. Meng; Y. Guan; S. Cheng; D. Cao; Y. Dong; J. Qie; K. Liu; Y. Zhang, *Sci. Rep.* **2017,** *7*, 5524.

[44]   B. Gupta; N. Thakur; N. Jain; J. Banweer; S. Jain, *Journal of Pharmacy & Pharmaceutical Sciences* **2010,** *13*, 571-588.

[45]   C. K. Sahoo; N. K. Sahoo; S. R. M. Rao; M. Sudhakar; K. Satyanarayana, *Bulletin of Faculty of Pharmacy, Cairo University* **2015,** *53*, 195-205.

[46]   R. K. Verma; D. M. Krishna; S. Garg, *Journal of Controlled Release* **2002,** *79*, 7-27.

[47]   K. Singh; M. Walia; G. Agarwal; S. Harikumar, *JDDT* **2013,** *3*, 156-162.

[48]   N. Arjun; D. Narendar; K. Sunitha; K. Harika; B. Nagaraj, *International Journal of Pharmaceutical Investigation* **2016,** *6*, 238-246.

[49]   A. Nokhodchi; M. N. Momin; J. Shokri; M. Shahsavari; P. A. Rashidi, *Drug Delivery* **2008,** *15*, 43-48.

[50]   G. A. McClelland; S. C. Sutton; K. Engle; G. M. Zentner, *Pharmaceutical Research* **1991,** *8*, 88-92.

[51]   A. Abd-Elbary; M. I. Tadros; A. A. Alaa-Eldin, *AAPS PharmSciTech* **2011,** *12*, 485-495.

[52]   G. M. Zentner; G. S. Rork; K. J. Himmelstein, *Journal of Controlled Release* **1985,** *1*, 269-282.

[53]   S. C. Chauhan; K. P. Choudhury, *Current Drug Delivery* **2006,** *3*, 193-198.

[54]   H. P. Thakkar; N. Pancholi; C. V. Patel, *AAPS PharmSciTech* **2016,** *17*, 1248-1260.

[55]   K. Adibkia; J. Hanaee; S. Ghanbarzadeh; R. Bahrami; J. Shokri, *Drug Res (Stuttg)* **2014,** *64*, 203-7.

[56]   L. A. Bahari; Y. Javadzadeh; M. B. Jalali; P. Johari; A. Nokhodchi; J. Shokri, *Colloids and Surfaces B: Biointerfaces* **2017,** *153*, 27-33.

[57]   V. Malaterre; J. Ogorka; N. Loggia; R. Gurny, *International Journal of Pharmaceutics* **2009,** *376*, 56-62.

[58]   V. Patel; A. Chudasama; M. Nivsarkar; K. Vasu; C. Shishoo, *Pharmaceutical Development and Technology* **2012,** *17*, 375-382.

[59]   R. Wakode; R. Bhanushali; A. Bajaj, *PDA Journal of Pharmaceutical Science and Technology* **2008,** *62*, 22.

[60]   R. W. Licht, *CNS Neuroscience & Therapeutics* **2012,** *18*, 219-226.

[61]   F. P. Pons-Faudoa; A. Ballerini; J. Sakamoto; A. Grattoni, *Biomedical Microdevices* **2019,** *21*, 47.

[62]   E. Chappel, Chapter 7 - Implantable drug delivery devices. In *Drug Delivery Devices and Therapeutic Systems*, Chappel, E., Ed. Academic Press: 2021; pp 129-156.

[63]   L. Baert; L. Schueller; Y. Tardy; D. Macbride; G. v. t. Klooster; H. Borghys; E. Clessens; G. Van Den Mooter; E. Van Gyseghem; P. Van Remoortere; P. Wigerinck; J. Rosier, *International Journal of Pharmaceutics* **2008,** *355*, 38-44.

[64]   K. H. Knight; F. M. Brand; A. S. McHaourab; G. Veneziano, *Croat Med J* **2007,** *48*, 22-34.

[65]   M. Lomanto, Baclofen. In *The Essence of Analgesia and Analgesics*, Watkins-Pitchford, J. M.; Jahr, J. S.; Sinatra, R. S., Eds. Cambridge University Press: Cambridge, 2010; pp 379-382.

[66]   V. C. Anderson; K. J. Burchiel, *Neurosurgery* **1999,** *44*.

[67]   S. Ferrati; D. Fine; J. You; E. De Rosa; L. Hudson; E. Zabre; S. Hosali; L. Zhang; C. Hickman; S. Sunder Bansal; A. M. Cordero-Reyes; T. Geninatti; J. Sih; R. Goodall; G. Palapattu; M. Kloc; R. M. Ghobrial; M. Ferrari; A. Grattoni, *Journal of Controlled Release* **2013,** *172*, 1011-1019.

[68]   F. Martin; R. Walczak; A. Boiarski; M. Cohen; T. West; C. Cosentino; M. Ferrari, *Journal of Controlled Release* **2005,** *102*, 123-133.

[69]   C. Cosentino; F. Amato; R. Walczak; A. Boiarski; M. Ferrari, *The Journal of Physical Chemistry B* **2005,** *109*, 7358-7364.

[70]   A. Grattoni; H. Shen; D. Fine; A. Ziemys; J. S. Gill; L. Hudson; S. Hosali; R. Goodall; X. Liu; M. Ferrari, *Pharmaceutical Research* **2011,** *28*, 292-300.

[71]   S. H. Lee; M. Park; C. G. Park; B.-H. Kim; J. Lee; S. Choi; S.-r. Nam; S.-H. Park; Y. B. Choy, *Journal of Controlled Release* **2014,** *196*, 52-59.

[72]   K. B. Sutradhar; C. D. Sumi, *Drug Delivery* **2016,** *23*, 1-11.

[73]   P. Gardner, *Expert Opinion on Drug Delivery* **2006,** *3*, 479-487.

[74]   A. I.-.-.-. Ziabicki, *Fundamentals of fiber formation*. John Wiley and Sons: London, 1976.

[75]   N. Joy; D. Venugopal; S. Samavedi, *European Polymer Journal* **2022,** *168*, 111102.

[76]   X. Liu; Y. Yang; D.-G. Yu; M.-J. Zhu; M. Zhao; G. R. Williams, *Chemical Engineering Journal* **2019,** *356*, 886-894.

[77]   A. Laha; C. S. Sharma; S. Majumdar, *Materials Science and Engineering: C* **2017,** *76*, 782-786.

[78]   D.-G. Yu; X.-Y. Li; X. Wang; W. Chian; Y.-Z. Liao; Y. Li, *Cellulose* **2013,** *20*, 379-389.

[79]   J. Xue; T. Wu; Y. Dai; Y. Xia, *Chemical Reviews* **2019,** *119*, 5298-5415.

[80]   A. S. Narang; S. H. S. Boddu, *Excipient Applications in Formulation Design and Drug Delivery*. Springer Nature: Switzerland, 2015.

[81]   S.-C. Chow, *WIREs Computational Statistics* **2014,** *6*, 304-312.

[82]   R. Panchagnula; N. S. Thomas, *International Journal of Pharmaceutics* **2000,** *201*, 131-150.

[83]   A. A. Somani; K. Thelen; S. Zheng; M. N. Trame; K. Coboeken; M. Meyer; K. Schnizler; I. Ince; S. Willmann; S. Schmidt, *British Journal of Clinical Pharmacology* **2016,** *81*, 137-147.

[84]   Y. Tsume; D. M. Mudie; P. Langguth; G. E. Amidon; G. L. Amidon, *Eur J Pharm Sci* **2014,** *57*, 152-63.

[85]   L. Z. Benet, *Journal of Pharmaceutical Sciences* **2013,** *102*, 34-42.

[86]   Y. Kawabata; K. Wada; M. Nakatani; S. Yamada; S. Onoue, *International Journal of Pharmaceutics* **2011,** *420*, 1-10.

[87]   J. Wadhwa; A. Nair; R. Kumria, *Acta Poloniae Pharmaceutica - Drug Research* **2012,** *69*, 179-191.

[88]   D. Xia; F. Cui; H. Piao; D. Cun; H. Piao; Y. Jiang; M. Ouyang; P. Quan, *Pharmaceutical Research* **2010,** *27*, 1965-1976.

[89]   A. T. M. Serajuddin, *Journal of Pharmaceutical Sciences* **1999,** *88*, 1058-1066.

[90]   R. Neslihan Gursoy; S. Benita, *Biomedicine & Pharmacotherapy* **2004,** *58*, 173-182.

[91]   D. L. Burcham; M. B. Maurin; E. A. Hausner; S. M. Huang, *Biopharmaceutics & Drug Disposition* **1997,** *18*, 737-742.

[92]   R. A. Schwendener; H. Schott, *Journal of Cancer Research and Clinical Oncology* **1996,** *122*, 723-726.

[93]   S. Davis; C. Washington; P. West; L. Illum; G. Liversidge; L. Sternson; R. Kirsh; , *Ann. N. Y. Acad. Sci.* **1987**, 75–88.

[94]   V. Patel; H. Kukadiya; R. Mashru; N. Surti; S. Mandal, *Iran. J. Pharm. Sci.* **2010,** *9*, 327-334.

[95]   A. D. Wickes; S. B. Howell, *Cancer Treat Rep* **1985,** *69*, 657-662.

[96]   Y. Mizushima; K. Hoshi; H. Aihara; M. Kurachi, *Journal of Pharmacy and Pharmacology* **1983,** *35*, 397-397.

[97]   P. M. Nigade; S. L. Patil; S. S. Tiwari, *Int J Pharm Bio Sci* **2012,** *2*, 42-52.

[98]   B. Tang; G. Cheng; J.-C. Gu; C.-H. Xu, *Drug Discovery Today* **2008,** *13*, 606-612.

[99]   A. Kumar; S. Sharma; R. Kamble, *Int J Pharm Pharm Sci* **2010,** *2*, 7-13.

[100]   S. C. Gupta; S. Patchva; B. B. Aggarwal, *The AAPS Journal* **2013,** *15*, 195-218.

[101]   S. Setthacheewakul; S. Mahattanadul; N. Phadoongsombut; W. Pichayakorn; R. Wiwattanapatapee, *European Journal of Pharmaceutics and Biopharmaceutics* **2010,** *76*, 475-485.

[102]   J. Li; D. J. Mooney, *Nature Reviews Materials* **2016,** *1*, 16071.

[103]   T. R. Hoare; D. S. Kohane, *Polymer* **2008,** *49*, 1993-2007.

[104]   F. Ullah; M. B. H. Othman; F. Javed; Z. Ahmad; H. M. Akil, *Materials Science and Engineering: C* **2015,** *57*, 414-433.

[105]   A. S. Hoffman, *Advanced Drug Delivery Reviews* **2012,** *64*, 18-23.

[106]   M. Vigata; C. Meinert; D. W. Hutmacher; N. Bock. Hydrogels as Drug Delivery Systems: A Review of Current Characterization and Evaluation Techniques *Pharmaceutics* [Online], 2020.

[107]   I. M. El-Sherbiny; R. J. Lins; E. M. Abdel-Bary; D. R. K. Harding, *European Polymer Journal* **2005,** *41*, 2584-2591.

[108]   C. Ma; Y. Shi; D. A. Pena; L. Peng; G. Yu, *Angew. Chem. Int. Ed.* **2015,** *54*, 7376-7380.

[109]   H. Dai; Q. Chen; H. Qin; Y. Guan; D. Shen; Y. Hua; Y. Tang; J. Xu, *Macromolecules* **2006,** *39*, 6584-6589.

[110] A. A. Obaidat; K. Park, *Biomaterials* **1997,** *18*, 801-806.

[111] J. D. Ehrick; M. R. Luckett; S. Khatwani; Y. Wei; S. K. Deo; L. G. Bachas; S. Daunert, *Macromolecular Bioscience* **2009,** *9*, 864-868.

[112] S. Zhang; A. M. Bellinger; D. L. Glettig; R. Barman; Y.-A. L. Lee; J. Zhu; C. Cleveland; V. A. Montgomery; L. Gu; L. D. Nash; D. J. Maitland; R. Langer; G. Traverso, *Nature Materials* **2015,** *14*, 1065-1071.

[113] R. J. Mumper; A. S. Huffman; P. A. Puolakkainen; L. S. Bouchard; W. R. Gombotz, *Journal of Controlled Release* **1994,** *30*, 241-251.

[114] S. Klein, *Aaps j* **2010,** *12*, 397-406.

[115] E. S. Stippler; S. Kopp; J. B. Dressman, *Dissolution Technologies* **2004,** *11*, 6-10.

[116] M. Farid-ul-Haq; M. A. Hussain; M. T. Haseeb; M. U. Ashraf; S. Z. Hussain; T. Tabassum; I. Hussain; M. Sher; S. N. A. Bukhari; M. Naeem-ul-Hassan, *RSC Advances* **2020,** *10*, 19832-19843.

[117] M. Kurisawa; F. Lee; L.-S. Wang; J. E. Chung, *Journal of Materials Chemistry* **2010,** *20*, 5371-5375.

[118] K. H. Bae; L.-S. Wang; M. Kurisawa, *Journal of Materials Chemistry B* **2013,** *1*, 5371-5388.

[119] M. Kurisawa; J. E. Chung; Y. Y. Yang; S. J. Gao; H. Uyama, *Chemical Communications* **2005**, 4312-4314.

[120] R. Duncan, *Nature Reviews Drug Discovery* **2003,** *2*, 347-360.

[121] S. H. Gehrke; L. H. Uhden; J. F. McBride, *Journal of Controlled Release* **1998,** *55*, 21-33.

[122] F. Lee; J. E. Chung; M. Kurisawa, *Journal of Controlled Release* **2009,** *134*, 186-193.

[123] K. Xu; F. Lee; S. J. Gao; J. E. Chung; H. Yano; M. Kurisawa, *Journal of Controlled Release* **2013,** *166*, 203-210.

[124] E. Caló; V. V. Khutoryanskiy, *European Polymer Journal* **2015,** *65*, 252-267.

[125] F. Vanpariya; M. Shiroya; M. Malaviya, *International Journal of Science and Research (IJSR)* **2021,** *10*, 847.

[126] Ajazuddin; A. Alexander; A. Khichariya; S. Gupta; R. J. Patel; T. K. Giri; D. K. Tripathi, *J. Control. Release* **2013,** *171*, 122-32.

[127] M. Talat; M. Zaman; R. Khan; M. Jamshaid; M. Akhtar; A. Z. Mirza, *Drug Development and Industrial Pharmacy* **2021,** *47*, 1193-1199.

[128] R. Koshani; M. Tavakolian; T. G. M. van de Ven, *ACS Sustainable Chemistry & Engineering* **2021,** *9*, 4487-4497.

[129] Y. Lu; L. Mao; Z. Hou; S. Miao; Y. Gao, *Food Engineering Reviews* **2019,** *11*, 245-258.

[130] K. Delmar; H. Bianco-Peled, *Carbohydrate Polymers* **2016,** *136*, 570-580.

[131] Y. Kapoor; A. Chauhan, *International Journal of Pharmaceutics* **2008,** *361*, 222-229.

[132] E. Josef; K. Barat; I. Barsht; M. Zilberman; H. Bianco-Peled, *Acta Biomaterialia* **2013,** *9*, 8815-8822.

[133] L. Wei; C. Cai; J. Lin; T. Chen, *Biomaterials* **2009,** *30*, 2606–2613.

[134] C. A. Weber; D. Zwicker; F. Jülicher; C. F. Lee, *Reports on Progress in Physics* **2019,** *82*, 064601.

[135] B. Rieß; J. Boekhoven, *ChemNanoMat* **2018,** *4*, 710-719.

[136] C. Wanzke; M. Tena-Solsona; B. Rieß; L. Tebcharani; J. Boekhoven, *Mater. Horiz.* **2020,** *7*, 1397-1403.

[137] M. Tena-Solsona; J. Janssen; C. Wanzke; F. Schnitter; H. Park; B. Rieß; J. M. Gibbs; C. A. Weber; J. Boekhoven, *ChemSystemsChem* **2021,** *3*, e2000034.

[138] P. S. Schwarz; L. Tebcharani; J. E. Heger; P. Müller-Buschbaum; J. Boekhoven, *Chemical Science* **2021,** *12*, 9969-9976.

[139] B. Rieß; C. Wanzke; M. Tena-Solsona; R. K. Grötsch; C. Maity; J. Boekhoven, *Soft Matter* **2018,** *14*, 4852-4859.

[140] A. B. Moshnikova; V. N. Afanasyev; O. V. Proussakova; S. Chernyshov; V. Gogvadze; I. P. Beletsky, *Cell. Mol. Life Sci.* **2006,** *63*, 229-234.

[141] S. Akhondzadeh, *Avicenna J Med Biotechnol* **2016,** *8*, 151-151.

[142] D. Krewski; M. E. Andersen; E. Mantus; L. Zeise, *Risk Analysis* **2009,** *29*, 474-479.

[143] A. Van Norman Gail, *JACC: Basic to Translational Science* **2019,** *4*, 845-854.

[144] H. A. Krebs, *Annual Review of Biochemistry* **1950,** *19*, 409-430.

[145] D. Richter; P. G. Croft, *Biochem J* **1942,** *36*, 746-57.

[146] M. D. Armstrong; U. Stave, *Metabolism* **1973,** *22*, 561-569.

[147] C. Daykin; R. Bro; F. Wulfert, *Metabolomics* **2012,** *8*, 52-63.

[148] G. Sezonov; D. Joseleau-Petit; R. D'Ari, *J Bacteriol* **2007,** *189*, 8746-9.

[149] M. KGaA Dulbecco's Modified Eagle's Medium (DME) Formulation. https://www.sigmaaldrich.com/DE/de/technical-documents/technical-article/cell-culture-and-cell-culture-analysis/mammalian-cell-culture/dulbecco-modified-eagle-medium-formulation (accessed 11.04).

[150] J. van der Valk; G. Gstraunthaler, *Alternatives to Laboratory Animals* **2017,** *45*, 329-332.

[151] I. Branzoi; M. Iordoc; F. Brânzoi; R. Mirea; S. Beatrice Gabriela, *Surface and Interface Analysis* **2010,** *42*, 502-509.

[152] G. Gstraunthaler; T. Lindl, *Zell- und Gewebekultur: Allgemeine Grundlagen und spezielle Anwendungen*. Springer Berlin Heidelberg: 2021.

[153] H. Büntemeyer; D. Lütkemeyer; J. Lehmann, *Cytotechnology* **1991,** *5*, 57-67.

[154] M. KGaA Fetal Bovine Serum (FBS) – What You Need to Know. https://www.sigmaaldrich.com/DE/en/technical-documents/technical-article/cell-culture-and-cell-culture-analysis/mammalian-cell-culture/serum-university (accessed 11.04).

[155] K. J. Laidler, *Journal of Chemical Education* **1984,** *61*, 494.

[156] S. L. Johnson, *The Journal of Physical Chemistry* **1963,** *67*, 495-496.

[157] F. Brotzel; Y. C. Chu; H. Mayr, *The Journal of Organic Chemistry* **2007,** *72*, 3679-3688.

[158] B. Meloun; L. Moravek; V. Kostka, *FEBS letters* **1975,** *58*, 134-137.

[159] D. C. Carter; X.-M. He; S. H. Munson; P. D. Twigg; K. M. Gernert; M. B. Broom; T. Y. Miller, *Science* **1989,** *244*, 1195-1198.

[160] M. B. Lerner; N. Kybert; R. Mendoza; R. Villechenon; M. A. Bonilla Lopez; A. T. Charlie Johnson, *Applied Physics Letters* **2013,** *102*, 183113.

[161] G. T. Williams; J. L. Kedge; J. S. Fossey, *ACS Sensors* **2021,** *6*, 1508-1528.

[162] D. Das; D.-M. Kim; D.-S. Park; Y.-B. Shim, *Electroanalysis* **2011,** *23*, 2036-2041.

[163] L. Zhao; Q. Huang; Y. Liu; Q. Wang; L. Wang; S. Xiao; F. Bi; J. Ding. Boronic Acid as Glucose-Sensitive Agent Regulates Drug Delivery for Diabetes Treatment *Materials* [Online], 2017.

[164] R. Tang; W. Ji; C. Wang, *Macromolecular Bioscience* **2010,** *10*, 192-201.

[165] A. Stubelius; S. Lee; A. Almutairi, *Accounts of Chemical Research* **2019,** *52*, 3108-3119.

[166] L. Li; Z. Bai; P. A. Levkin, *Biomaterials* **2013,** *34*, 8504-8510.

[167] L. Sun; X. Zhang; J. An; C. Su; Q. Guo; C. Li, *RSC Advances* **2014,** *4*, 20208-20215.

[168] Z. Zhao; X. Yao; Z. Zhang; L. Chen; C. He; X. Chen, *Macromolecular Bioscience* **2014,** *14*, 1609-1618.

[169]   M. A. Al-Ni'mat; S. Parcero-Bouzas; S. P. Amaral; E. Fernandez-Megia, *ChemRxiv. Cambridge: Cambridge Open Engage* **2021**.

[170]   R. Bernardini; A. Oliva; A. Paganelli; E. Menta; M. Grugni; S. D. Munari; L. Goldoni, *Chemistry Letters* **2009,** *38*, 750-751.

[171]   S. Kheirjou; A. Abedin; A. Fattahi, *Computational and Theoretical Chemistry* **2012,** *1000*, 1-5.

[172]   S. Einmahl; F. Behar–Cohen; F. o. D'Hermies; S. Rudaz; C. Tabatabay; G. Renard; R. Gurny, *Investigative Ophthalmology & Visual Science* **2001,** *42*, 695-700.

[173]   R. Tang; W. Ji; D. Panus; R. N. Palumbo; C. Wang, *Journal of Controlled Release* **2011,** *151*, 18-27.

[174]   R. A. Swaringen, Jr.; J. F. Eaddy; T. R. Henderson, *The Journal of Organic Chemistry* **1980,** *45*, 3986-3989.

[175]   P. Wipf; T. Tsuchimoto; H. Takahashi, *Pure Appl. Chem.* **1999,** *71*, 415-421.

[176]   M. R. Clarkson; C. N. Magee; B. M. Brenner, Chapter 24 - The Kidney and Hypertension in Pregnancy. In *Pocket Companion to Brenner and Rector's The Kidney (Eighth Edition)*, Clarkson, M. R.; Magee, C. N.; Brenner, B. M., Eds. W.B. Saunders: Philadelphia, 2011; pp 487-510.

[177]   B. W. Trautner; R. O. Darouiche, *American Journal of Infection Control* **2004,** *32*, 177-183.

[178]   B. Lin; H. Chen; D. Liang; W. Lin; X. Qi; H. Liu; X. Deng, *ACS Applied Materials & Interfaces* **2019,** *11*, 11157-11166.